CRCLEME

Cooperative Research Centre for
Landscape Environments
and Mineral Exploration

MINERAL RESOURCES NEW SOUTH WALES

OPEN FILE REPORT SERIES

REGOLITH ARCHITECTURE AND GEOCHEMISTRY OF THE BYROCK AREA, GIRILAMBONE REGION, NORTH-WESTERN NSW

A joint project between CRC LEME and NSW DMR

R.A. Chan, R.S.B. Greene, M. Hicks, M. Le Gleuher, K.G. McQueen, K.M. Scott and S.E. Tate

CRC LEME OPEN FILE REPORT 159

August 2004

CRCLEME

(NSW DMR Report GS2004/122)

CRC LEME is an unincorporated joint venture between CSIRO-Exploration & Mining, and Land & Water, The Australian National University, Curtin University of Technology, University of Adelaide, Geoscience Australia, Primary Industries and Resources SA, NSW Department of Mineral Resources and Minerals Council of Australia, established and supported under the Australian Government's Cooperative Research Centres Program.

CRC AUSTRALIA

© CRC LEME

The Girilambone (Cobar-Bourke) Project is providing a new knowledge base and developing methodologies for improved mineral exploration in areas of regolith cover in central western NSW. This integrated project has a multidisciplinary team with skills in regolith geology, geomorphology, bedrock geology, geochemistry, geophysics and soil science, working to understand the processes and controls on element dispersion in a variable regolith terrain. This report is the third part of a planned series of three reports on work in progress.

Copies of this publication can be obtained from:
The Publications Officer, CRC LEME, c/- CSIRO Exploration & Mining, PO Box 1130, Bentley WA 6102, Australia. Information on other publications in this series may be obtained from the above, or from http://crcleme.org.au
Cataloguing-in-Publication:
Chan, R.
Regolith architecture and geochemistry of the Byrock Area, Girilambone Region, North-western NSW
ISBN 0 643 09152 1
1. Regolith – New South Wales
2. Geochemistry – New South Wales
3. Landforms – New South Wales
I. Chan, R.A.
II. Title
CRC LEME Open File Report 159.
ISSN 1329-4768

Addresses and affiliations of authors:

R.A. Chan
Cooperative Research Centre for Landscape Environments and Mineral Exploration
c/- Geoscience Australia
Division of Minerals
GPO Box 378, Canberra 2601
Australian Capital Territory

R.S.B. Greene
Cooperative Research Centre for Landscape Environments and Mineral Exploration
c/- Australian National University
School of Resource and Environmental Management
Department of Geography
PO Box 4, Canberra 0200
Australian Capital Territory

M. Hicks
Cooperative Research Centre for Landscape Environments and Mineral Exploration
c/- NSW Department of Mineral Resources
Geological Survey of New South Wales
Level 5, 29-57 Christie Street
St Leonards, Sydney 2065
New South Wales

M. Le Gleuher
Cooperative Research Centre for Landscape Environments and Mineral Exploration
c/- Australian National University
Department of Earth and Marine Sciences
PO Box 4, Canberra 0200
Australian Capital Territory

K.G. McQueen
Cooperative Research Centre for Landscape Environments and Mineral Exploration
c/- Australian National University
Department of Earth and Marine Sciences
PO Box 4 Canberra 0200
Australian Capital Territory

K.M. Scott
Cooperative Research Centre for Landscape Environments and Mineral Exploration
c/- Commonwealth Scientific and Industrial Research Organisation
Division of Exploration and Mining
P.O. Box 136, North Ryde, Sydney 1670
New South Wales

S.E. Tate
Previously: Cooperative Research Centre for Landscape Environments and Mineral Exploration
c/- Australian National University.
School of Resource and Environmental Management
Department of Geography
PO Box 4, Canberra 0200
Australian Capital Territory

© Cooperative Research Centre for Landscape Environments and Mineral Exploration, 2004

Abstract

Stage 3 of the Girilambone (Cobar-Bourke) Project has involved collaborative work between CRC LEME and the NSW Department of Mineral Resources in the Byrock area. This work has provided 2713 m of drilling for regolith study with 60 holes, generally 1-3 km apart along a major road traverse across the Byrock 1:100 000 sheet area and more widely spaced across parts of the Glenariff 1:100 000 sheet area.

Regolith-landform mapping conducted in association with drill hole logging reveals that colluvial and alluvial sediments cover most of the Byrock area. Islands of *in situ* regolith are surrounded by sheetwash deposits on rises grading to depositional plains, and large areas of stagnant alluvial plains, especially towards the northwest. Analysis and interpretation of aircore drill samples has allowed identification of two sequences of sediments, weathered bedrock lithologies (altered and unaltered), as well as various types of induration of both transported and *in situ* regolith. A 16.8 Ma leucitite lava marker flow separates the younger sequence of sediments (Sequence 1) with inferred arid alluvial, colluvial and aeolian sediments from the older sequence of sediments (Sequence 2) with inferred lacustrine sediments. Sequence 1 includes magnetic sediments whose areal extent can be detected on first vertical derivative airborne magnetic imagery.

Major and trace element geochemical data from the drilling program indicate a different geochemical terrain to that previously examined further south. There appears to be a greater abundance of weathered mafic rocks (probably including dykes and volcanics) and fractionated granites. There are a number of areas where gold is elevated in the regolith. These appear to be in a "gold-only" association and some are spatially associated with mafic rocks, including those in the western part of the Byrock sheet near the Mt Dijou – Bald Hills area. In the Lord Carington area, northeast of Byrock, anomalous gold values (>0.04 and up to 0.15 g/t Au) were intersected over a 39 m interval in weathered chlorite-phengite-magnetite schists. There is potential for vein and lode-style gold mineralisation associated with mafic rocks in regolith concealed areas.

Detailed work on the soils in the Byrock and adjacent areas has clearly established the presence of a significant aeolian component. This is predominantly in the near 70 μm size fraction. To reduce the diluting effect of this extraneous component, the >100 μm fraction is the most appropriate fraction for geochemical analysis.

CONTENTS

APPENDICES

PLATES

1 INTRODUCTION

The aim of this study is to assist the geological mapping and mineral exploration of the Girilambone belt by providing a more detailed understanding of the regolith geology (transported and *in situ*) and the regolith geochemistry of the Byrock area. The study provided an opportunity to determine geochemical and regolith material associations in sediments and over a variety of bedrock lithologies, some of which were altered. The study also enabled geochemical and geomorphological dispersion processes to be characterised for areas with background geochemical values, as well as for areas with anomalous values indicative of potential mineralisation.

The study is one of a series of projects being undertaken within the Girilambone belt, covering the general area between Nyngan-Cobar-Bourke-Nymagee. Two previously completed projects cover the Sussex-Coolabah and Hermidale areas of this region (Chan *et al.*, 2003a,b; Figure 1). This work is being conducted in collaboration with the Geological Survey of NSW, Department of Mineral Resources (NSW DMR). The results of these projects will be synthesised in a final report due for release in late 2004.

Samples from 60 air core drill holes along road traverses predominantly across the Byrock sheet area, but also on the Glenariff and Gunderbooka sheet areas (Figure 2) were subjected to geochemical, mineralogical and petrographic analyses. Regolith-landform mapping and field analysis of surficial materials were conducted in conjunction with the drilling program in order to provide a context for interpreting the drill hole data. Regional geophysical data (airborne magnetics and radiometrics) were used to assist with regolith-landform mapping, to obtain information on subsurface regolith materials, and to plan drill hole positions.

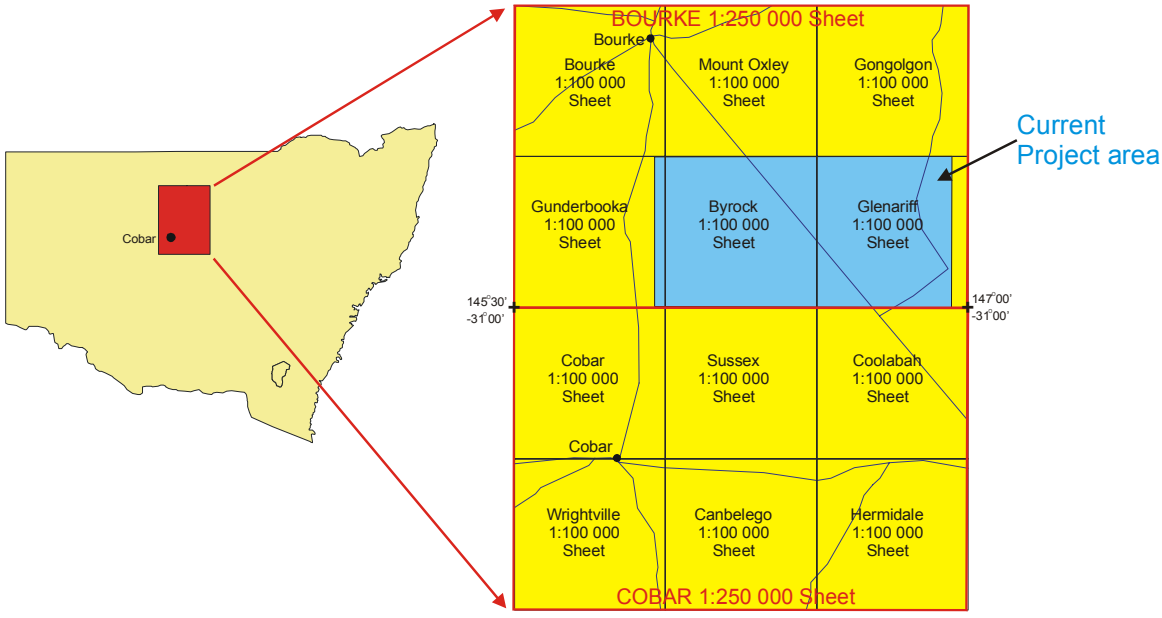

Figure 1. Locality diagram

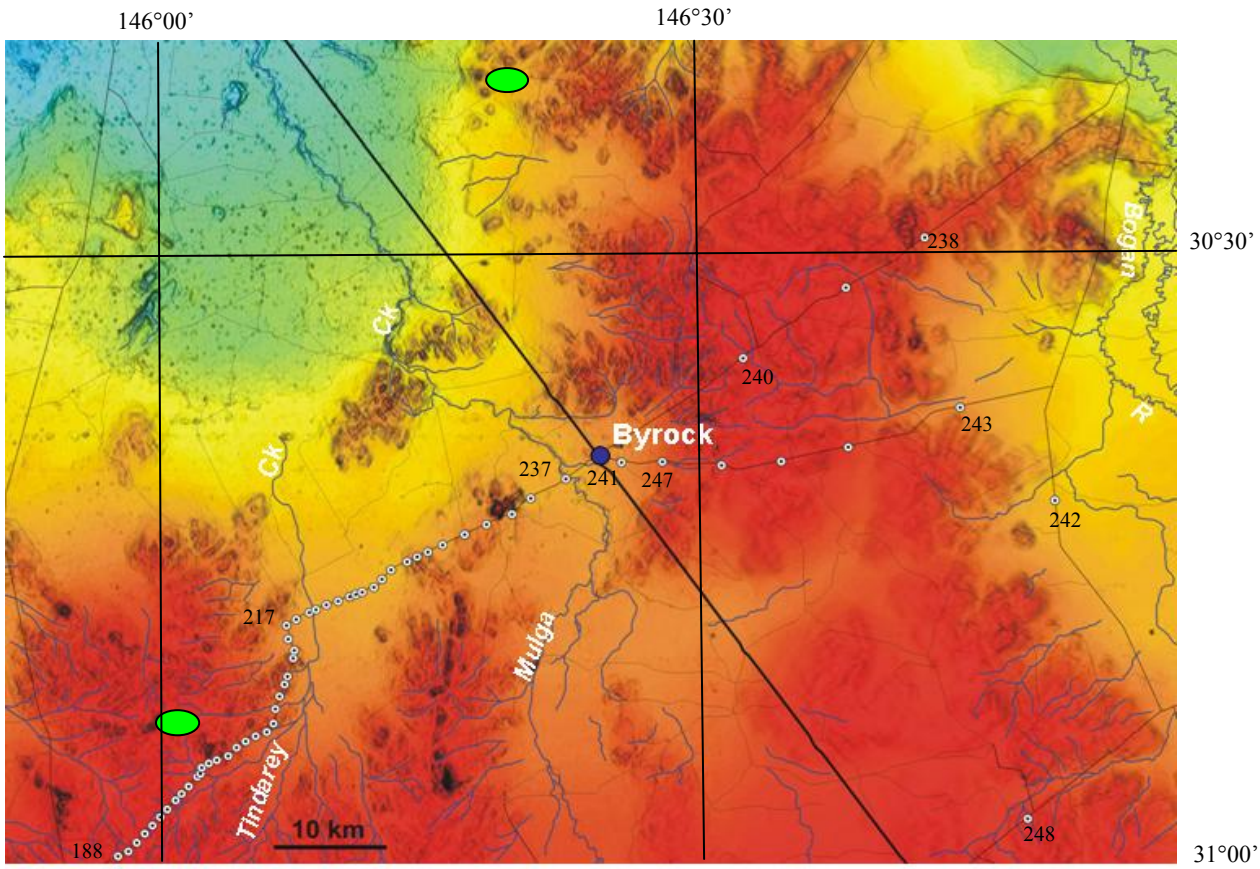

Figure 2. Digital elevation model of the Byrock study area with present drainage, roads and CBAC drill holes. Red – high elevation, blue – low elevation. Green symbols locate the two main known areas of significant mineralisation: Mount Dijou – Bald Hills in the south and Doradilla in the north. Black numbers are Cobar air core (CBAC) drill hole numbers.

2 REGIONAL SETTING

2.1 Location

The Byrock area is in central-western New South Wales, approximately 550 km northwest of Sydney (Figure 1). It lies between Cobar and Bourke and is contained within the Bourke 1:250 000 topographic map sheet. The area of this study covers the Byrock 1:100 000 sheet and parts of the Glenariff and Gunderbooka 1:100 000 sheets where drilling was undertaken (CBAC188 to CBAC248: Figure 2).

The Byrock area has a sub-arid climate with a mean maximum summer temperature (measured at Bourke) of 36.5ºC (January) and a mean winter maximum temperature of 17.9ºC (July). The mean minimum temperature is 21ºC and 4.6ºC for summer and winter respectively (Bureau of Meteorology, 2003).

Two main creeks intermittently flow to the north: Tindarey Creek in the west fades out in plains in the central part of the study area; and Mulga Creek, which persists to join the southwest flowing Darling River to the north of the Byrock study area. Elevation and relief in the Byrock study area generally decrease to the northwest (Figure 2). Elevation ranges from 414 m asl in the central south of the Byrock 1:100 000 sheet area to 120 m asl in the northwest of this area. The relief ranges from 190 m at Coronga Peak in the south to less

than a few metres on plains along the two main creeks and in the northwest. The relief is mostly less than 30 m with large areas less than 9 m relief. The variation in relief and elevation is reflected in the regolith-landforms of the Byrock area.

2.2 Regional Geology of Byrock and Glenariff Sheet areas

The Byrock and Glenariff map sheet area represents a transitional surficial environment between eroded colluvial domains and depositional, fluvial domains. Zones of strongly weathered bedrock in the central portion of the area are flanked by the Darling and Bogan River drainage systems. A prominent hill and ridge of leucitite dominate the landscape west of Byrock village. These Miocene lavas are relatively unweathered. However, over the remainder of the project area outcrop is highly weathered and poorly exposed, commonly sub-cropping within creeks, roadside drains and borrow pits.

The basement, other than the granitoid intrusions, can be divided into two major structural zones. The predominantly northerly trend, which follows the trend of the Gilmore Suture zone, occurs over most of the area. However, these structures are truncated and dragged into a major northeast trending zone in the northwest corner of the Byrock sheet (Figure 3). This major northeast lineament probably marks the southern edge of the Thompson Fold Belt. The Thompson Fold Belt is thought to overthrust the Lachlan Fold Belt, with a possible sinistral transgressive deformational component (Gray and Foster, 2004).

The bedrock geological interpretation is shown in Figure 3. The oldest exposed rocks in the study area are the Cambro-Ordovician Girilambone Group. The Girilambone Group is composed of strongly foliated, bedded and laminated quartzo-feldspathic sandstone, quartzite, shale, phyllite, chert, minor mafic volcanics and intrusives. The chert and quartzite form distinct mappable beds, which can be traced from south of the study area, on the Sussex sheet to well onto the Byrock sheet. On the western margin of the Byrock map sheet area there is a block composed of mafic volcanic rocks (including pillow lavas) and intercalated metasedimentary rocks. These are referred to as the Mt Dijou Volcanics and are an enigmatic group generally considered to be Ordovician in age.

Major crustal extension in the latest Silurian to Early Devonian in the Cobar region led to the formation of a number of shallow water shelf areas. The shallow marine Kopyje Group is one shelf sequence, which developed on, and adjacent to, the Girilambone Group, and borders the deeper water Cobar basin (Byrnes, 1993). Recent work by the Department of Mineral Resources has shown that the Kopyje Group covers an extensive part of the western side of the Byrock sheet. This is indicated in the “overburden filtered” magnetic imagery for the study area (Hicks and Fleming, 2004) and has been confirmed by drilling in this project.

The Bourke 1:250 000 geological map shows extensive areas of Girilambone Group in the Byrock area. Detailed petrographic descriptions of “core stick” samples collected during drilling, together with field investigations, however, have led to the realisation that large areas of the Byrock sheet, especially in the south, are Siluro-Devonian in age. These Siluro-Devonian units form distinctly magnetic, north trending “fingers” of imbricate thrust faulted sedimentary rocks which are clearly visible in the “overburden filtered” 1VD (first vertical derivative) airbourne magnetic data (Hicks and Fleming, 2004).

Very highly strained polymictic conglomerates, which crop out in distinct north trending ridges across the Sussex and southern portion of the Byrock sheet areas, show evidence of

a Siluro-Devonian age. These conglomerates are currently mapped as Ordovician, however particular pebble lithologies, including radiolarian cherts, crenulated phyllites and siltstones, together with the presence of volcanic quartz within both the matrix and some sandstone pebbles, all support a much younger age. Petrographic evidence from pebbles collected from conglomerates at Mount Boppy and Tara suggests a provenance of both Girilambone Beds (θg) and Siluro-Devonian formations (L Barron, *pers. comm*., 2004). Pebble lithologies and the presence of volcanic quartz in the matrix suggest a comparison with the less strained Siluro-Devonian Cobar Supergroup conglomerates.

A number of granite intrusions occur within the Byrock and Glenariff map sheet areas. These are mostly SiO_2 rich, compositionally evolved and I-type in character (Blevin and Jones, 2004). They include the weakly magnetic to non-magnetic biotite dominant Byrock Granite and the weakly magnetic pink feldspar Glenariff Granite. The Glenariff Granite is distinct from the others in having salmon-pink alkali feldspar and abundant miarolitic cavities. It also has associated microgranite zones and pegmatitic phases. The highly evolved, texturally diverse and high silica Midway Granite occurs to the north of the Byrock 1:100 000 sheet area, and the Gongolgon Granite occurs to the north of the Glenariff 1:100 000 sheet area. The Midway Granite is extremely fractionated and is associated with tin and copper mineralisation at Doradilla. The granites are generally poorly exposed. The Byrock Granite is well exposed over a small area at the Byrock Rock Holes.

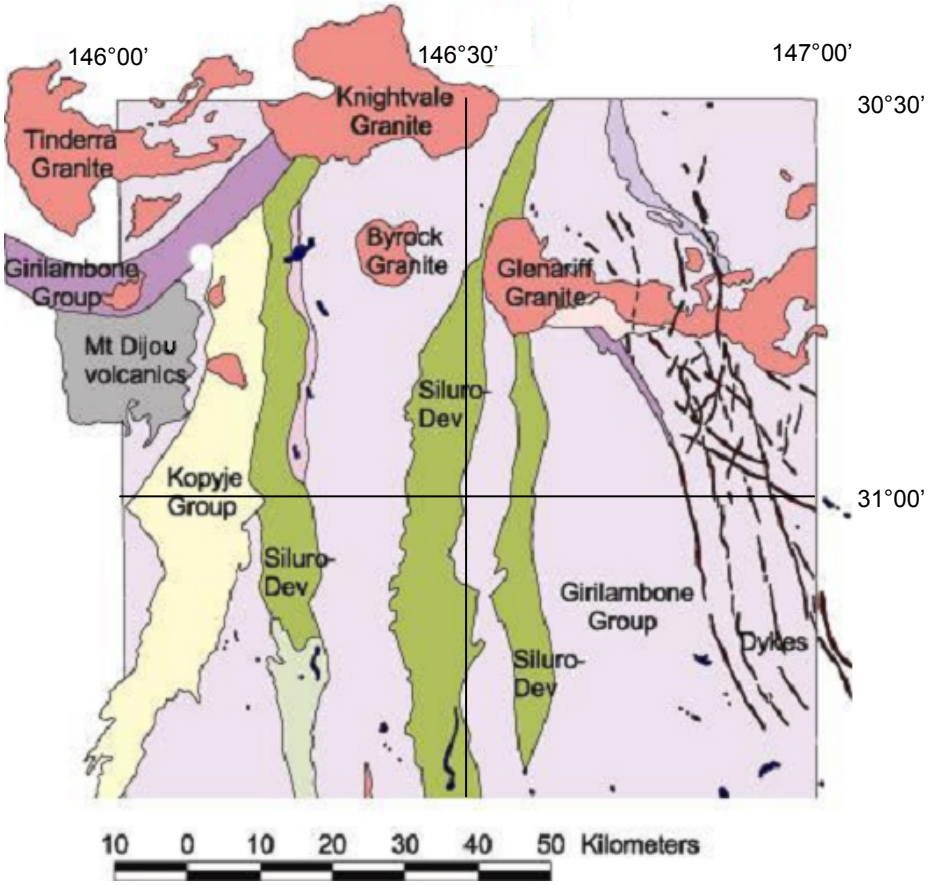

Figure 3: Bedrock geological interpretation by NSW DMR of Byrock and Glenariff 1:100 000 map sheet areas in the north, and part of the Sussex and Coolabah 1:100 000 sheet areas to the south. Darker mauve colours are more mafic parts of the Girilambone Group. Green colours are Siluro-Devonian metasedimentary rocks, possibly equivalent to the Cobar Supergroup.

2.3 Economic Geology and Mineralisation

The Byrock area straddles a major northeast-trending boundary between two distinct geological and metallogenic provinces (see Section 2.2). South of the boundary, on the southern portion of the Byrock 1:100 000 sheet, major structural trends are northerly, and the rock associations are similar to those typical of the Girilambone terrain. To the north there is a pronounced northeast-trending structural grain and a granitoid suite chemically distinct from the granitoids in the Lachlan Fold Belt to the south (Blevin and Jones, 2004). Known areas of significant mineralisation in this region include the Mount Dijou – Bald Hills area near the southwestern boundary of the Byrock 1:100 000 sheet and the Doradilla area, north of Byrock (Figure 2).

2.3.1 Mount Dijou – Bald Hills

Small deposits of Au-Ag±Cu mineralisation have been worked at Mount Dijou and Bald Hills (Figure 2). The area was prospected from the 1890's until the early 1900's, with the main workings centred on the better-exposed, topographically higher areas at Mount Dijou and Bald Hills. More recent exploration of this area was conducted in the 1970's and 1980's (Byrnes, 1993). At Mount Dijou the host rocks are deformed mafic volcanic rocks, including pillow lavas (Mount Dijou Volcanics), and adjacent metasedimentary rocks. At Bald Hills to the southeast host rocks include mafic schists, quartzites, cherts and deformed pelitic rocks. The age of the Mount Dijou Volcanics is uncertain although they have been correlated with the Girilambone Group and considered to be of Ordovician age (Byrnes, 1993). Other workers have suggested that they may be correlated with andesitic rocks near Louth considered to be of possible Devonian age (Scheibner, 1987).

Mineralisation at Mount Dijou and Bald Hills appears to be structurally controlled occurring in fault breccias and quartz veins and lodes with associated silicification. Lodes are reported to be up to 300 m long and 5 m wide. Byrnes (1993) noted that there is "perhaps a tendency for lodes to be situated close to the boundaries between basalt and sediments, especially at Mount Dijou". Sulfide minerals recorded are pyrite, pyrrhotite, sphalerite, galena, chalcopyrite and marcasite (McClatchie, 1970). Magnetite and sulfides (mainly pyrite) occur as disseminations, stringers and bands in the mafic volcanic rocks and interpillow material. Early descriptions of the deposits (*cf.* Thomson, 1949; Braithwaite, 1974) refer to mineralisation occurring in vughy horizons or jasper-ironstone lodes, probably reflecting near surface oxidised portions of the mineralisation.

The major workings in the Bald Hills area occur at the Perseverance mine (also known as the Rocky Ned and Lucky Ned mine). Here there are several shafts, pits and surface stopes developed along a northerly trending structure. The orebodies were 0.6-1.8 m wide with grades up to 15-17 g/t Au, and 4-7 g/t Au in the wallrocks (Byrnes, 1993), but the mineralisation appears to have been discontinuous and average grades were probably much lower. The lodes were quartz-veined and quartz-filled breccias developed in sheared pelitic and mafic schists. Similarities have been drawn between the style of mineralisation at Mount Dijou – Bald Hills and the vein gold deposits in the Forbes – Parkes – Peak Hill – Tomingley gold belt and also ophiolite-hosted mineralisation, such as that at Miners Beach near Port Macquarie (Byrnes, 1993). Previous workers have suggested that the deposits formed as epigenetic mineralisation related to underlying granitic rocks or by hydrothermal remobilisation of gold from the host mafic volcanics. However, the deposits are too poorly understood at this stage to ascribe a definite genesis.

Maximum assay values recorded for the Mt Dijou – Bald Hills area are 92 g/t Au, 8.4 g/t Ag, 0.19% Cu, 150 ppm Pb, 775 ppm Zn, 1% Bi, 9% As and 6.7 ppm Hg (Byrnes, 1993). These grades are probably from gossanous material that has been supergene enriched. The known gold production from the Mount Dijou – Bald Hills deposits is small (total <1 kg), the main producers being the Mount Dijou Mine (249 g) and the Perseverence (Rocky Ned or Lucky Ned) mine (280 g; Byrnes, 1993).

2.3.2 Doradilla

Doradilla is the largest known metalliferous occurrence in the Byrock area (Figure 2) and, more regionally, on the Bourke 1:250 000 sheet. Copper mining commenced at Doradilla in the early 1900's and in the period 1900-1920 about 20 tonnes of Cu were produced (Byrnes, 1993). More recent exploration has demonstrated the presence of significant tin reserves. Much of the tin is apparently present in fine-grained malayaite, rendering metallurgical treatment difficult and costly.

Mineralisation in the Doradilla area is mainly developed along a narrow northeast-trending calc-silicate zone that extends for over 16 km through the Doradilla, Midway, Midway East and 3Kel prospects (Metals Exploration Pty Ltd., 1981). There are also some smaller, separate areas of mineralised calc-silicate rocks (*e.g.* at Bob's Tank). The calc-silicate zone appears to overly a major, possibly poly-phase, granite pluton. A small body of leuco-adamellite crops out at the Midway prospect and at the Doradilla prospect there is a high-level porphyry dyke complex. Foliated to massive biotite-hornblende granite and granodiorite have been intersected in drilling WSW of the old Doradilla copper mine. The host sequence to the skarn style mineralisation contained calcareous rocks, probably including original limestone, dolomite and calcareous shales. Ultramafic rocks are also present on both sides of the calc-silicate zone. This calcareous sequence has been considered part of the Girilambone Group, better known and exposed to the south (but deficient in limestones), or alternatively part of a Devonian sequence, similar to limestones of the Kopyje Group in the Cobar Basin. However without better control on the bedrock stratigraphy or dating of the calcareous rocks, correlation with other known sequences remains speculative.

The mineralised calc-silicate zone at Doradilla appears to be an extensive and zoned skarn system with well developed prograde and retrograde skarn assemblages (Byrnes, 1993). There are a number of styles of mineralisation including: tin silicate mineralisation in calc-silicate rocks, with tin mainly in malayaite; sulfide-bearing zones in calc-silicate, with both stannite and cassiterite; oxide zone secondary tin concentrations; as well as cassiterite in porphyry dykes and mineralisation associated with breccia zones and within granite. Quartz-tourmaline veining is associated with quartz-feldspar porphyry dykes and these rocks are also cut by veins of microgranite, greisen and quartz-fluorite. Base metals are also present in the system, with thin bands of sulfides containing up to 3% Cu and wider zones with up to 2% Pb and 5.1% Zn (Byrnes, 1993). Ore minerals recorded include, malayaite, cassiterite, stannite, wolframite, scheelite, molybdenite, bismuthinite, bismuth, chalcopyrite, bornite, sphalerite, galena, pyrrhotite, pyrite, arsenopyrite and magnetite.

2.3.3 Mineral occurrences in the Byrock-Glenariff sheet areas

There are very few recorded mineral occurrences on the Byrock and Glenariff 1:100 000 sheet areas. This probably reflects, in large part, the very extensive cover of transported regolith and poor exposure of strongly weathered bedrock in erosional areas. Mineral

occurrences and prospects are described from the Byrock and Glenariff 1:100 000 sheet areas in the metallogenic notes for the Bourke 1:250,000 sheet (Byrnes, 1993). These include the following types.

2.3.3.1 Granite-related mineralisation

Highly fractionated granites occur across the northern half of the Byrock-Glenariff region. These are likely to be the source of heat systems for the polymetallic tin-tungsten and base metal mineralisation. Known examples of this style of mineralisation are concentrated in the east-northeast trending Galambo-Mount Kelly magnetic zone, which passes through the northwestern portion of the Byrock sheet (Byrnes, 1993).

Recorded deposits (with Bourke metallogenic map number) include:

- Mulga Tank (37):
  An area of old workings with disseminated pyrite-pyrrhotite and minor Cu (Pb, Zn) mineralisation and reported possible Sn and W. This area contains intensely quartz-veined chloritic siltstones and is on the margin of the Galambo Granitic Complex.
- Knightvale prospect (38):
  An area of ironstone float close to granite. The ironstone float contains anomalous Cu, Pb, Zn, As and W. Drilled granodiorite contains disseminated pyrite and rare chalcopyrite.

2.3.3.2 Mafic-andesite volcanic-associated gold deposits

These deposits occur in the Mt Dijou-Bald Hills area on the extreme southwestern edge of the Byrock sheet and onto the Gunderbooka sheet (see above). The aircore drilling traverse has indicated the Bald Hills sequence and mineralisation extends further to the south and southeast than the area of known outcrop. Drill holes CBAC198-204 have intersected anomalous gold values, in some cases with associated copper. Some of these holes have intersected thin mafic units, possibly dykes (see Sections 4.4.3.2 and 4.5.1). There is thin cover in this area, but the surface is littered with highly ferruginous quartz and "ironstone" float and lag. Some of the latter consists of specular hematite with magnetite, of interest given the description of magnetite-bearing jasper with some of the known Bald Hills - Mt Dijou mineralisation. A bulk sample of this specular ironstone collected near drill hole CBAC201 was found to contain 0.04 ppm Au, 124 ppm Cu, 15 ppm As, 61 ppm Pb and 95 ppm Zn. A bulk sample of ferruginous quartz lag in the same area contained 0.04 ppm Au, 36 ppm Cu, 36 ppm As, 1 ppm Pb and 46 ppm Zn. Several samples of calcrete collected from exposures and borrow pits along the road in this area (between CBAC194 and 209) contain elevated levels of Au (14-18 ppb).

Recorded deposits on the Byrock sheet (with Bourke metallogenic map number) include:

- Perseverance (56):
  Extensive workings along a north-trending, near vertical, cleavage-parallel shear zone (recorded production 280 g Au);
- Turner prospect (57):
  Shallow workings developed along two north- trending and steep west-dipping, parallel quartz vein systems and associated stringers;
- Wilson mine (58):
  Shallow pits on a north-trending zone of mineralisation;
- Kennedy mine (59):
  Workings along 35 m of a narrow north-trending zone with siliceous fault breccias;
- Mulvays Last Try (60):
  Workings along a very narrow, north-trending and steep west-dipping quartz vein.

2.3.3.3 Mafic-ultramafic intrusive related mineralisation

Enigmatic, low grade Cu-Pb-Zn mineralisation is recorded from the Wilga Downs – Anomaly 5A area, 10 km north of Bald Hills (Byrnes, 1993). This includes disseminated mineralisation in schists and deformed "mafic volcanics". Pyroxenites and amphibolites are also reported from this area and these various mafic rocks may be related to the Mt Dijou – Bald Hills sequence. The possible presence of intrusive mafic-ultramafic rocks (including serpentitites) is interesting given the indications of widespread mafic dykes in the recent aircore drilling program.

Recorded deposits (with Bourke metallogenic map number) include:

- A5 Prospect (36):
  Small equant aeromagnetic anomaly consisting of pyroxenite-peridotite, with minor Cu sulfides in surrounding quartz-chlorite schists;
- White Tank Prospect (54):
  Disseminated Cu-Pb-Zn sulfides in schists and phyllites along an EW-trending magnetic zone about 800 m long;
- Wilga Downs Prospect (55):
  Stringers and patches of Pb-Zn-Cu sulfides in sheared metavolcanics within metasediments.

2.3.3.4 Shear-hosted and vein-style gold mineralisation

To the northeast of Byrock (between Byrock and Gongolgon) there are areas of quartz veining with anomalous gold (Capnerhurst, 2003). This includes the area around Wyuna Downs and Lord Carrington Hill. Byrnes (1993) mentions that old gold workings southeast of Congolgon are apparently on a quartz vein swarm.

A prominent magnetic high centred on Lord Carrington Hill has significant ferruginous quartz float in an area of chloritic schists, where it crosses the Byrock- Gongolgon road. Drilling at this site (drill hole CBAC238) intersected weathered magnetite-bearing schists with abundant illite and zones of apatite. Sections of this hole contained elevated Au, including 6 m of 0.03-0.15 g/t (see Section 4.5.2).

In the area around Belah Tank, 23 km south of Byrock, sampling of an extensive zone of gossanous float reveals anomalous Cu, Pb and Zn (including up to 0.13% Cu). At the southern end of this trend, near Rosies Tank, samples of gossanous quartz contain up to 0.18 g/t Au (Capnerhurst, 2003). The geology of this area is not well known but it appears to be within Girilambone Group rocks and the gold mineralisation is probably of vein style.

Major east-northeast trending structures near the major terrane boundary across the Byrock sheet may have potential for shear hosted mineralisation. A borrow pit on the north side of the Cobar-Byrock road (near drill hole CBAC229) exposes strongly sheared metasediments with included pods of felsic granite and aplite. A calcrete sample from this site contains 9 ppb Au (significantly above the regional threshold of 3 ppb).

Some recent unpublished company drilling on Kenilworth Station near the Three Sisters, possibly directed at magnetic targets, has intersected highly chloritic zones along the margins of quartzite units. The precise nature of any mineralisation associated with these zones is not known.

2.3.3.5 The Byrock Leucitite

Leucite, with similar properties to basalt, is quarried at Bye Trig for blue metal aggregate. The occurrence consists of an eruptive vent with a surrounding lava mound. It has been radiometrically dated at 16.8±0.2 Ma (Sutherland, 1985). There has been some diamond exploration centred west of Byrock around the leucitite occurrence (CRA Exploration Pty Ltd., 1982) but the single micro-diamond reported in the area is regarded as contamination (M. Rangott, pers. comm., 2004).

2.4 Economic Potential

The greatest potential for metalliferous mineralisation in the Byrock-Glenariff area appears to be for shear-hosted gold mineralisation and granitoid-related systems, including skarns. Strata-bound metasediment-hosted copper mineralisation (Girilambone-style) may extend into covered areas in the southern part of the region (south of the major terrane boundary). This project has indicated the presence of abundant mafic rocks (mainly as dykes) concealed in the deeply weathered terrain. These may have associated gold mineralisation (Sections 4.4.3.2 and 4.5.1).

3 METHODS

3.1 Mapping

Regolith-landforms were mapped over the Byrock 1:100 000 sheet (Plate 1) by P. Buckley (CRC LEME / NSW DMR). Photo interpretation, together with the use of Discovery 2000 airborne geophysical data and Landsat data, and field inspection were the basis of this mapping. Details of the methodology are reported in Fleming and Hicks (2003). Seventeen regolith-landform units are depicted on the Byrock 1:100 000 scale regolith-landform map (Plate 1) and overlaid on airborne geophysics images (Plates 2 and 3). These units portray the dominant associations between surficial regolith types and associated landforms types. For example, CHep refers to sheetwash colluvium (regolith type in capital letters) on erosional plains (landform type in lower case letters). Where there is more than one unit with the same broad association but with minor significant variations, a numeric subscript is used, for example, Aas1 (see Pain *et al*., 2002, for more details). An underlying principle in this mapping methodology is that the same geomorphic processes that operate on the formation of surficial regolith materials also operate on their associated landforms. Landforms can thus be mapped as a surrogate for mapping surficial regolith materials.

3.2 Soil analysis

A range of particle size, mineralogical, geochemical, and micromorphological techniques were used to investigate the characteristics of soils from the Byrock area.

3.2.1 Particle size analysis (PSA)

For the purposes of this research, when characterising the particle size distribution (PSD) of soils, it is necessary that there should be minimum disturbance of the samples. In order to do this, Mason *et al.* (2003) recommend that samples should not be pre-treated. Their studies revealed that particularly in Australian aeolian materials, disaggregation methods

result in the dominance of finer materials than those that occur without pre-treatments. Therefore, it was decided in this study that no chemical or physical pre-treatment or disaggregation methods should be applied to the soil samples prior to PSA.

The PSD of selected soil samples, with no chemical or mechanical pre-treatments, were determined using the laser detection technique on the Malvern Mastersizer 2000. Each sample was briefly dispersed in water and analysed: 30 seconds, break 10 seconds, and then repeated three times. The average calculation(s) within the 0.2µm to 2000µm detection limits were collected from the Malvern built-in software, and for all data points 2µm<1000µm data was interpolated at 2µm intervals. The weighted frequency (dV/d logD) was calculated for all data points, weighting the data according to the width of the interval or particle diameter and plotted on a log scale (Bagnold, 1960).

NB: Caution needs to be taken concerning the bias effects of the laser detection technique (of the Malvern Mastersizer 2000), particularly when the sample is dominated by both sand and silt fractions. In such a case, the clay fraction may be underestimated (Campbell, 2003).

3.2.2 Mineralogy and geochemistry

The mineralogy of selected soils and soil fractions were determined by powder X-ray diffractometry with a Siemens Diffractometer D501 equipped with graphite monochromator and scintillation detector. CuK-alpha radiation was used, with scans carried out from 2θ (2-70°), with a step width of 0.02°, and a scan speed of 1° per minute. Scans were interpreted with SIEMENS computer software package Diffrac*plus* Eva (1996-2001) and Siroquant 2.5 (2000).

Major elemental compositions of selected soil and soil sample fractions were determined by standard XRF methods. ICP-MS was used to determine trace elements after complete dissolution with HF/H/NO_3/$HClO_4$/HCl following Li-tetraborate fusion.

3.2.3 Micromorphological analysis

3.2.3.1 Scanning Electron Microscopy (SEM)

Undisturbed soil samples were coated 3 times with Au using a "Sputter Coater" to improve sample conductivity and eliminate possibilities of organic material collapsing. Analysis was performed on the Cambridge 360 and JEOL JSM6400.

3.2.3.2 Thin Section observations

Surface samples (0-0.1m) were dried in the Kubinia tins at 40°C and then impregnated with polyester resin for 6 weeks. Thin sections, vertical to the soil surface, were cut, polished, mounted on a glass slide, and reduced to 25µm thickness. The optical properties of the specimen were viewed using a petrographic microscope and photographed.

3.2.4 Soil sampling sites

A detailed study was made of the characteristics of regolith materials found at selected study sites. The sites were chosen to:

- include a range of transported and *in situ* materials reworked to different extents, and
- highlight areas where there was a marked contrast in the nature of the transported material compared with the underlying substrate.

The selected study sites are within two domains:

3.2.4.1 Leucitite lava outcrops in the Girilambone Region

Three leucitite lava outcrops (named El Capitan Knob, Mountain Tank, and Byrock Hill) were chosen to represent "natural dust traps" (NDT). These young Tertiary basaltic outcrops were formed by lava flow inflation and have been positive landscape features since the Miocene (Gonzalez, 2001 and K. McQueen, pers. comm., 2003). They are lithologically distinct from the surrounding bedrock and any aeolian transported material. Only skeletal soils, to a maximum depth of approximately 0.1m, exist on the leucitite basalts. Sampling sites were chosen towards the top of these topographic highs to avoid any alluvial or colluvial contamination, thus leaving the only options available for the derivation of the soils to be residual or aeolian (Tate *et al.*, 2003).

3.2.4.2 Girilambone Region Profiles.

Sampling sites throughout the Girilambone Region were chosen to examine trends across various mapped regolith landform units. Four different regolith landform units were chosen and the drill hole numbers for each of the sites are as follows:

- Colluvial sheetwash depositional plain: CBAC217;
- Alluvial plain: CBAC243;
- Colluvial rise: CBAC248;
- Alluvial channel: CBAC219.

3.3 Drilling/Logging/Profiling

A total of 60 holes (2713 m) were drilled along roads in the Byrock study area, using a small 6-wheel air core rig supplied by Geological Ore Search, Cobar. The drilling was conducted at approximately 1-2 km spacing, with holes varying between 6 m and 72 m deep. To avoid cross-hole contamination, a hole was drilled to 2 m at each new site to purge the vacuum system before moving a few metres away and restarting the drilling. The air core drill holes are designated by the prefix CBAC (Cobar air core).

Chip tray samples were collected at 1 m intervals for the first 9 m, and then either continued at 1 m intervals (20 drill holes) or changed to 2 m intervals (40 drill holes) thereafter. Samples were also collected for palynological examination where appropriate, with a total of 26 samples being analysed.

Bags of samples collected for geochemical analysis (approximately 4 kg) were taken at 1 m intervals for the first 9 m, and then composite samples were collected to the bottom of the hole. Composite samples were collected by taking a sample from each interval and then bulking these together. Following geochemical analysis of the initial samples, intervals with interesting results were re-sampled at 1 m intervals for additional geochemical analysis.

A standard set of drill log sheets combining requirements for both CRC LEME and NSW Department of Mineral Resources were used for field logging (see Chan *et al.*, 2003a). The field logging was done by A. Senior (CRC LEME/ANU). The water table level was noted in the field at the time of drilling. The 60 field logs are reproduced in the NSW DMR Byrock Report (GS2003/048).

Upon return from the field, samples from all 60 drill holes were logged in more detail and profiled along traverse section lines (Plate 4). The detailed logging was done using a binocular microscope, hand texturing, a pencil magnet, acid attack and a Portable Infrared Mineral Analyser (PIMA). Characteristics noted included Munsell colour, major minerals, clast and bedrock lithologies, texture, fabric, grain size and roundness, induration, attraction to pencil magnet, and affect of acid attack. The carbonate content was tested for each hole using concentrated HCl. Results were recorded as "M" for a major reaction, and "m" for a minor reaction, with samples containing no carbonate left blank (Appendix 1).

Through detailed binocular microscopic petrography and textural analyses, with some specific validation from geochemistry, all saprolith lithologies were nominally identified, and a variety of weathering overprints (*e.g*. pink saprolite, pallid saprolite, and induration) and degree of weathering (saprolite versus saprock) were ascertained. Saprolite, being moderately to completely weathered bedrock, ranges from clay and/or individual mineral grains to chips with some fabric. Saprock, being slightly weathered bedrock, appears as competent, often greyish coloured, rock chips.

Topographic profiles along traverses in direct line between drill holes were derived from digital elevation data (DEM) from the NSW DMR Discovery 2000 Initiative and were constructed to scale, incorporating drill hole locations, by P. Milligan (GA) using Research Systems IDL (Interactive Data Language) software. The profile was adjusted using photo interpretation on either side of CBAC247 where a major discrepancy in elevation data occurred between the differential GPS reading at CBAC247 and the DEM. The topographic profiles were drawn to a standard scale with vertical exaggeration of 50 (horizontal scale of 1:50 000 and vertical scale of 1:1 000). Elevation is displayed as metres above sea level (m a.s.l.; see Plate 4 and Appendix 8).

Following the detailed laboratory logging and PIMA analysis (Appendix 2 and Section 3.4) of the 60 holes, regolith profile units were determined for all drill holes based upon the dominant regolith materials (*e.g.* clay, silt, sand, gravel, saprolith chips, and mineral grains). Comparison between adjacent holes was used to construct the 2.5D-regolith architecture (Plate 4), to help interpret the evolution of the landscape in the Byrock area.

3.4 PIMA analysis

A Portable Infrared Mineral Analyser (PIMA) was used to analyse all the samples (1916 samples) from the 60 holes from the Byrock area. The use of the PIMA is important to confirm the depth of the unconformity (transported sediments *vs*. *in situ* boundary; Appendix 3) and to identify parent bedrock lithology.

The PIMA is an instrument that records the 1300-2500 nm Short Wavelength Infrared (SWIR) reflectance spectrum of samples. In this spectral region discrete wavelengths of light are absorbed due to the bending and stretching of molecular bonds. The types of mineral groups which display absorption features within the PIMA range include phyllosilicates, hydroxylated silicates, carbonates, sulfates and ammonium-bearing minerals, plus Al-OH, Fe-OH, Mg-OH. Absorption features at the same wavelength may overlap, *i.e*. kandite minerals (kaolinite, dickite and nacrite), all of which have very similar Al-OH features which may sometimes be difficult to distinguish.

A number of algorithms, such as absorption feature depths or wavelengths within a certain range, may be created to extract information from a spectrum. The algorithms used for this study include:

- Depth of the water peak (1880-1960 nm);
- Depth of the Al-OH peak (2180-2230 nm);
- Wavelength of the Al-OH peak (2180-2230 nm);
- Depth of the Fe-OH peak (2240 – 2280 nm & 2235-2245 nm);
- Kaolinite Disorder (Crystallinity) using the KX index [2180 slope - (2160 slope-2180 slope)].

The PIMA II spectrometer was used for all analyses. The Spectral Geologist (TSG), Version 2 software (AusPec International Pty. Ltd), has been used in the presentation and interpretation of the PIMA data for this report. The TSG provides graphical interpretation by applying a series of algorithms to the spectra. In these samples, five algorithms have been used to display down-hole changes in the regolith profile. TSG scale has been applied to the algorithms to provide lateral correlation between holes. For this report, PIMA data is provided as pdf files of stacked spectra and graphical interpretation logs (Appendix 2).

Refer to Chan *et al.* (2003a) for further details of the PIMA methodology.

3.5 Geochemistry

Bulk samples collected by aircore drilling were prepared and chemically analysed by ALS-Chemex in their Orange and Brisbane laboratories. Samples were analysed for Au (by *aqua-regia* digest, solvent extraction and graphite furnace AAS analysis: method Au-GF42) and 28 other elements using a combination of ICP OES and ICP MS techniques following a multi acid digest (HF-HNO_3HClO_4 digestion, HCl leach: method: ME – ICP61). This method of analysis provides a good first pass indication of element abundances, particularly for most (but not all) elements of direct interest as commodities or pathfinders. It should be remembered that it is not a "total" analysis technique for a number of elements. All geochemical analyses are listed in Appendix 4.

A small number of calcrete samples were collected from borrow pits and other available exposures in the Byrock region. These samples were submitted to AMDEL laboratories in Adelaide for pulverisation and analysis for gold (analysis by graphite furnace AAS following aqua regia digestion and solvent extraction: method AA9) and a suite of other elements (HF-HNO_3HClO_4 digestion, HCl leach: method A9612-12 amended) using a combination of ICP OES and ICP MS analytical techniques. Calcrete analyses are listed in Appendix 5.

3.6 Databases

The location data for the 60 drill holes, as well as specific geochemical data (XRF analyses of bottom of the holes samples) and palynological sample data were entered into the Geoscience Australia's (GA) corporate Oracle database, DEVIANT. (Refer to Appendix 3 for GA's site IDs, and Appendix 6 for end of hole depths for the 60 drill holes.) Processing aspects of the palynology data were also entered into GA's corporate Oracle database, PALSED. The regolith-landform unit symbols (Appendix 3) and descriptions (Plate 1)

were entered into GA's corporate Oracle regolith units database, RTMAP. NSW DMR has entered site data into their corporate SITES database, petrological data into ROCKS, and drill hole location data into INTERSECT.

4 RESULTS AND DISCUSSION

4.1 Regolith-Landform mapping

Most of the Byrock area is covered by transported regolith, which is comprised of alluvial and colluvial sediments with minor paludal (swamp) and aeolian source bordering dunes (ISub - in the far northwest corner of map sheet). However, analysis of drill hole materials (see Section 4.3) and detailed soil analyses (see Section 4.2) indicate that aeolian silt-size quartz grains with clay coatings have impregnated the upper regolith layer within most regolith-landforms across the area. Areas of saprolith occur as islands of *in situ* regolith surrounded by rises covered by colluvial sheetwash deposits (CHer) and erosional plains (CHep) in the south, and depositional sheetwash plains (CHpd) and alluvial plains towards the north. Networks of ephemeral drainage lines with headwater erosion gullies (Aed) and downstream alluvial plains (Aap) dissect the saprolith rises covered by sheetwash deposits. Most of the saprolith occurs as highly weathered bedrock (saprolite) rises (SHer), with a linear north trending spine of slightly weathered bedrock (saprock) rises (SSer) and a local hill (SSeh - Coronga Peak) in the central south of the Byrock sheet. Slightly to moderately weathered leucitite lava mounds (VFvp) occur as volcanic plateaus to the southwest of Byrock village, with a chain of north trending swamps (Paw) to the south which result from north flowing drainage being impeded by the lava mound. An alluvial terrace (Aat) and an alluvial fan (Afa) occur on the southern edge of the Byrock map sheet along the boundary with the Sussex 1:100 000 map sheet. Alluvial flood plains (Aaf) with channels (ACar) occur along Tindarey and Mulga Creeks, with Tindarey Creek fanning out into a distributary system at its termination in the northwest of the map area. Stagnant alluvial plains (Aas) adjacent in the south to the two main creeks broaden out into vast plains to the northwest towards the Darling River. Chains of closed stagnant alluvial depressions (Aas1) within the stagnant alluvial plains are indications of formerly active channels associated with prior drainage.

Chains of alluvial depressions to the east and south of the volcanic plateaus indicate migration of Mulga Creek to the east to its present position just west of Byrock village. The northwest trend of the chain of depressions in the northwest of the map area indicate the prior northwest extension of Mulga Creek, which has since diverted to the north on the western edge of an island of saprolite. A long northwest-trending linear depression to the northeast of this northerly island of saprolite may indicate an even earlier drainage line prior to Mulga Creek flowing to the northwest and eroding through the saprolite island. P. Buckley noted a correlation between the northeast trend of some of these prior drainage lines and northeast striking sub-vertical strike-slip faults (Fleming and Hicks, 2003). Two of these northeast trending faults align with either side of the island of saprolite in the north of the map area that Mulga Creek presently bisects.

The airborne gamma spectroradiometric imagery ("radiometrics"), flown as part of the Exploration NSW Initiative (Figure 4), provides additional information on the mapped regolith-landforms (Plate 2). The patchy white, pink and yellow areas indicate that much of the rises covered by sheetwash deposits, and to a lesser extent the erosion plains covered by sheetwash deposits, have a relatively thin and discontinuous colluvial sheetwash cover.

The depositional plains formed of sheetwash deposits, on the other hand, have a darker and, in places, greener signature which is indicative of a thicker colluvial sheetwash cover. The dark radiometric response relates also to the stagnant alluvial plains with implied thick cover. The teal green radiometric signature, which relates to ferruginous magnetic lag, occurs on depositional plains formed of sheetwash deposits, erosional plains covered by sheetwash deposits, and to a lesser extent on rises covered by sheetwash deposits. This lag may be concentrated due to winnowing of the fine material from the sheetwash. This same teal signature on highly weathered bedrock rises may indicate ferruginous mottled saprolite and scattered ferruginous magnetic lag. The variable radiometric response in saprolith dominant regolith-landforms is associated with variation in parent lithology of outcrop and subcrop: red (relatively high potassium, *e.g.* a component of Mount Dijou Volcanics), white (high in all channels - potassium, thorium and uranium, *e.g.* leucitite lava, and black (low in all channels, *e.g.* quartzite of Caronga Peak).

It is important to note that the regolith materials and landform type at a particular site (*e.g.* a drill hole, see Appendix 3) in a given regolith-landform unit polygon may not always be the same, as the site may be a sub-dominant element of the polygon at the scale of mapping. This is evident for a few of the 60 aircore drill holes in the Byrock area. More detailed regolith-landform units were used over part of the area where available (Glanville, 2004).

The high frequency component of airborne magnetic data (first vertical derivative) acquired as part of the Exploration NSW initiative (Figure 5) reveals broad dendritic drainage systems. These palaeodrainage systems contain magnetic sediments that are mostly buried under stagnant alluvial plains and adjacent low relief depositional plains (Plate 3). Some of these magnetic sediments are exposed on erosional plains and in some headward valleys, as indicated by the teal green radiometric signature (Figure 4).

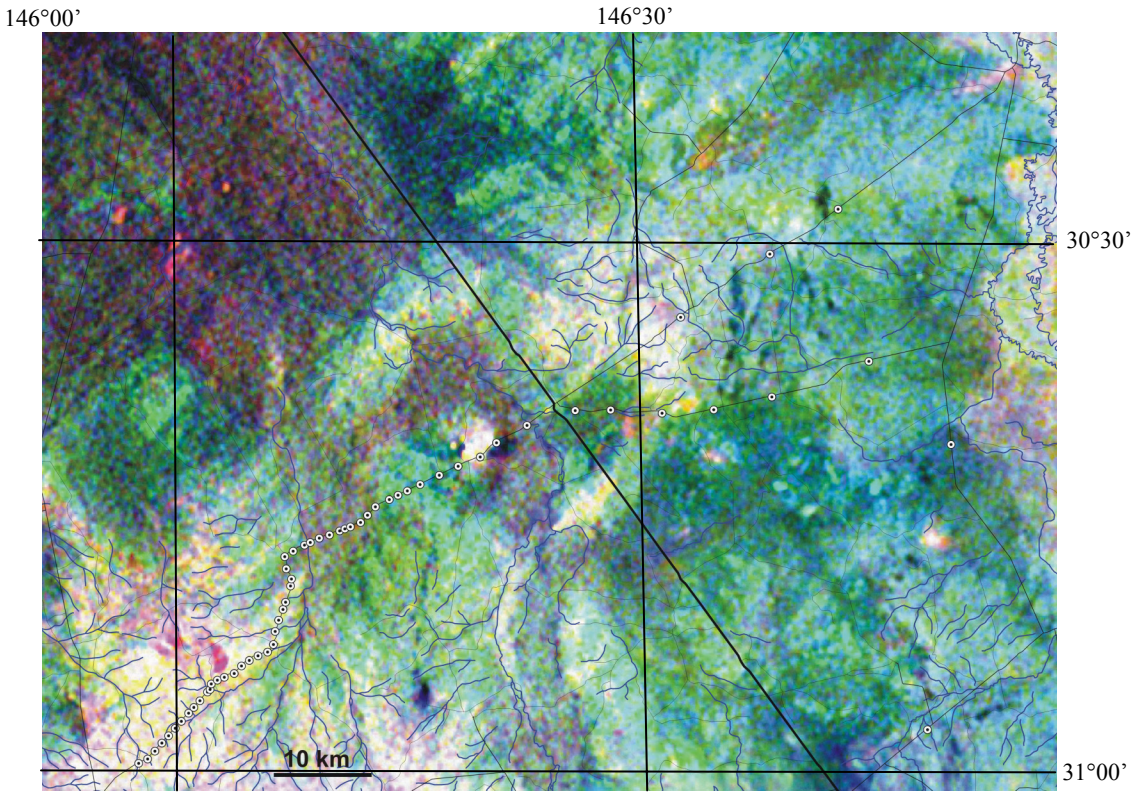

Figure 4. Ternary airborne radiometric image (Exploration NSW Initiative) of the Byrock –Glenariff area with present drainage, roads and CBAC drill holes. White – high in all channels (K, Th U), Green – relatively high in Th, Red – relatively high in K, Black – low in all channels.

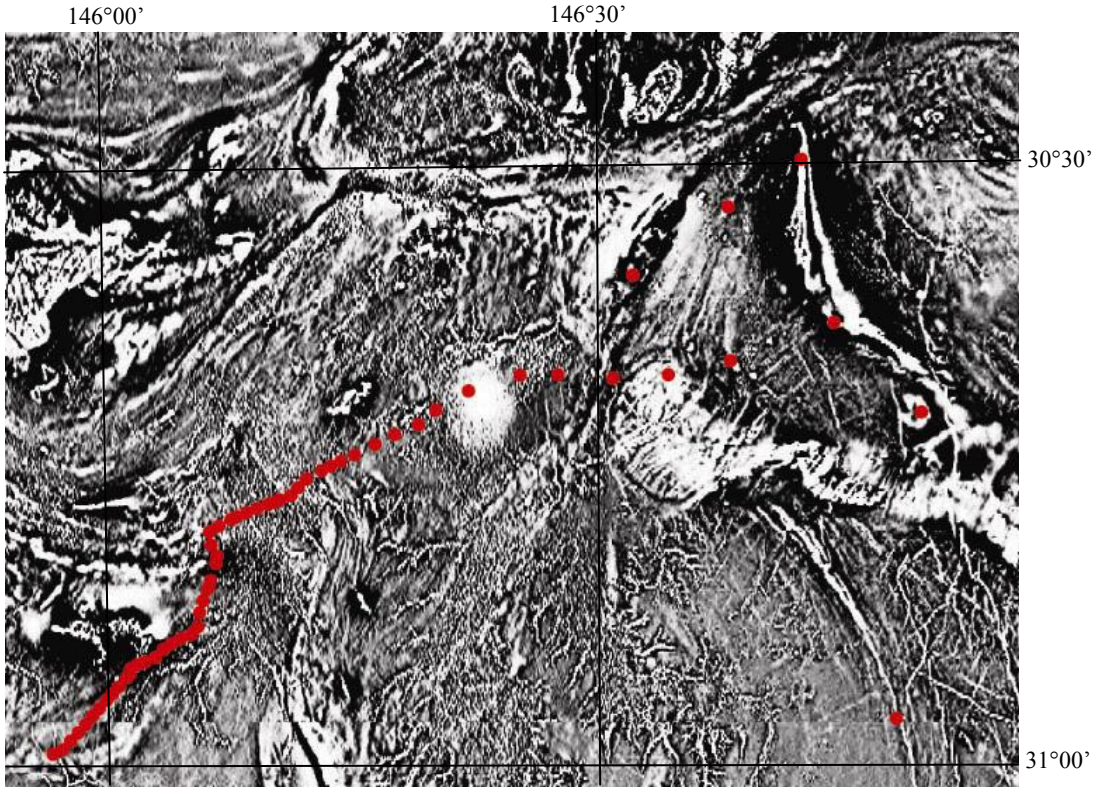

Figure 5. First vertical derivative airborne magnetic image (Exploration NSW Initiative).

4.2 Aeolian Material

Analysis of the soils in the Byrock region confirmed the presence of a significant aeolian component (Tate *et al.*, 2003). This was clearly demonstrated for soils on the elevated leucitite ridges which represent natural dust traps (NDT). The particle size distributions (PSD) of all NDT soils display a distinct tri-modal pattern with a dominant size fraction peak at 70 µm (Figure 6). Determination of major mineral composition by XRD analysis of bulk soil samples (Figure 7) and investigations of micromorphological characteristics using SEM and thin section microscopy (Figure 8 and Figure 9 respectively) revealed that the underlying leucitites contain no quartz, but the NDT soils contain both aeolian quartz and mafic-derived clays, some of which coat the quartz grains. The geochemical and major mineral compositions of the NDT soils show that they are quite dissimilar to the underlying leucitite (Table 1 and Figure 7). These soils contain abundant quartz, as spherical grains and show higher SiO_2 contents than the underlying leucitite. This quartz could only have been derived from an aeolian addition. Spherical quartz particles around the 70 µm size range (Figures 8 and 9), coated with clay, were taken as indicative of aeolian materials that would also have been deposited in the surrounding Girilambone Region.

Similar aeolian materials were detected across different regolith landform units throughout the Girilambone region. For example, PSD of the upper 0-0.5 m of a colluvial rise (Figure 10), indicates that the 70 µm particles are present at all depths sampled, but particularly in the upper 0.3 m. Similarly, the XRD analysis of the major mineral composition (Figure 11) also shows that the quartz is concentrated in the upper 0.5 m of the profile. Thus the aeolian particles are most concentrated in the upper 0.2-0.3 m of the profile, and subject to a range of post-depositional processes.

Through integrating a range of techniques and study site attributes, it was possible to derive a set of distinguishing characteristics for aeolian materials in the Girilambone region (Tate *et al.*, 2003). These are:

1. 70 µm quartz particles, *that are*
2. highly-abraded and spherical, *that have*
3. well-rounded clay coats, *and are*
4. dominant in the surface 0.2 m, *with preservation* subject to:
    a) redistribution and reworking by alluvial, colluvial and subsequent aeolian processes,
    b) post-depositional addition of alluvial and colluvial material, and/or
    c) post-depositional surface processes, *e.g.* wind and water erosion.

To reduce the diluting effect of this extraneous component in sampling for geochemical exploration, the >100 µm fraction is recommended for geochemical analysis.

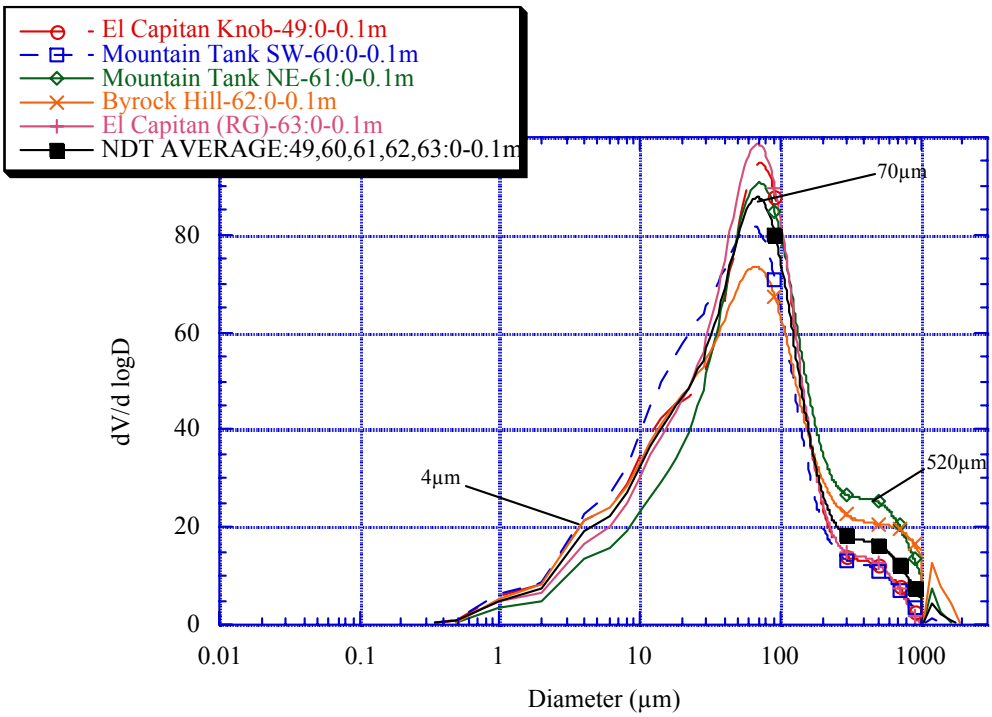

Figure 6. Particle size distribution of all NDT 0-0.1m bulk soil samples, plus their calculated average.

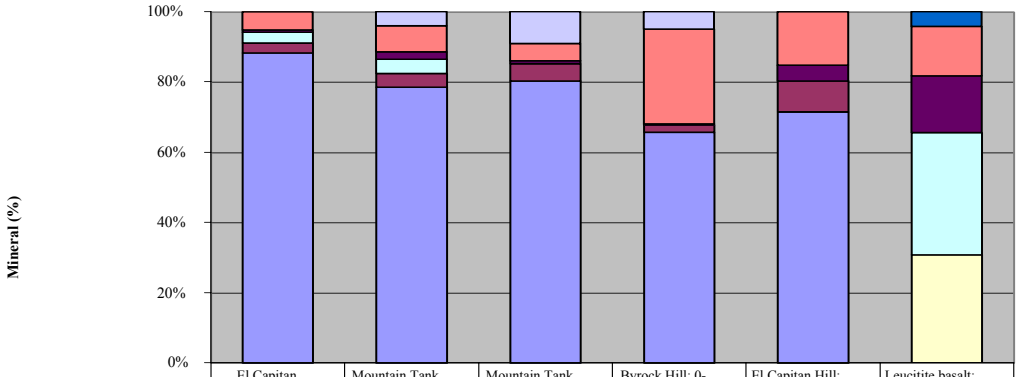

	El Capitan Knob: 0-0.1m	Mountain Tank SW: 0-0.1m	Mountain Tank NE: 0-0.1m	Byrock Hill: 0-0.1m	El Capitan Hill: 0-0.1m	Leucitite basalt: El Capitan Hill
Other Minor Phases (Wt%)	0	4	9	5	0	0
Amphibole	0	0	0	0	0	4
Mica + (including muscovite, biotite)	5	7	5	27	15	14
Fe, Ti Oxides (including hematite, rutile)	1	2	1	0	5	16
Pyroxene	3	4	0	0	0	35
Leucite	0	0	0	0	0	31
Kaolin	3	4	5	2	9	0
Quartz	88	79	80	66	71	0

Figure 7. Major mineralogical analyses (wt%) on all NDT soil bulk samples, as determined by quantitative XRD (SIROQUANT).

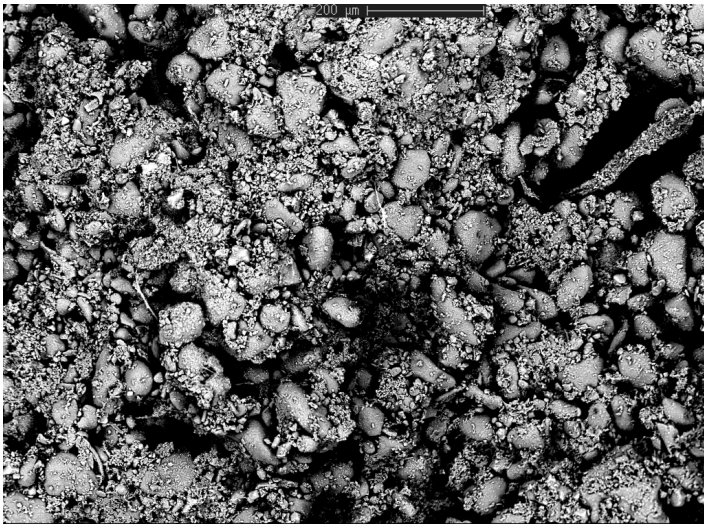

Figure 8. SEM image of soil (0-0.1m) from El Capitan Knob NDT. Note abundant, rounded quartz grains and clay aggregates. Scale bar at top is 100µm.

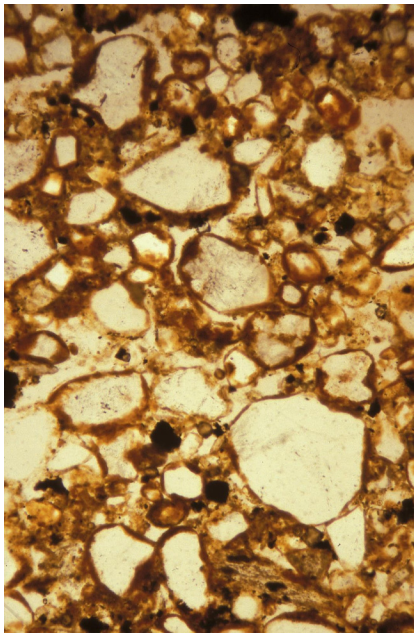

Figure 9. Thin section image of soil sample from El Capitan NDT showing abundant quartz grains, some with clay and iron oxide coatings. Scale: width of image is 625µm.

Sample	**SiO_2 wt. %**	**Al_2O_3 wt. %**	**Cr ppm**	**Nb ppm**	**Ti wt. %**	**Zr ppm**	**Ti/Zr**
Byrock Hill bulk soil sample	58.7	9.8	204	130	2.79	735	38
Mountain Tank bulk soil sample	58.6	10.6	263	126	2.57	777	33
El Capitan bulk soil sample	66.0	9.7	228	120	2.19	770	28
Leucitite sample: WT6*	42.1	7.8	348	179	3.24	883	37
Leucitite sample: WT7/8*	41.6	7.7	360	184	3.34	862	39
Leucitite sample: MT28*	42.8	7.8	438	174	3.08	762	40

Table 1. Selected geochemical analyses for the soils overlying NDTs at Mountain Tank, Byrock Hill and El Capitan for 0-0.1m: bulk sample, and also selected analyses for three leucitite samples from the El Capitan area* (from Gonzalez, 2001). Analyses by XRF.

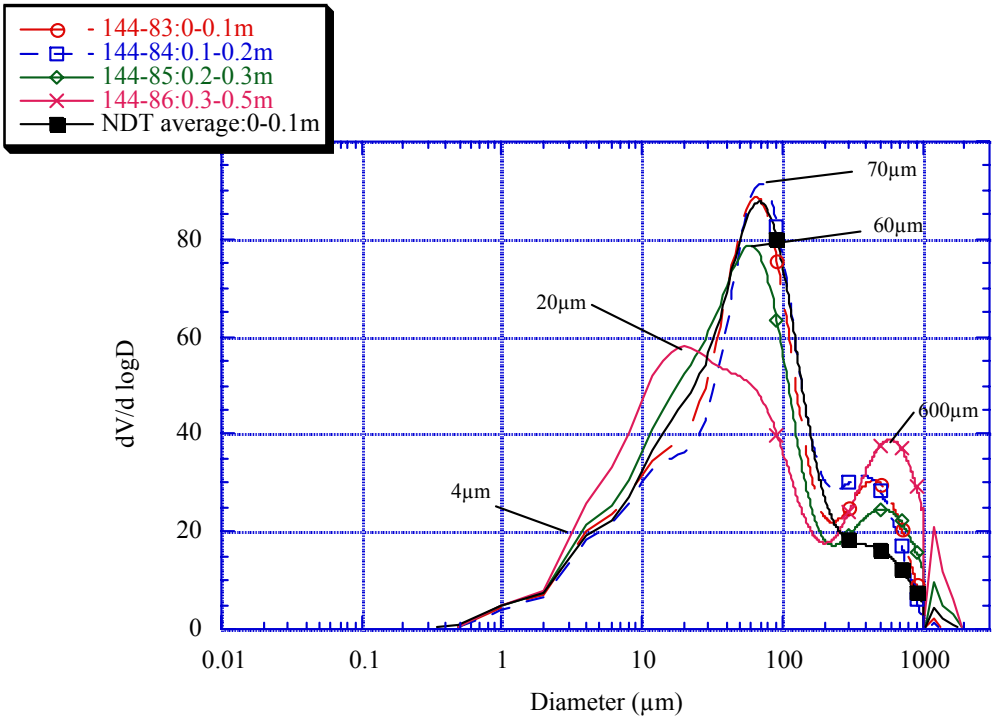

Figure 10. PSD for the upper 0-0.5 m of a colluvial rise profile (CBAC144), plus the NDT average PSD curve.

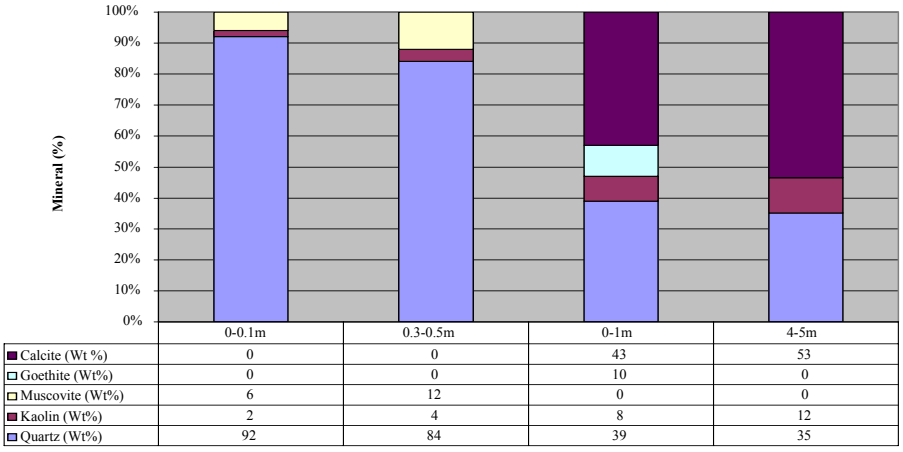

	0-0.1m	0.3-0.5m	0-1m	4-5m
Calcite (Wt %)	0	0	43	53
Goethite (Wt%)	0	0	10	0
Muscovite (Wt%)	6	12	0	0
Kaolin (Wt%)	2	4	8	12
Quartz (Wt%)	92	84	39	35

Figure 11. Major mineralogical analysis (wt%) of bulk samples from a range of depths for the colluvial rise profile (CBAC144), as determined by quantitative XRD analysis (SIROQUANT).

4.3 Regolith Profiles

Detailed information on regolith profiles has been obtained by petrographic logging, spectral analysis (using the PIMA) and geochemical analysis of samples from the 60 air core holes drilled during the project. This has been supplemented by observations of available exposures into the regolith and surface materials. Petrographic logging, combined with spectral analysis (PIMA), is particularly important for distinguishing transported from *in situ* regolith, and for defining the boundary (unconformity) between these materials in drill sections (Appendix 3). Detailed regolith profiles encompassing both transported and *in situ* regolith materials are graphically displayed on Plate 4, and will be attributed in a spreadsheet in a later report. Figure 12 summarizes the salient regolith architecture for the profile section along the western half of the drill hole traverse (CBAC188 to CBAC245). Figure 13 summarizes the simplified inferred landscape evolution associated with the transported regolith for the same traverse section as for Figure 12.

4.3.1 Transported Regolith in Palaeovalleys

Interpretation of drill chips from air core drilling across the Byrock area shows that magnetic (maghemite-bearing) sediments, as detected in the first vertical derivative magnetics image (Figure 5), occur in buried palaeovalleys and on some interfluves, the latter indicating relief inversion (*e.g.* CBAC229 and CBAC230, Plate 4). These magnetic sediments are just one component of the widespread and relatively thick palaeovalley sediments (up to >66 m thick *e.g.* in CBAC236). These palaeovalley sediments have been divided into two sequences: Sequence 1 containing magnetic sediments; and the underlying Sequence 2 containing clays and no magnetic sediments (Figure 12). Sequence 1 sediments are up to at least 40 m thick in the Mulga Creek palaeovalley (CBAC235 to CBAC246) which is 18 km wide along the drill hole section line. Sequence 1 palaeovalleys tend to have gentler slopes than Sequence 2 palaeovalleys, which have steep-sided and relatively deep palaeovalleys up to at least 60 m deep and at least 8 km wide west of Mulga Creek. The base of Sequence 1 palaeovalleys forms an erosion hiatus with the underlying Sequence 2 sediments. Palynological dating of these sediments has been attempted, but has been unsuccessful to date. (Dates of sediment deposition from palynological determinations reported previously in the Hermidale report (Chan *et al.*, 2003b) have been reviewed and found to be in error.) Palynological studies are on-going and complete results will be presented in a subsequent report. However, based on the 16.8 Ma (Miocene) K/Ar date of the leucitite (Sutherland, 1985) which overlies Sequence 2 sediments in CBAC235, these lower sediments are Early Miocene or older. Sequence 1 sediments overlie baked sub-lava sediments in CBAC236 from which the overlying leucitite lava has all but been eroded, thus indicating an erosion hiatus prior to deposition of sediments in Sequence 1 (Figure 13).

Carbonate induration occurs more commonly in Sequence 1 sediments (*e.g.* CBAC191 and CBAC225), but does occur in Sequence 2 sediments, *e.g.* CBAC210. The deepest carbonate induration is to 21m below ground level in Sequence 2 sediments in CBAC236. For details of carbonate determinations for drill holes refer to Appendix 1.

4.3.1.1 Sequence 1

Sequence 1, being the upper sequence, has a ubiquitous top layer of red-brown silt size quartz with or without sand and gravel, which is interpreted to be the result of aeolian attrition of the silt and its incorporation into existing transported (*e.g.* CBAC201 and

CBAC210) and *in situ* (CBAC229 and CBAC230) regolith profiles by bioturbation or mixing during transport. Sequence 1 at the southwestern end of the drill hole traverse in the southeast of the adjoining Gunderbooka 1:100 000 map sheet and continuing onto the southwest of the Byrock map sheet is mostly 1-2 m thick red-brown silt +/- sand and gravel, thickening to 3-5 m at CBAC204, CBAC210, CBAC211, CBAC213 and CBAC215 (Figure 12). Sequence 1 begins to thicken significantly from CBAC216 under sheetwash depositional plains to the west of Tindarey Creek, and increases in depth to a variable degree towards the east across broad stagnant alluvial plains, reaching a maximum observed sediment thickness of 34 m in the bottom of the palaeovalley at CBAC226. Numerous gravel layers containing ferruginous and magnetic pisoliths and rock fragments occur, especially on the flanks of the palaeovalley. Immature clay indurated sandstone and siltstone to silty claystone beds, that also have ferruginous and siliceous induration in places, occur towards the centre (CBAC222 to CBAC228) of this broad (19 km wide along drill hole traverse) Tindarey Creek palaeovalley, with buff to red-brown sandy beds towards the base of Sequence 1 in the deepest part of the palaeovalley at CBAC226. Sequence 1 is interpreted as colluvial, alluvial and aeolian sediments with an inferred arid environment of deposition.

Sequence 1 in Tindarey Creek palaeovalley thins further towards the east wedging out fairly sharply between CBAC228 and CBAC229 on the eastern edge of the stagnant alluvial plain which is buttressed by ferruginised and silicified bedrock (Figure 12). A thinner Sequence 1, (11 m thick) occurs in a palaeovalley further east under alluvial plains and sheetwash depositional plains between CBAC230 and CBAC233, with a still thinner Sequence 1 (9 m thick) containing basal transported (remnant layers visible under microscope) granitic sand in a palaeovalley at CBAC234. Further east again on the west bank of Mulga Creek a thick Sequence 1 (43 m thick) occurs at CBAC237 in the central part of the Mulga Creek palaeovalley, which extends between CBAC235 and CBAC246 on the eastern edge of the Byrock map sheet. The thickest sequence towards the middle of the Mulga Creek palaeovalley is sand-rich and reflects the provenance of the easterly migrating Mulga Creek.

Sequence 1 becomes relatively thin (<5 m thick) over granitic high terrain along the drill hole traverse further to the east in the Glenariff 1:100 000 sheet area (CBAC244-246, but thickens further towards the east (10 m thick at CBAC243) and to the south (18 m thick at CBAC242) where it overlies strongly compacted Early Cretaceous (Aptian) Surat Basin sediments (palynological date of micaceous silty clay sediment at the bottom of CBAC242, Appendix 7). Thin Sequence 1 sediments (< 3 m thick) occur over *in situ* regolith in the other four drill holes in the Glenariff sheet area (CBAC238 to CBAC240 in the north; CBAC248 in the south). Ferruginous staining and induration from weathering is common in Sequence 1 sediments, whereas siliceous induration is widespread but of patchy and limited extent (*i.e.* CBAC225, CBAC226 CBAC236, CBAC239, CBAC243, CBAC244, CBAC245, CBAC246, CBAC247).

4.3.1.2 Sequence 2

Sequence 2 underlies Sequence 1 (Figure 12). In no location that was drilled in the Byrock area has Sequence 1 been entirely eroded away leaving Sequence 2 at the surface, as occurs in places in the more elevated and generally more eroded terrain of the Sussex-Coolabah area. On the other hand, there are many places in the Byrock area where Sequence 2 has been completely eroded away and consequently Sequence 1 sits directly on *in situ* regolith (*e.g.* CBAC218, CBAC225, CBAC227 and CBAC 231).

Palaeovalleys containing Sequence 2 sediments become increasingly deeper as elevation decreases from west to east along the drill hole traverse from CBAC204 (base of palaeovalley 8 m depth at 168 m asl) to CBAC226 (base of palaeovalley >52 m depth at <93 m asl). Intervening palaeovalley thalwegs occur at CBAC210, and CBAC221 to CBAC223. Palaeovalleys further east are at CBAC226 (>51 m depth), CBAC232 (only 25 m deep), and a wider (8 km) and deep (>66 m thick at CBAC236) palaeovalley between CBAC234 and CBAC237. Sequence 2 palaeovalleys are narrower and deeper than the superimposed Sequence 1 palaeovalleys, whose thalwegs vary from being coincident (*e.g.* CBAC210, CBAC226, CBAC232) to somewhat displaced (*e.g.* CBAC237).

Sequence 2 sediments are dominantly white to pale grey to dark grey clays and silts with some similarly coloured sandy beds. Beds of white rounded quartz gravels and sands occur in CBAC237, and very coarse sands occur in CBAC228. These coarser beds indicate a fluvial phase within the inferred dominantly lacustrine depositional environment for Sequence 2 sediments. A ferruginous clay, silt and sand layer (23-25 m depth) above the very coarse sand in CBAC228 seems to be a buried palaeosol representing a hiatus in deposition prior to an increase in water depth, as indicated by the overlying silt then clay. In CBAC221 two periods of increasing and decreasing water depth, or conversely valley infilling, may be interpreted from sequence stratigraphy. Some clays have quartz clasts, perhaps indicating vegetation rafting in a near shore environment, or possibly a debris flow; whereas other clays have dispersed quartz grains, perhaps indicating further distance from shore, or the tail of a debris flow. Colour banding of clays and silts was noted: white to pale grey, and medium to dark grey. There is no correlating change in mineralogy, as indicated by PIMA. Alunite possibly occurs sporadically in clays without any quartz clasts or grains (*e.g.* CBAC226; see Section 4.4.2.4). Ferruginous induration from weathering is variable, ranging from little to none (*e.g.* CBAC216 and CBAC221) to major induration (*e.g.* CBAC223 and CBAC232). Siliceous induration occurs only in the bottom of CBAC241.

4.3.2 In situ Regolith

Drill holes along the southwestern end of the traverse (CBAC188 to CBAC216) are on gradually descending terrain with dominantly rises covered with sheetwash deposits. The saprolite in these drill holes is predominantly a variety of sandstone/siltstone to meta-sandstone/siltstone, claystone to shale/phyllite (micaceous in places), and silty claystone/phyllite. Saprock is encountered in two of these holes: CBAC198 at 48 m depth; and CBAC204 at 51 m depth. Drill holes CBAC200 and 201 have mafic dykes and altered sedimentary clay saprolith towards the bottom of the holes, with CBAC201 having magnetite altered saprock at 63 m depth. Micaceous sandstone/siltstone saprolite occurs sub-dominantly in CBAC188 CBAC190 to CBAC195, CBAC209 and CBAC210, with saprock occurring in CBAC209 at 37 m depth, and dominantly in CBAC202 and CBAC217.

Further along the drill hole traverse to the northeast, on the depositional plains just west of the stagnant alluvial plain associated with Tindarey Creek, micaceous schist saprolite is the exclusive lithology in CBAC218 and CBAC220, as it is for CBAC238 (magnetite also

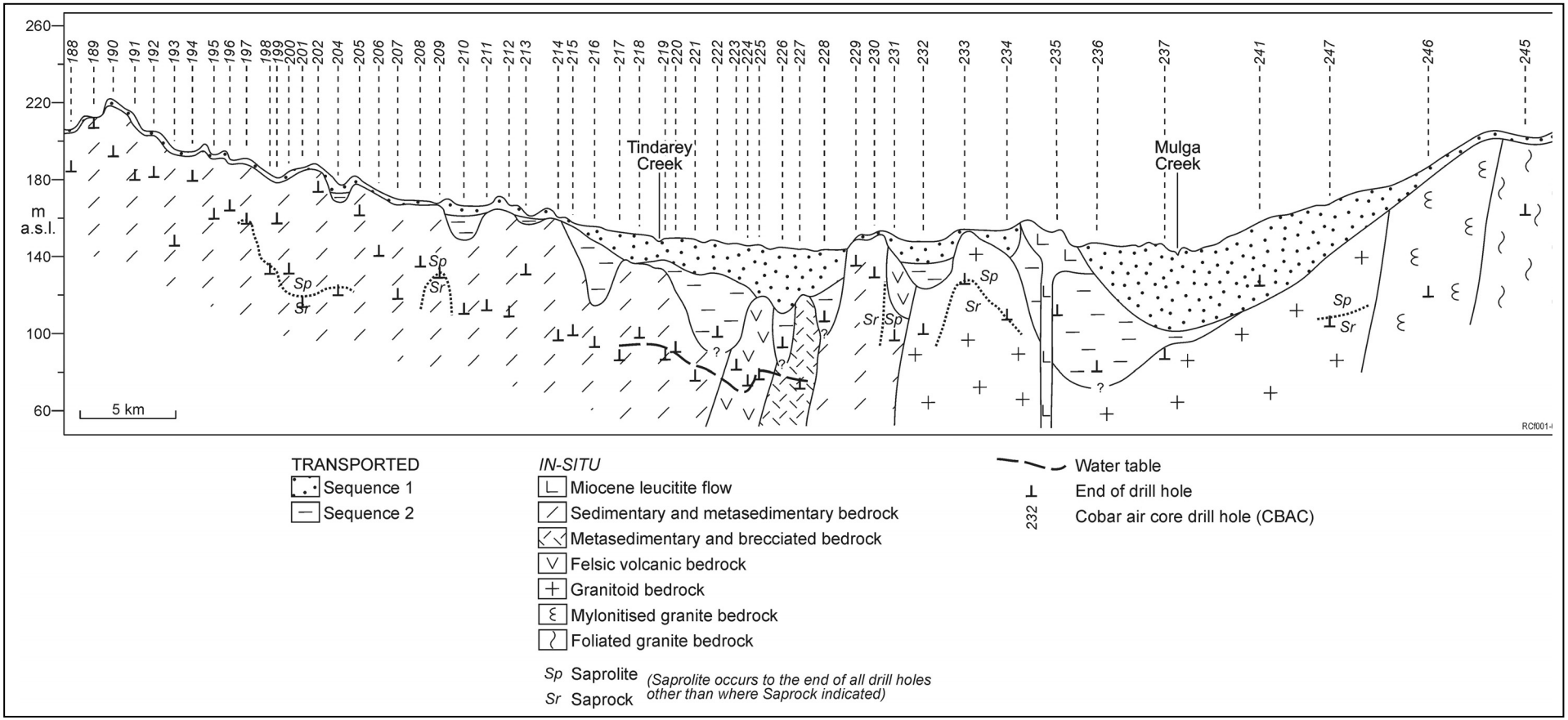

Figure 12. Regolith architecture derived from drill hole profiles along drilling traverse in the Byrock area.

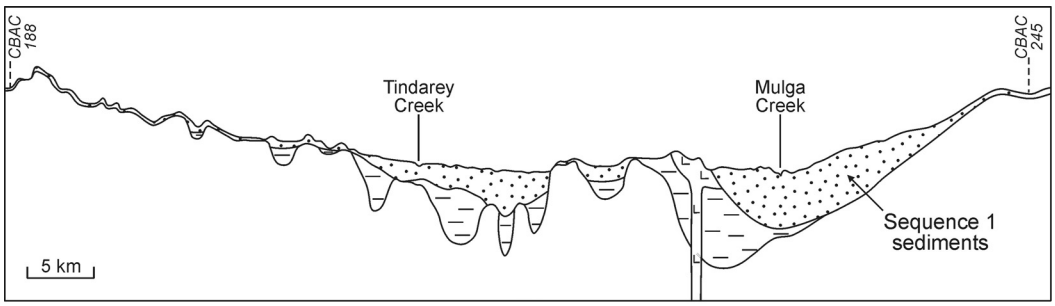

D. Deposition of Sequence 1 sediments infilling lower landscape and continued erosion of upper landscape to present time.

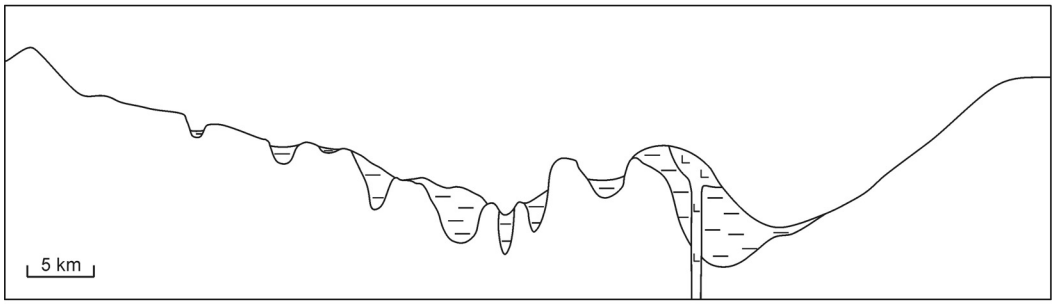

C. Continued erosion of Sequence 2 sediments, leucitite flow and bedrock interfluves.

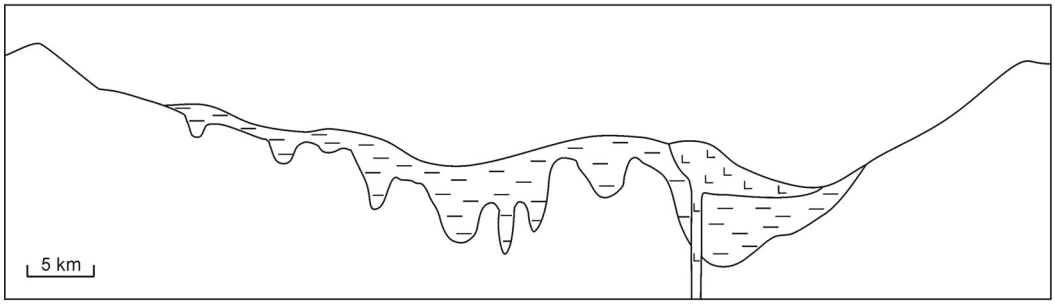

B. Erosion of Sequence 2 sediments and bedrock interfluves. Eruption of Miocene (16.8Ma) leucitite flow.

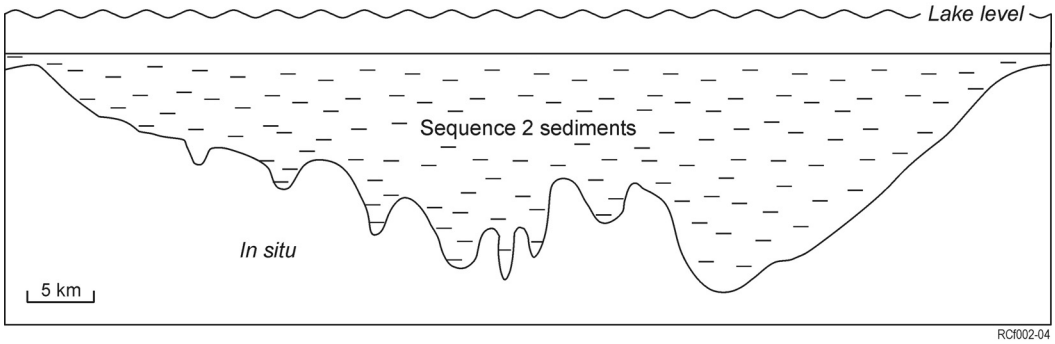

A. Flooding of high relief landscape by lake and deposition of Sequence 2 sediments.

Figure 13. Simplified diagram of landscape evolution along drilling traverse in the Byrock area.

occurs throughout this profile) and CBAC243 in the Glenariff map sheet to the east. Adjacent drill holes to CBAC218 and CBAC220, *i.e.* CBAC219 and CBAC221, have the same range of sandstone/siltstone/claystone saprolite as already described for drill holes further southwest. Felsic volcanic saprolite, including rhyolite, is the prime lithology in CBAC223 to CBAC225, forming a buried interfluve beneath the stagnant alluvial plain and sediments of Sequences 1 and 2. Another buried interfluve occurs at CBAC227 just to the northeast on claystones/phyllite underlain by meta-siltstone and breccia. The eastern edge of the stagnant alluvial plain associated with Tindarey Creek is buttressed by silicified claystone/phyllite saprock in CBAC229, and sandstone/siltstone saprock in CBAC230.

Lithologies beneath the smaller and shallower palaeovalley to the east of the stagnant plains associated with Tindarey Creek are felsic volcanic saprolite overlying micaceous sandstone/siltstone saprolite in CBAC231, and granitoid saprolite in CBAC232 which continues to the east, sub-cropping at CBAC233 and covered by granitoid derived sediments at CBAC234. Granitoid saprock occurs at 25 m depth in CBAC233 and at 45 m depth in CBAC234. Slightly weathered leucitite lava overlies baked Sequence 2 sediments in CBAC235 at 17-23 m depth, or, alternatively, hyaloclastite sediments derived from the venting and mounding of the lava as it burst through the lacustrine sediments and lake water. Similar baked sediments with or without a thin layer of highly weathered remnant basalt may occur in CBAC236 between 15 m and 22 m depth. Additional detailed geochemical studies are being undertaken to fully resolve the situation.

Granitoid saprolite reappears at depth beneath the stagnant alluvial plains associated with Mulga Creek at CBAC237. The granitoid saprolite continues to the east to the eastern edge of the Byrock map sheet and on to the Glenariff map sheet from CBAC244 to CBAC247 (east to west), forming significantly higher terrain with relatively shallow Sequence 1 sediments as mentioned above. The granitoid saprolite in CBAC247, which changes to saprock at 63m depth, varies to mylonitised granite saprolite with a schistose texture at CBAC246 and CBAC244, and foliated granite saprolite in between at CBAC245. This is interpreted as a possible shear zone.

Slate saprolite occurs in CBAC239 and CBAC240 in the north of Glenariff map sheet, and in CBAC248 in the south of Glenariff, indicating low grade regional metamorphism in the Glenariff area. Low grade regional metamorphism in the Byrock area is also indicated by meta-sandstone/siltstone and meta-shale/phyllite. Felsic volcanic saprolite occurs beneath the slate in CBAC240, and micaceous schist is the dominant lithology in CBAC248 with saprock at 55 m depth, and slate interbeds.

Pallid saprolite is common beneath palaeovalleys in a range of lithologies, *e.g.* CBAC204 (micaceous schist), CBAC213 and CBAC219 (claystone/phyllite), and CBAC231 (felsic volcanics and micaceous sandstone/siltstone). This is indicative of an environment with little or no oxidation of iron. However, pallid saprolite is common in granitoid saprolite both under palaeovalleys (*e.g.* CBAC232 and CBAC247) and where there is shallow cover (*e.g.* CBAC233, CBAC245 and CBAC246). This also applies to micaceous schist (*e.g.* CBAC238 and CBAC248) where there is only a couple of metres of sediment cover. This occurrence of pallid granitoid and micaceous schist saprolite independent of cover may relate to the more porous nature of these lithologies. Pallid saprolite also occurs as discrete relatively thin layers scattered through profiles with little, if any, sediment cover, *e.g.* CBAC190 and CBAC205.

Pink saprolite is an indication of accumulation of iron oxides in the *in situ* profile and occurs in variable parts of the profile and in a range of lithologies, but notably in CBAC215 and CBAC216 (sandstone/siltstone/claystone), CBAC217 (micaceous sandstone/siltstone), CBAC218 (micaceous schist), CBAC224 (acid volcanics), CBAC227 (meta-siltstone and breccia), and CBAC234 (granitoid). Goethitic staining (yellow) is common in non-pink and non-pallid parts of the profile. Ferruginous induration, as noted in competent red to black drill chips and less pervasive iron oxide staining in mottles and veins, is common in various parts of the profile and in various lithologies. Siliceous induration is less common than ferruginous induration and occurs alone (*e.g.* CBAC201 and CBAC205), associated with ferruginous induration (*e.g.* CBAC207, CBAC217, and CBAC238), and associated with quartz veining (*e.g.* CBAC194, and CBAC198). Quartz veining is disparate but common, occurring notably in CBAC211, CBAC212, CBAC215, CBAC217, CBAC218, CBAC220, CBAC231, CBAC239, CBAC240, CBAC243, and CBAC246. Quartz veining is strongly associated with pallid saprolite in CBAC239 and CBAC246. Carbonate induration is common at and within a few metres below the transported / *in situ* interface, *e.g.* CBAC193 and CBAC217 (Appendix 1).

The water table level ranges from 27 m below ground level at CBAC242 on the western alluvial plains of the Bogan River (a north flowing tributary of the Darling River in the Glenariff area) to 66 m below ground level at CBAC225 on the stagnant alluvial plains associated with Tindarey Creek palaeovalley in the Byrock area. Strongly compacted yellow and grey mottled clays occur below the water table in CBAC242 at 31-39 m and 43-45 m depths. A zone of ferruginous induration occurs at 65-67 m depth in CBAC221 at the water table. Refer to Figure 12 and Plate 4 for depth of water table where encountered in drill holes.

4.4 Mineralogy determined by PIMA and X-Ray diffraction

4.4.1 Identification of Transported / In situ Regolith Boundary

The PIMA data have been used in conjunction with the field and laboratory logging data to distinguish the transported material from the *in situ* material. Transported material consists of aeolian, alluvial and colluvial sediments and a lava flow overlying the bedrock, and the sediments tend to contain less crystalline kaolinite and more bound water in their minerals than those of *in situ* regolith (Chan *et al.,* 2003b).

Figure 14 shows the stacked spectra obtained for material from the surface to a depth of 34 m of drill hole CBAC212. Kaolinite and mica are the dominant clays of the 13 top metres of the hole. However, the boundary is indicated by an increase in kaolinite crystallinity below 2 m and a decrease in bound water content (1900 nm absorption feature) towards the bottom of the hole.

The depths of the transported / *in situ* regolith boundaries in the 60 drill holes are listed in Appendix 3. The thickness of transported regolith varies greatly, ranging from less than 10 cm to more than 60 m.

In the upper parts of the landscape such as erosional rises (CHer), the transported regolith is reduced to a surface layer (*e.g.* CBAC190) and is typically 1 m thick. The thickness of the sediments ranges from 1 to > 60 m in alluvial (Aap, Aed, Aas, ACar) and colluvial

(CHpd, CHep) regolith-landform units. The thickest transported regolith is found in the Mulga Creek palaeovalley (CBAC234 to CBAC246), west of Byrock (Figure 15).

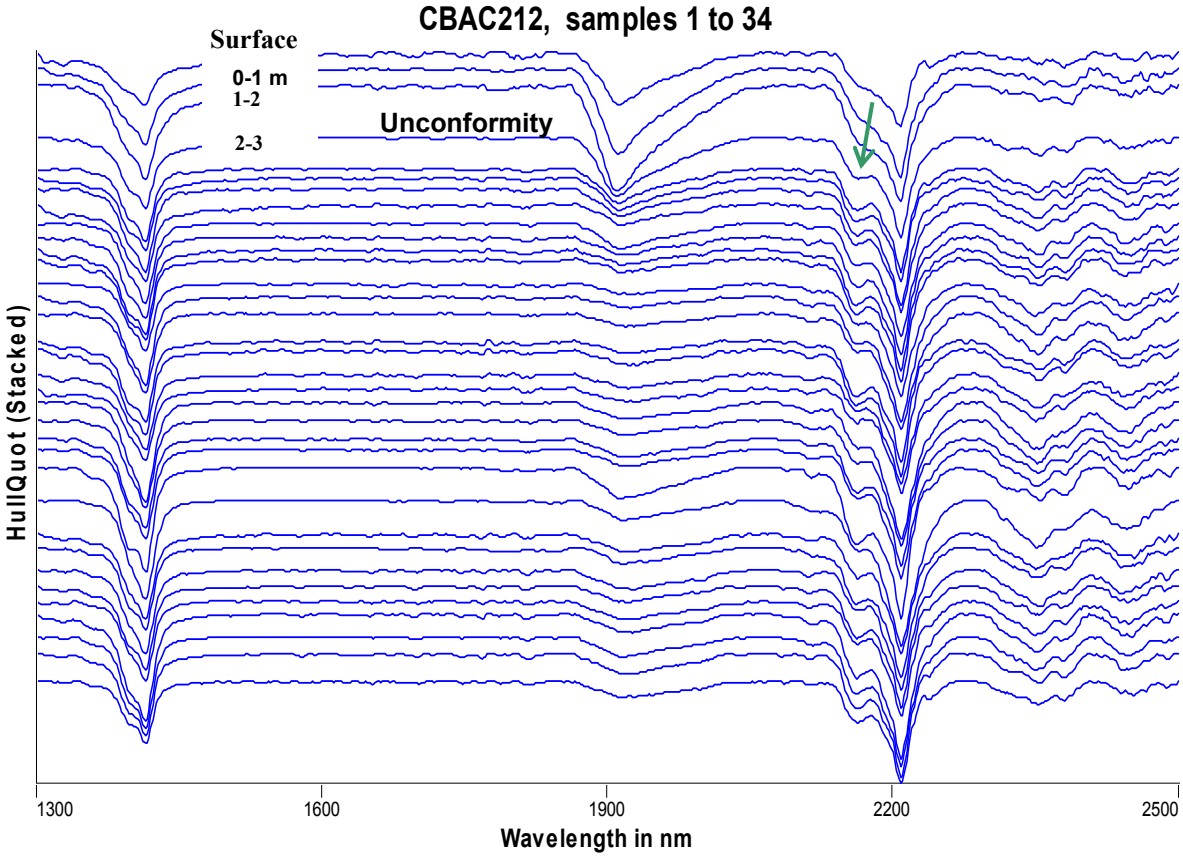

Figure 14. Stacked PIMA spectra from drill hole CBAC212. The unconformity lies at 2 m. The green arrow points at an absorption feature characteristic of an increase of kaolinite crystallinity.

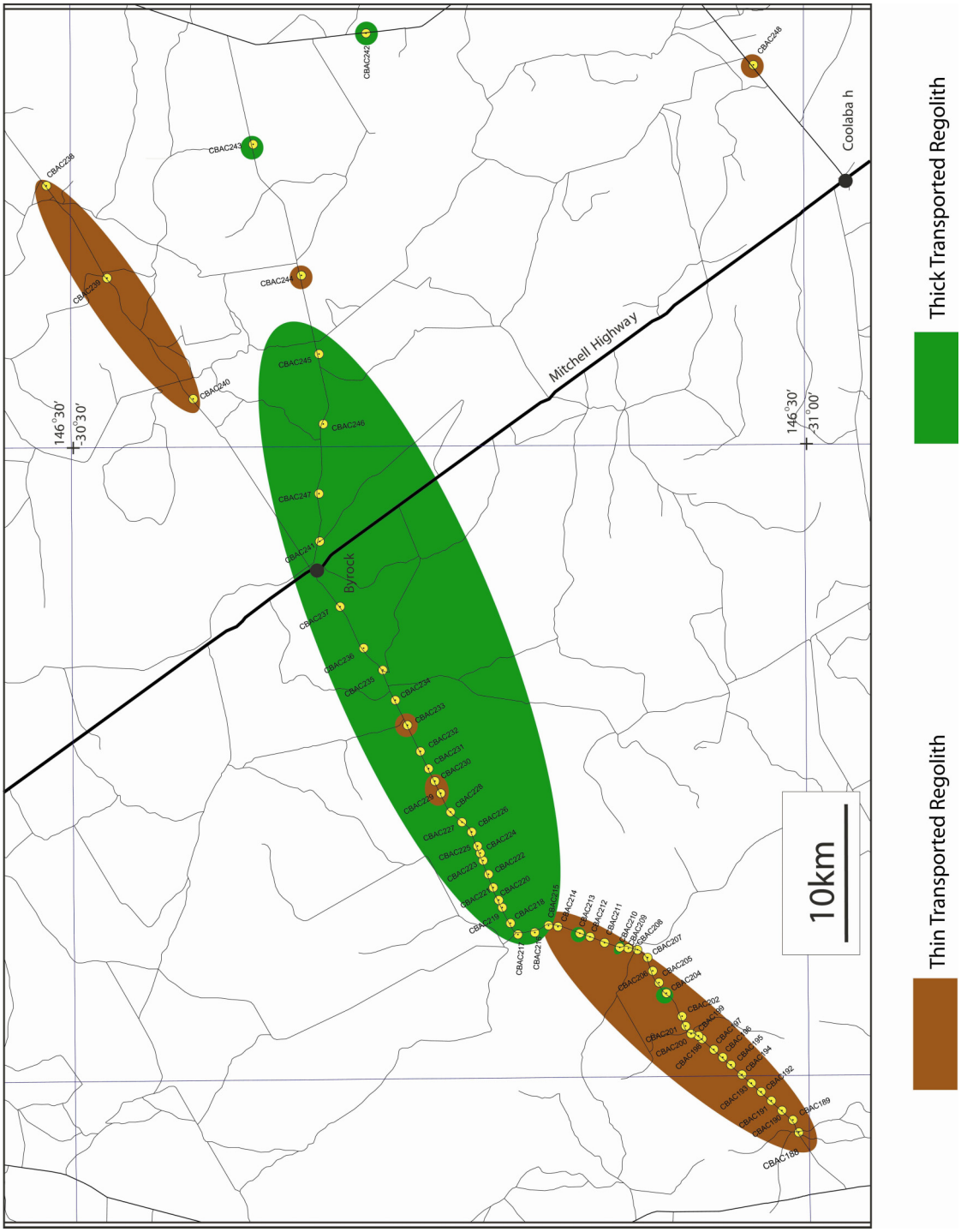

Figure 15. Thickness of the transported cover in the Byrock area. Thin cover ≤ 3 m contains kaolinite and illite. Thick cover > 3 m contains kaolinite, and smectites

4.4.2 Mineralogy of the Transported Regolith

The clay minerals identified by PIMA in the transported material are kaolinite (as indicated in previous reports, identification of the kaolinite polymorphs, nacrite and dickite, by PIMA should be confirmed by other methods and such identifications are regarded as kaolinite in this report), halloysite, illite, muscovite and smectites. Kaolinite is present in 59 drill holes as a major or minor clay mineral. Alunite has been detected in two drill holes, although in one case it may occur just below the unconformity (see below).

The clay mineralogy of the transported material in the 60 drill holes is shown in Appendix 8.

Four types of transported material are observed in the Byrock region:

- Transported material composed of a mixture of alluvial, colluvial and aeolian sediments;
- Leucitite lava flows;
- Lacustrine sediments;
- Alunite-bearing sediments.

4.4.2.1 Mineralogical Assemblages in Sequence 1 Alluvial, Colluvial and Aeolian Sediments

Transported regolith consisting of variable amounts of alluvial, colluvial and aeolian material in Sequence 1 occurs in all 60 of the drill holes of this study. Two main clay mineral assemblages reflecting a toposequence association have been observed:

- Kaolinite + illite ± muscovite ± halloysite (no smectite): assemblage observed in 23 drill holes. This assemblage is mostly observed in low relief areas (CHer) as thin (≤3 m) sequences (Figure 15) west of the Mulga Creek valley. A typical spectral response produced by this material is shown in Figure 16 (CBAC244). Kaolinite is not detected in CBAC206;

- Kaolinite + illite + smectites ± halloysite ± muscovite: the most common mineralogical assemblage found in more than half of the holes analysed (37 drill holes). This material contains abundant smectites and forms thick sequences (> 3 m) associated with the Tindarey Creek and Mulga Creek palaeovalleys, and also 2 drill holes further east (Figure 15). Typically the smectitic intervals are overlain by material (up to 3 m thick) rich in kaolinite (or halloysite) and illite. The smectite-rich sediments are about 2 m thick in the areas of slight topographic relief and become thicker (up to 22 m in CBAC225) in low relief areas. In addition, smectites and halloysite are commonly present at the base of the transported regolith (Figures 17 and 18). The presence of smectites probably reflects less well drained conditions.

4.4.2.2 Mineralogy of Leucitite Flow

Leucitite subcrops under a 50 cm layer of red-brown soil containing partially weathered leucitite cobbles in drill hole CBAC235. Some smectites have been detected with the PIMA in the interval 18-19 m in generally fresh leucitite, which is characterised by the absence of phyllosilicates (Figure 19). The leucitite lava flow, which is 23 m thick, overlays kaolinitic Sequence 2 sediments.

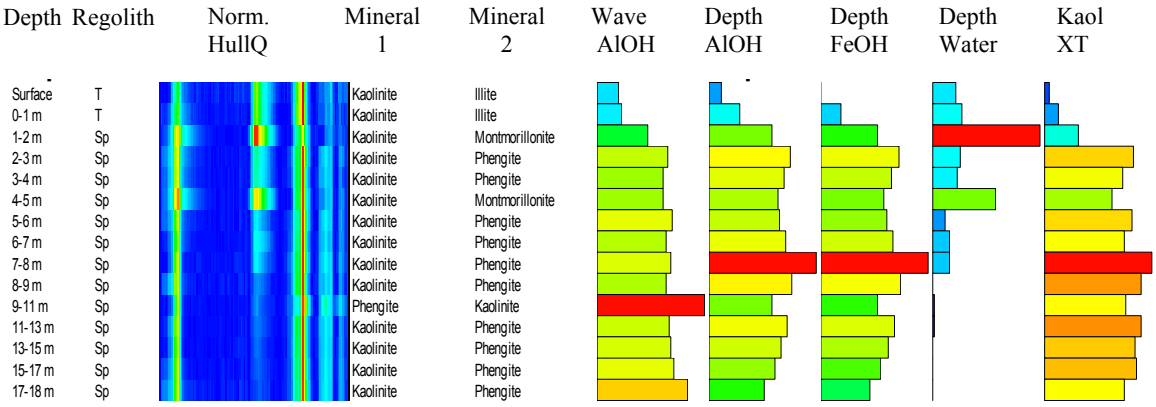

Figure 16. PIMA analysis of the regolith from drill hole CBAC244. The transported material is 1 m thick and contains kaolinite and illite. T: Transported regolith; Sp: Saprolite (*in situ* regolith).

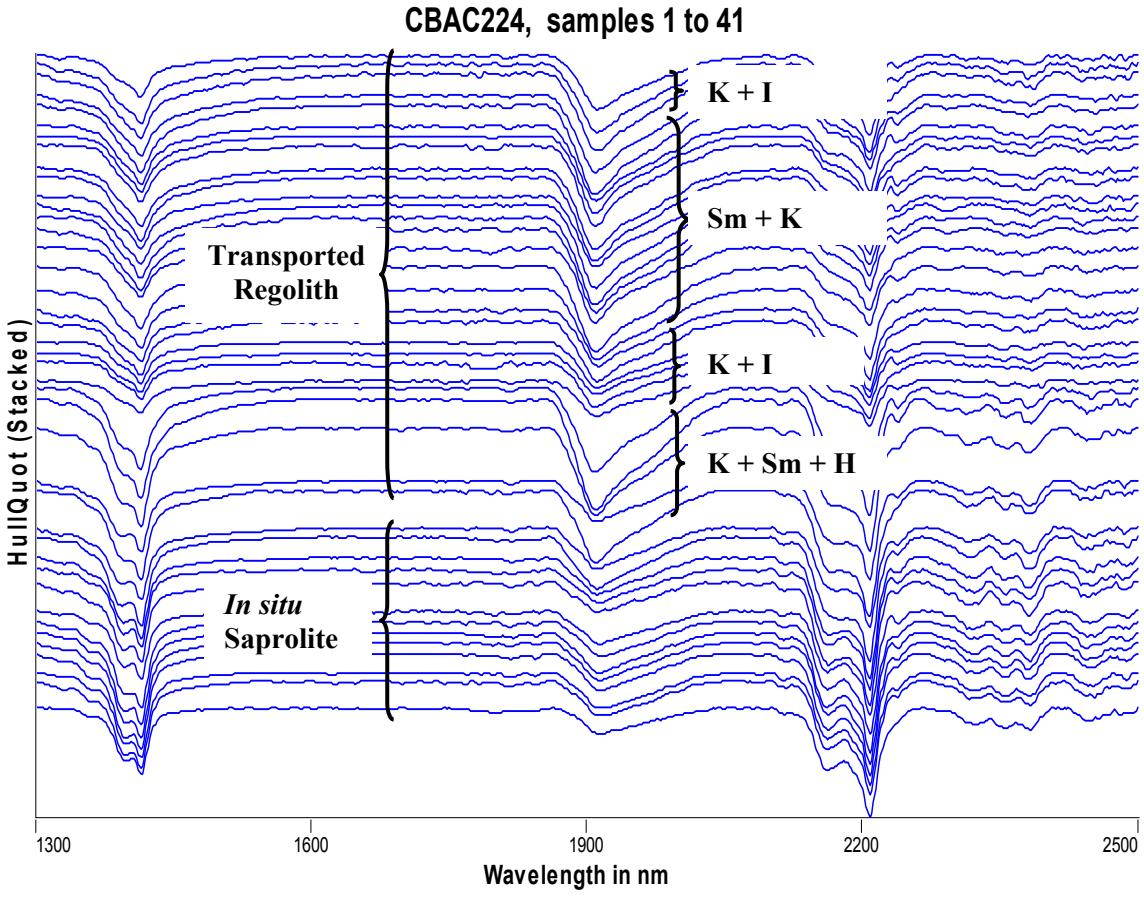

Figure 17. Stacked PIMA spectra from drill hole CBAC224. The unconformity lies at 29 m. K: Kaolinite; I: Illite; Sm: Smectite; H: Halloysite.

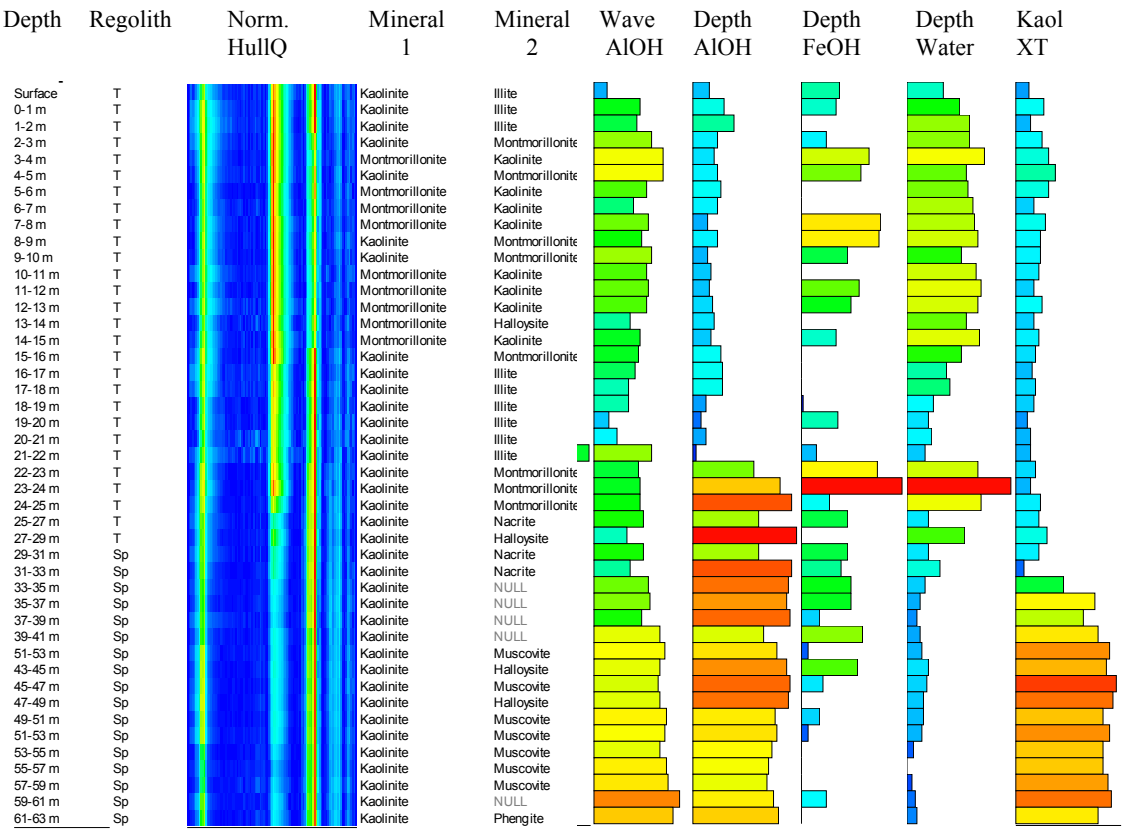

Figure 18. PIMA analysis of the transported material from drill hole CBAC224. The smectitic layer is evidenced on the Normalised Hull Quotient colour slice by the depth and asymmetry of the water absorption features. T: Transported regolith; Sp: Saprolite (*in situ* regolith).

4.4.2.3 Mineralogy of Sequence 2 Sediments

The lacustrine sediments consist of pale to dark grey clays. They are composed of kaolinite, and abundant illite, halloysite and smectites.

4.4.2.4 Alunite-Bearing Sediments

Drill hole CBAC226 intersects an alunite-rich horizon from 36 to 41 m. Figure 20 shows the characteristic PIMA spectra produced by alunite-kaolinite assemblages. The elevated K_2O content in this interval (Appendix 4) may also reflect the presence of the alunite. Alunite is also found in CBAC 213 at 4-6 m, but here it appears to occur in *in situ* material just below the unconformity. The alunite is probably associated with the lake sediments, and not the result of the weathering of sulfides. This hypothesis could be checked by doing sulfur isotope analyses.

4.4.3 Mineralogy of the In situ Regolith

The *in situ* regolith results from the weathering of the Girilambone Group rocks, felsic and mafic intrusions and mafic volcanics. The *in situ* clay composition for each hole is summarised in Appendix 9. Within the Girilambone Group, the clay mineralogy of the *in situ* saprolite varies with the nature and degree of weathering of the original sedimentary rock.

Within weathered Girilambone Group rocks three main mineralogical assemblages have been distinguished:

- Kaolinite + muscovite ± halloysite ± smectites ± illite. This type of assemblage has been observed in the following 33 drill holes:
  CBAC188 CBAC189 CBAC190 CBAC191 CBAC192 CBAC193,
  CBAC194 CBAC195 CBAC196 CBAC197 CBAC199 CBAC202,
  CBAC204 CBAC205 CBAC206 CBAC207 CBAC208 CBAC212,
  CBAC213 CBAC214 CBAC215 CBAC216 CBAC217 CBAC218,
  CBAC219 CBAC220 CBAC223 CBAC227 CBAC229 CBAC230,
  CBAC231 CBAC239 CBAC240.

  Two types of profiles are observed with this mineralogical assemblage: those with muscovite and kaolinite as the only clays detected; and those with hydrated clays such as illite, halloysite and smectites in association with kaolinite or muscovite at the top of the saprolite, immediately under the unconformity (Figure 21). Alunite has been detected in CBAC213 at the top of the residual material just below the unconformity.

- Kaolinite + muscovite + phengite ± halloysite ± illite ± smectites. This assemblage has been observed in the following 9 following drill holes: CBAC198, CBAC200, CBAC201, CBAC209, CBAC210, CBAC211, CBAC221, CBAC224 and CBAC225. Phengite occurs as the main clay in one interval in CBAC198, two intervals in CBAC200 and CBAC221 and five intervals in CBAC209 (Figure 22). Drill holes CBAC198, CBAC200 and CBAC201 are intersected by mafic intrusions and show anomalous Pb-Zn±Cu±Au values (see Section 4.5.1).

- Kaolinite + phengite ± halloysite ± illite ± smectites (no muscovite). Weathered sediments containing phengite and kaolinite but no muscovite) have been intersected in CBAC238, CBAC243, and CBAC248 (Figure 23). Figure 24 shows stacked spectra taken from mainly weathered rocks in the depth interval 37 to 66 m in drill hole CBAC238. The 2200 nm (Al-OH) absorption feature, which is sharp in kaolinite-rich material, broadens in intervals dominated by phengite. Phengite is the only clay detected in interval (63-65 m). Its spectrum is characterised by a shift to higher wavelengths of the Al-OH absorption band, due to Fe-Mg substitution for Al in muscovite. The drill hole CBAC238 intersects a mineralised shear system in the Lord Carrington area, 20 km northeast of Byrock. Disseminated magnetite, present throughout the saprolite, becomes abundant halfway down the hole. Samples from the intervals, 37-39 m, 49-51 m, 51-53 m and 65-66 m were also analysed by X-ray diffraction (Figure 25). Phengite, kaolinite, K-feldspar, quartz and hematite are the main minerals in material between 37-53 m, with apatite accounting for the high Ca and P contents in the 37-39 m sample (Section 4.5.2 and Appendix 4). Plagioclase is abundant in interval 65-66 m. Small amounts of chlorite, which have not been detected with the PIMA, are present below 49 m. Interstratified chlorite / smectite (or chlorite / vermiculite), a common weathering product of chlorite, has also been detected in these samples.

4.4.3.1 Regolith Derived from Felsic Rocks

Granite, displaying a variable degree of weathering, is intersected in four drill holes: CBAC237, CBAC244, CBAC245 and CBAC246.

In drill holes CBAC237 and CBAC245, the granite is intensively weathered and mica has been completely replaced by kaolinite. In CBAC237, west of Byrock, kaolinite is the major clay in the saprolite buried under a thick transported cover (50 m). Halloysite is present in the material located just underneath the transported sediments. Both clays result from the weathering of feldspars and muscovite. In CBAC245 the granite is weathered to kaolinite with no other phyllosilicates. Smectites (montmorillonite) and kaolinite are present in the overlying transported sediments (Figure 26).

In drill holes CBAC244 and CBAC246, the granite is less weathered: the material contains abundant fresh mica (muscovite/phengite) and the foliated structure is retained.

Weathered granitoid rocks, possibly monzodiorite, are present in 4 drill holes: CBAC232, CBAC233, CBAC234 and CBAC247. The saprolite is composed of kaolinite, halloysite and smectites (montmorillonite and nontronite).

Partially weathered felsic volcanics (possibly rhyolite) containing abundant fresh mica and kaolinite have been identified in the bottom ten metres of drill hole CBAC240.

4.4.3.2 Regolith Derived from Mafic Rocks

Mafic rocks are intersected in drill holes CBAC198, CBAC200, CBAC201 and CBAC243.

The presence of weathered mafic rocks is indicated by:

- The clay mineralogy: kaolinite, halloysite and smectites/vermiculite are the only clays formed during the weathering of mafic rocks (mica and illite are not present);
- The clay chemical composition: kaolinite and smectites generally contain iron in their structure. The presence of a FeOH absorption feature in the 2230-2295 nm wavelength interval in the PIMA spectra indicates Fe substitution for Al in the kaolinite. Nontronite (Fe-smectite) and saponite (Mg-smectite) instead of montmorillonite (Al-smectite) may also be present;
- PIMA TSG results show Kaol + NULL or NULL + NULL.

Phengite has been identified in the saprolite of these 4 drill holes. The formation of this mica is likely to be primary, being related to the mafic intrusive event.

High levels of base metals and / or gold have been detected in all the drill holes intersected by mafic intrusions: Pb-Zn±Cu±Au values are present in CBAC198, CBAC200 and CBAC201, and anomalous Au levels of gold have been detected in CBAC243 (see Section 4.5.1).

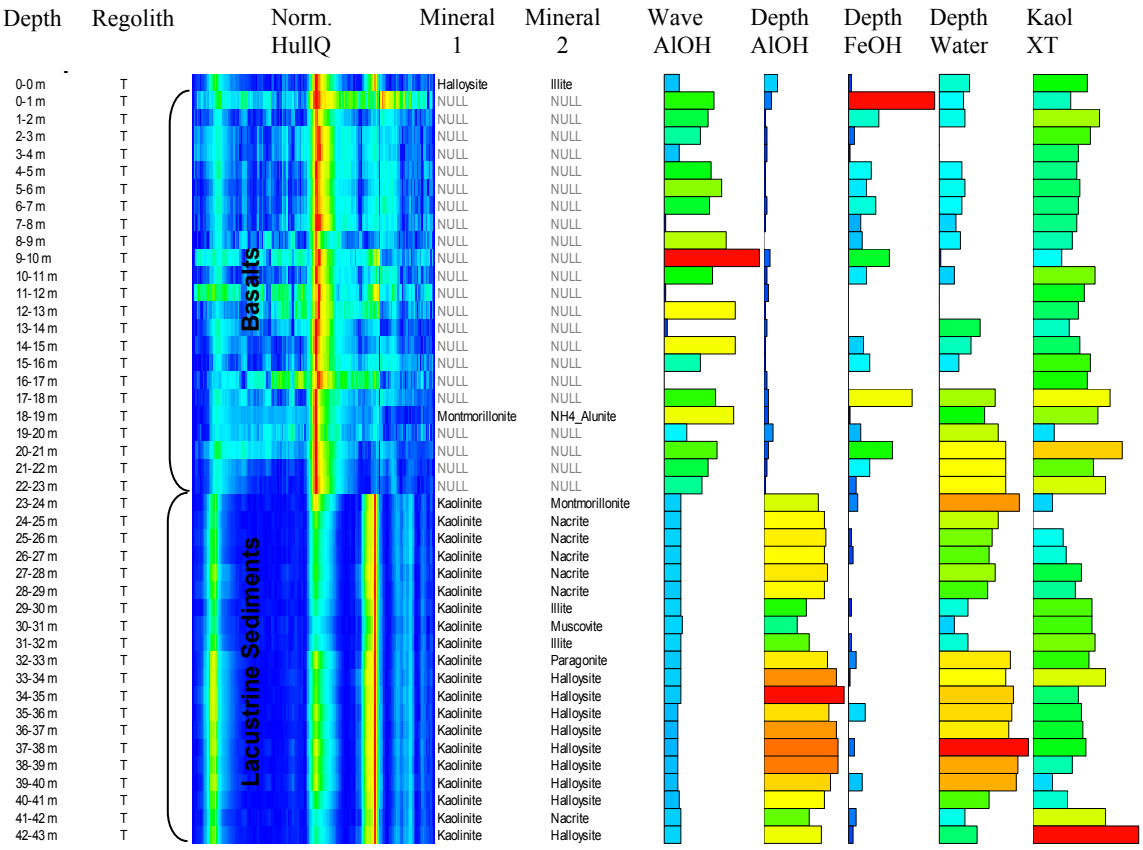

Figure 19. PIMA analysis of the regolith from drill hole CBAC235. The leucitite flow is 23 m thick and covers kaolinitic lacustrine sediments. T: Transported regolith.

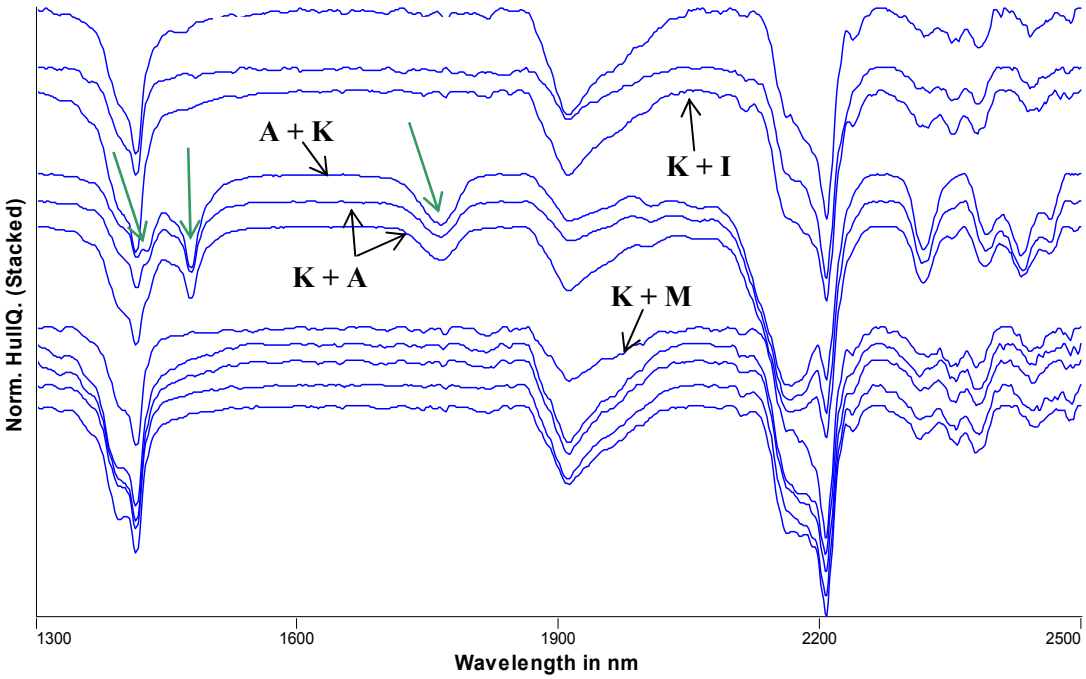

Figure 20. PIMA stacked spectra from drill hole CBAC226. Alunite is the main mineral detected by PIMA in one interval and is associated with major kaolinite in two intervals. The green arrows point at diagnostic alunite absorption features. A: Alunite; K: Kaolinite; I: Illite; M: Muscovite.

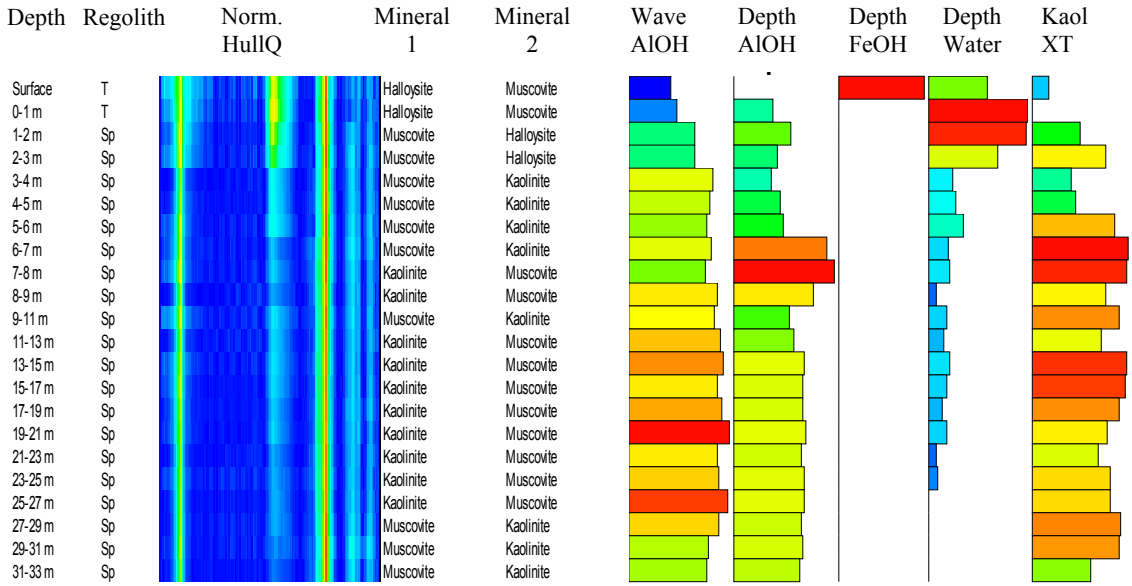

Figure 21. PIMA analysis of the regolith for drill hole CBAC206. Halloysite is present in 2 intervals under the unconformity. T: Transported regolith; Sp: Saprolite (*in situ* regolith).

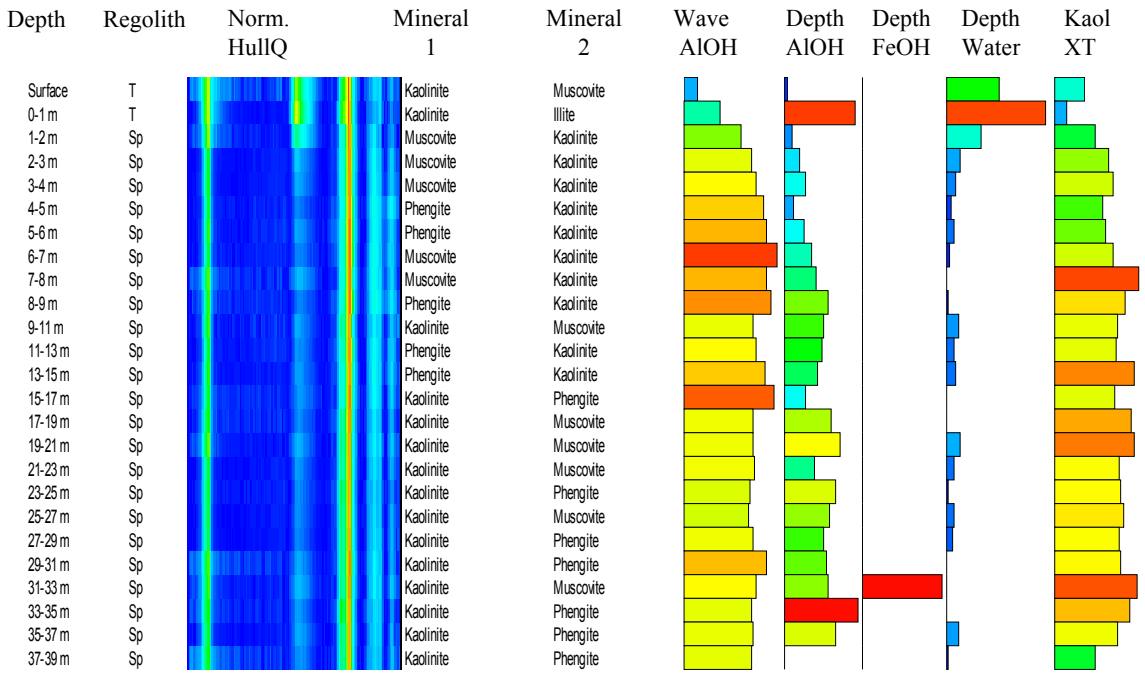

Figure 22. PIMA analysis of the regolith profile for drill hole CBAC209. The saprolite contains abundant kaolinite and muscovite and phengite has been detected in 12 intervals. T: Transported regolith; Sp: Saprolite (*in situ* regolith).

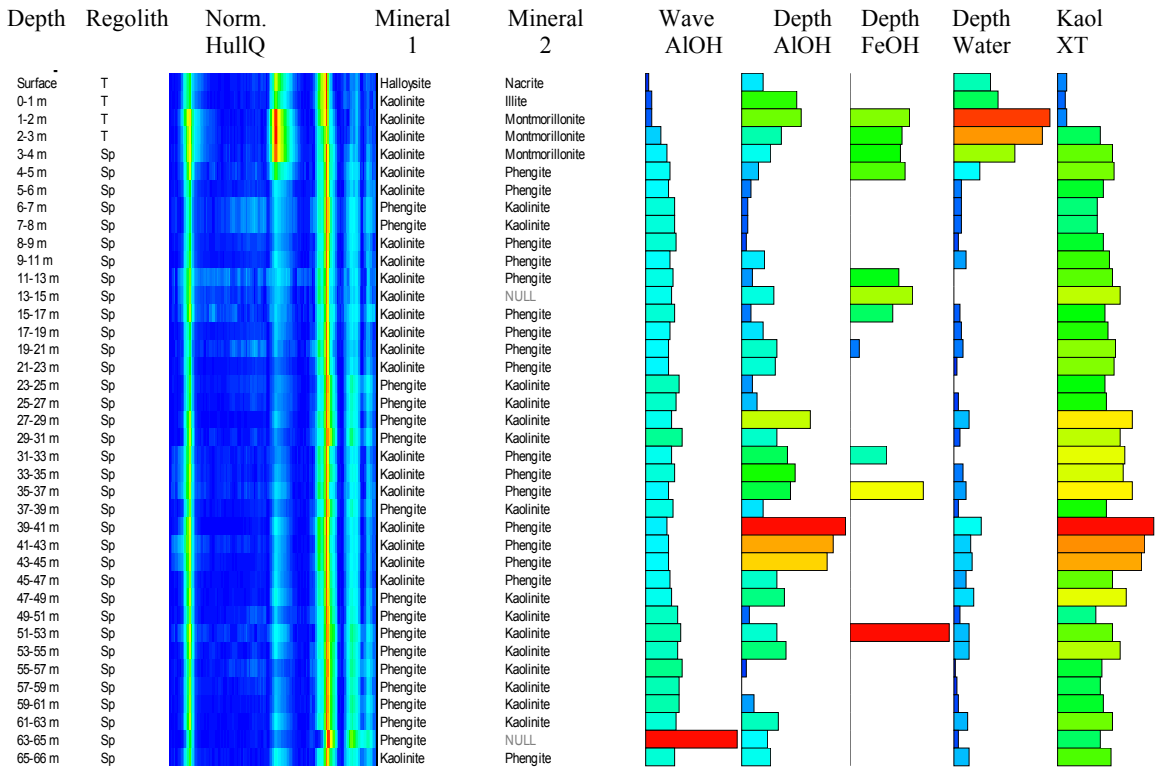

Figure 23. PIMA analysis of the regolith profile for drill hole CBAC238. Phengite is abundant through all the *in situ* regolith. T: Transported regolith; Sp: Saprolite (*in situ* regolith).

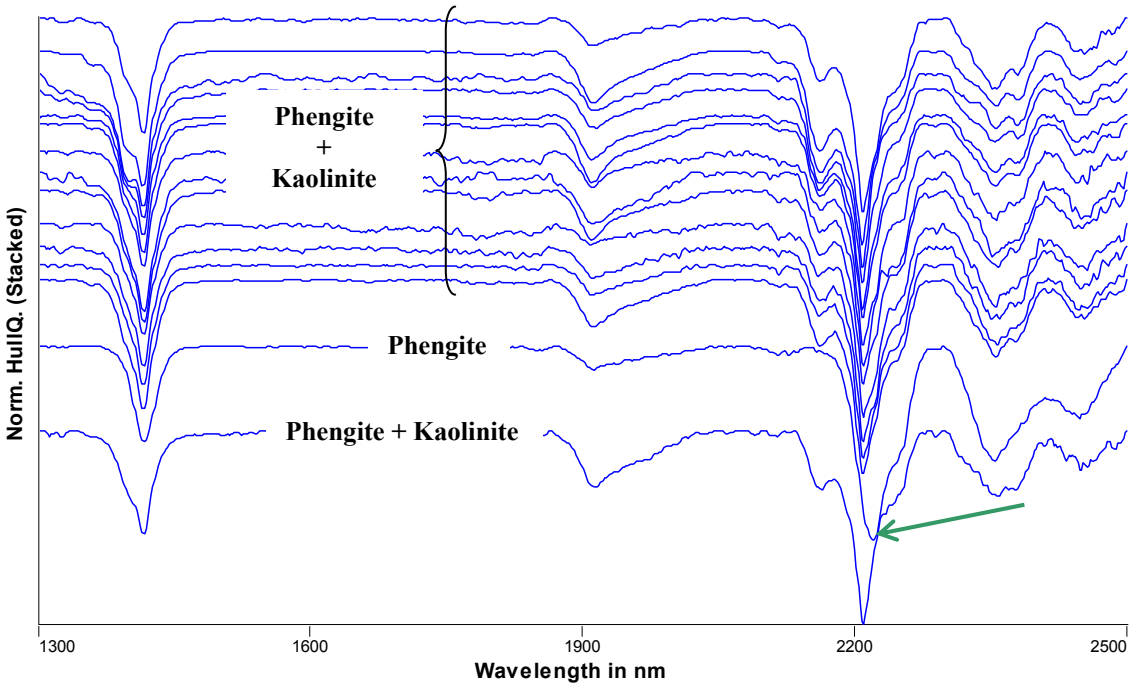

Figure 24. Stacked PIMA spectra from drill hole CBAC238, from 37 to 66 m. Phengite is partially weathered into kaolinite except in interval (63-65 m) where it is fresh. The green arrow points at the shift in the wavelength of the AlOH absorption feature.

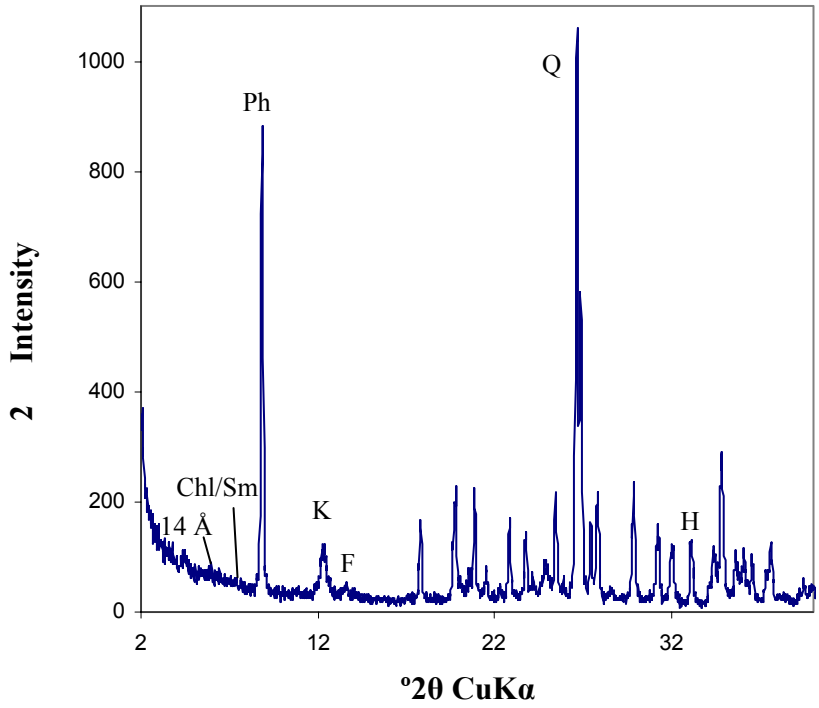

Figure 25. X-Ray diffraction pattern of the saprolitic material in interval 51-53 m CBAC 238. Ph: Phengite; K:Kaolinite; F: Feldspar; H: Hematite; Q: Quartz; Chl/Sm: Interstratified clay mineral chlorite/smectite (or chlorite/vermiculite).

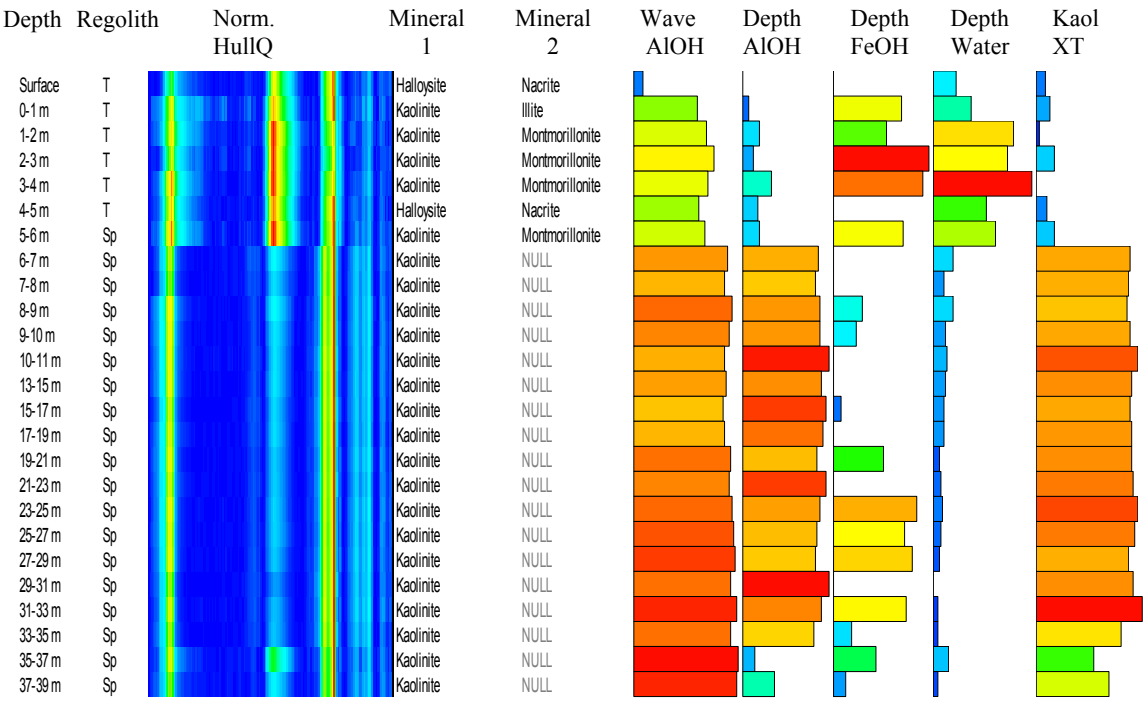

Figure 26. PIMA analysis of the regolith profile from drill hole CBAC245 derived from granite. Mica has been completely weathered into kaolinite. T: Transported regolith; Sp: Saprolite (*in situ* regolith).

4.5 Geochemistry

Inspection of the geochemical data from the Byrock drilling program revealed that several profiles contain samples with anomalous levels of base metals. Nine of these profiles were selected for detailed investigation of their geochemistry relative to mineralogy in order to understand the significance of the geochemistry (see Appendix 10 for geochemical data quality and reliability and Appendix 11 for ALS-Chemex data certificate for the Byrock drilling program). Mineralogical data were provided by PIMA (and in some cases, X-ray Diffraction traces) (Section 4.4 and Appendix 2) and interpretation of the distribution of carbonate (as determined by HCl acid attack: Appendix 1).

4.5.1 Mineralisation associated with mafic rocks

Gold mineralisation, with no consistent presence of pathfinders, occurs in and adjacent to mafic material in CBAC198, CBAC200, CBAC201 and CBAC243.

Drill hole CBAC198 contains 0.02 g/t Au between 14 and 18 m. In detail the hole passes from kaolinite and illite into *in situ* material characterised by calcite and dolomite with muscovite and kaolinite from 1 to 9 m. Smectite tends to be present in the upper 3 m of saprolite (Figure 27). Zinc is elevated in the interval 1-5m and Pb from 3-18 m, especially between 6-15 m where Pb is commonly >1000 ppm but no other pathfinder elements are present, although elevated Au occurs between 14 and 18 m. The basal portion of this hole (48-51 m *i.e.,* 30m below the mineralisation) is characterised by a PIMA spectrum, NULL+NULL, typical of weathered mafic material (*cf.* Section 4.4.3.2). Such an identification is verified by the elevated Fe, Mg, Mn, Ni, P, Sr, Ti and V (Figure 27 and Appendix 4) and the Ti/Zr in the basal material = 91. Mineralisation in the hole varies upwards from Au to Pb to Zn with distance from the mafic material.

Anomalous Au (0.006 g/t) occurs from 22-66 m in CBAC243. Transported material characterised by 2 m of kaolinite overlying 8 m of kaolinite and montmorillonite overlies residual material in this drill hole (Figure 28). No calcrete is observed in this drill hole (Appendix 1). PIMA signatures of kaolinite+NULL occur from 12-33 m generally coincide with the interval defined by elevated Fe and sporadic Cr, V and P. These associations suggest the presence of mafic material (Figure 28 and Appendix 4). The anomalous Au occurs partly in this mafic interval and for 30 m into the underlying sedimentary rocks. No chalcophile elements are associated with the Au, although elevated As occurs higher in the profile (at 8 and 21 m), on the edges of the mafic material.

4.5.2 Gold mineralisation not obviously associated with mafic material

A thick sequence of anomalous Au (39 m @ 0.04g/t) occurs from 27 m to the base of the hole in CBAC 238 associated with a shear in the Lord Carrington area, 20 km northeast of Byrock. Three metres of transported material in this hole contains kaolinite and montmorillonite with calcrete also occurring about the unconformity (see Ca contents: Figure 29 and Appendix 1). The phyllosilicates of the residual saprolite are kaolinite and phengite but magnetite, feldspars, quartz and hematite are also present with chlorite present at depth (Section 4.4.3). High Ca and P contents between 33-47 m (Figure 29) reflect apatite. Although Zn varies from >100 ppm below the unconformity to 15 m and >150 ppm below that, no other chalcophile element is present in the Au-rich interval.

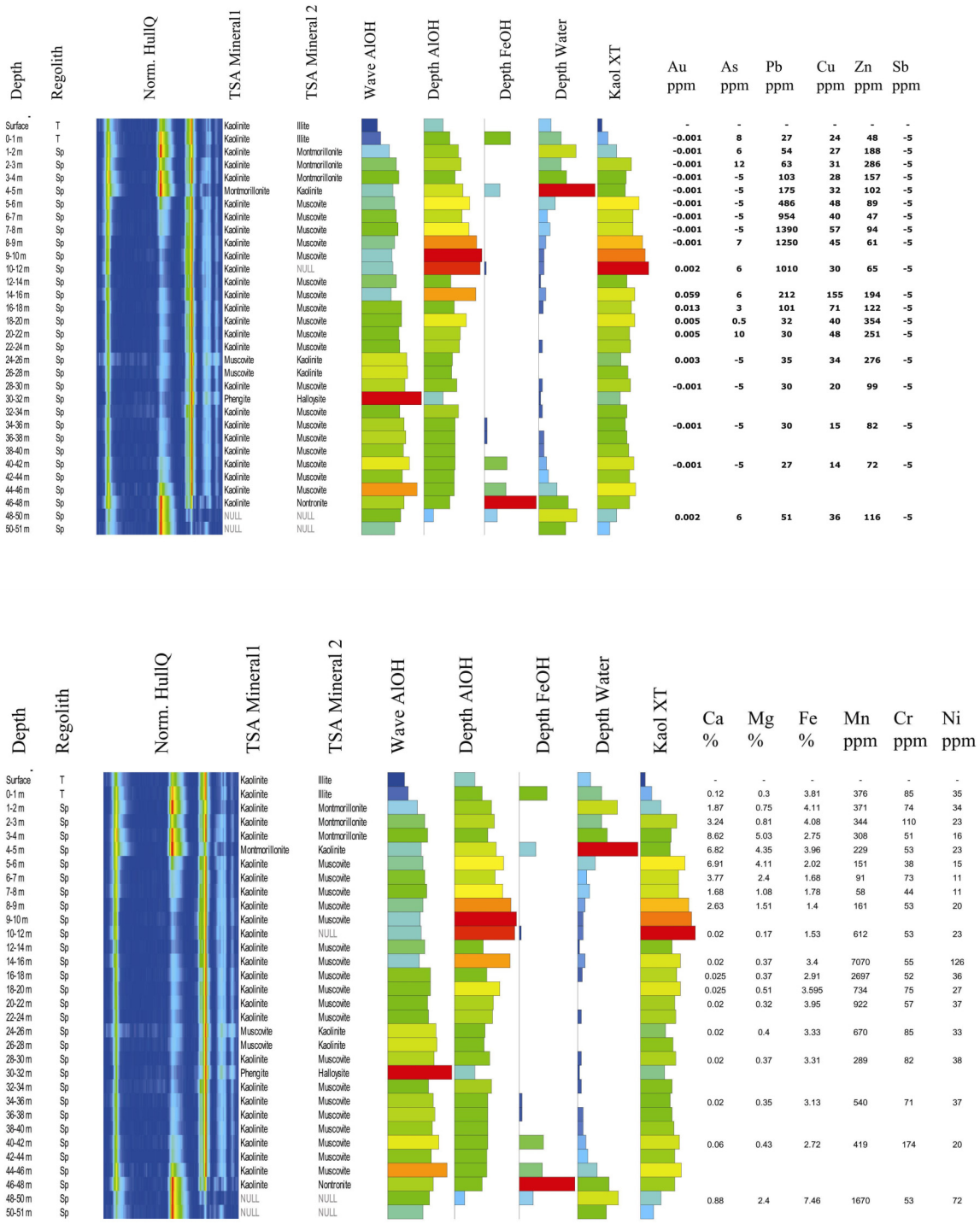

Figure 27. PIMA analysis and selected geochemical data of the regolith profile for drill hole CBAC198.

In CBAC191, Au values >0.01 g/t (and exceeding 0.03 g/t in some metre intervals) occur intermittently from 5-24 m but is not associated with elevated chalcophile element contents, except perhaps Zn (Figure 30). Although calcrete occurs to 3 m *i.e.,* about the unconformity (Appendix 1), Au is not elevated in this horizon.

Gold >0.008g/t occurs from 43 m to the base of the hole (54 m) in CBAC211. Although there are elevated As, Sb and Zn values in this hole they occur above the Au zone and in the case of a As-Sb association, at the base of the calcrete zone (around 7 m: Appendix 1) and are not specifically associated with the Au (Figure 31). Montmorillonite is associated with the upper portion of the calcrete horizon and increasing Mg relative to Ca below the unconformity at 3 m (Appendix 4) suggests that the calcrete horizon may vary from calcite- to dolomite-dominant. Again there is no elevated Au in the carbonate-rich samples.

4.5.3 Anomalous As occurrences

Arsenic values > 50 ppm occur intermittently throughout CBAC206 (Figure 32) but there are no substantial amounts of other chalcophile elements or Au present. Calcrete (probably dominantly dolomite, based on Ca vs Mg: Appendix 6) occurs in the top 5 m of the hole (see also Appendix 1) but there is no smectite development or Au association.

4.5.4 Anomalous Zn occurrences

In CBAC234, Zn ≥100 ppm, and even > 200 ppm, occurs from 35 m to the base of the hole (46 m: Figure 33). Such occurrences are associated with elevated Fe, Co, Cr, V, Mg and Mn (Figure 33 and Appendix 4) but no chalcophile elements. This elemental association suggests the presence of intermediate rocks, a suspicion confirmed by Ti/Zr=54 and the petrographic identification of monzodiorite (Barron *in* Fleming and Hicks, 2003). Thus the presence of Zn appears to be related to the occurrence of the intermediate rock and its depletion up the profile reflects normal weathering/dispersion processes. Calcrete, dominantly dolomite (see Ca *vs* Mg: Appendix 6), occurs from 2-7 m and is associated with smectite development in the transported material.

4.5.5 Anomalous Co±Zn occurrences

Highly anomalous Co occurs associated with Mn in the basal sample of CBAC215 and Co+Zn occurs with thousands of ppm Mn from 15-33 m in CBAC 201 (Figure 34). Although this latter case is associated with the presence of mafic material below 51 m, such occurrences with no other associated chalcophile elements are stongly suggestive of an association of Co and Zn with Mn oxides at a former water table (*cf*. McQueen, 2004).

4.5.6 Sulfate occurrences

Sulfur >0.1% is present over at least 5 m, and commonly >10 m, in drill holes CBAC207, **213**, **216**, 221, 222, 223, **226**, 235, **236** and 242 (with the drill holes outlined in bold having >0.5% in at least one sample). The occurrence of most of these drill holes in a tight geographical area is interesting. High S contents in the absence of chalcophile elements and Au, suggests that the S may be present as gypsum, consistent with deposition in a lacustrine environment. However not all the S is necessarily present as gypsum. Alunite was identified in CBAC226 and close to the unconformity in CBAC213 (Section 4.4.2.4; Figure 35). The presence of alunite would also be consistent with development in a lacustrine environment.

4.5.7 Calcrete Geochemistry

Calcrete samples collected across the Byrock area included nodular and bedrock-coating morphologies (see Appendix 5 for analyses and sample locations). The calcrete samples comprise both calcite- and dolomite-rich varieties. Dolomite-rich samples are from near Bald Hills and possibly reflect the presence of weathered mafic source rocks in this area. One dolomite sample is from an area along the Byrock-Gongolgon road near the Tarcoom turnoff. The gold contents of the calcrete samples range from below detection (<1 ppb) to 18 ppb. Calcrete samples from the Bald Hills area (between drill hole sites CBAC194-209) have gold contents greater than 13 ppb, well above the regional threshold of 4 ppb. A calcrete sample (CC168) from within palaeovalley sediments near Pine Tree Tank (in the vicinity of CBAC215) contains 9 ppb Au and 6 ppm Ag. Calcrete developed in the underlying saprolite contains no detectable Au. The palaeovalley sediments appear to have been sourced to the west in the Bald Hills area. A calcrete sample from a small borrow pit along the Byrock road about halfway between Byrock and the Cobar-Bourke road turnoff contains 9 ppb Au. This borrow pit exposes highly sheared metasedimentary rocks and granite pods that appear to lie in a major shear zone. All the calcrete samples contain <30 ppm Cu, <20 ppm Pb and most have <50 ppm Zn, although one sample (CC180) had 105 ppm Zn.

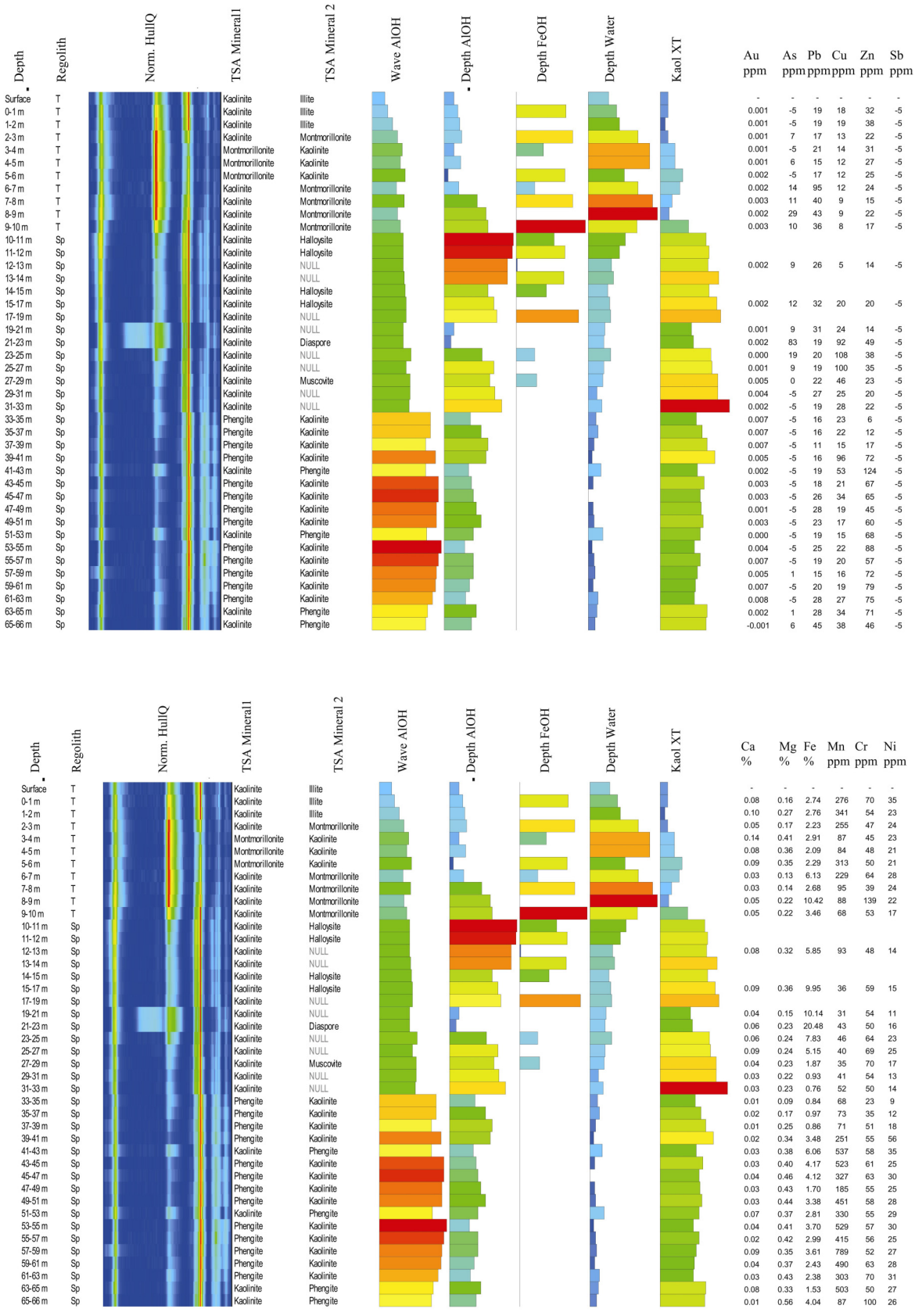

Figure 28. PIMA analysis and selected geochemical data of the regolith profile for drill hole CBAC243.

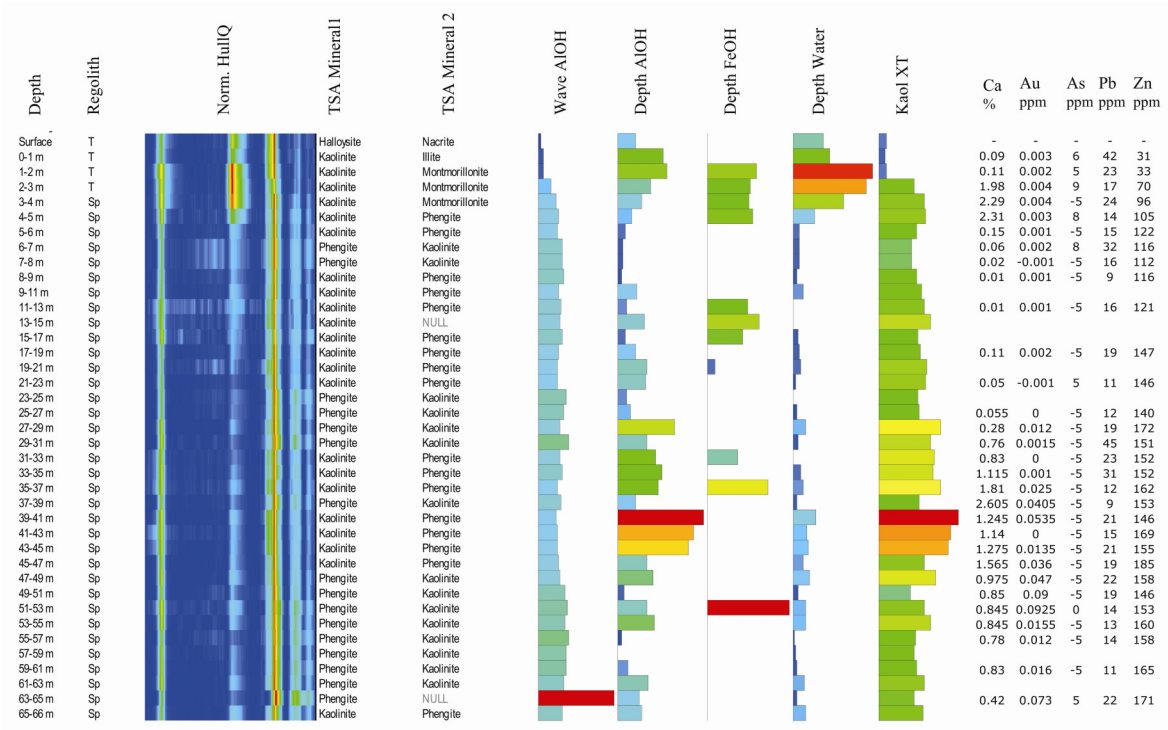

Figure 29. PIMA analysis and selected geochemical data of the regolith profile for drill hole CBAC238.

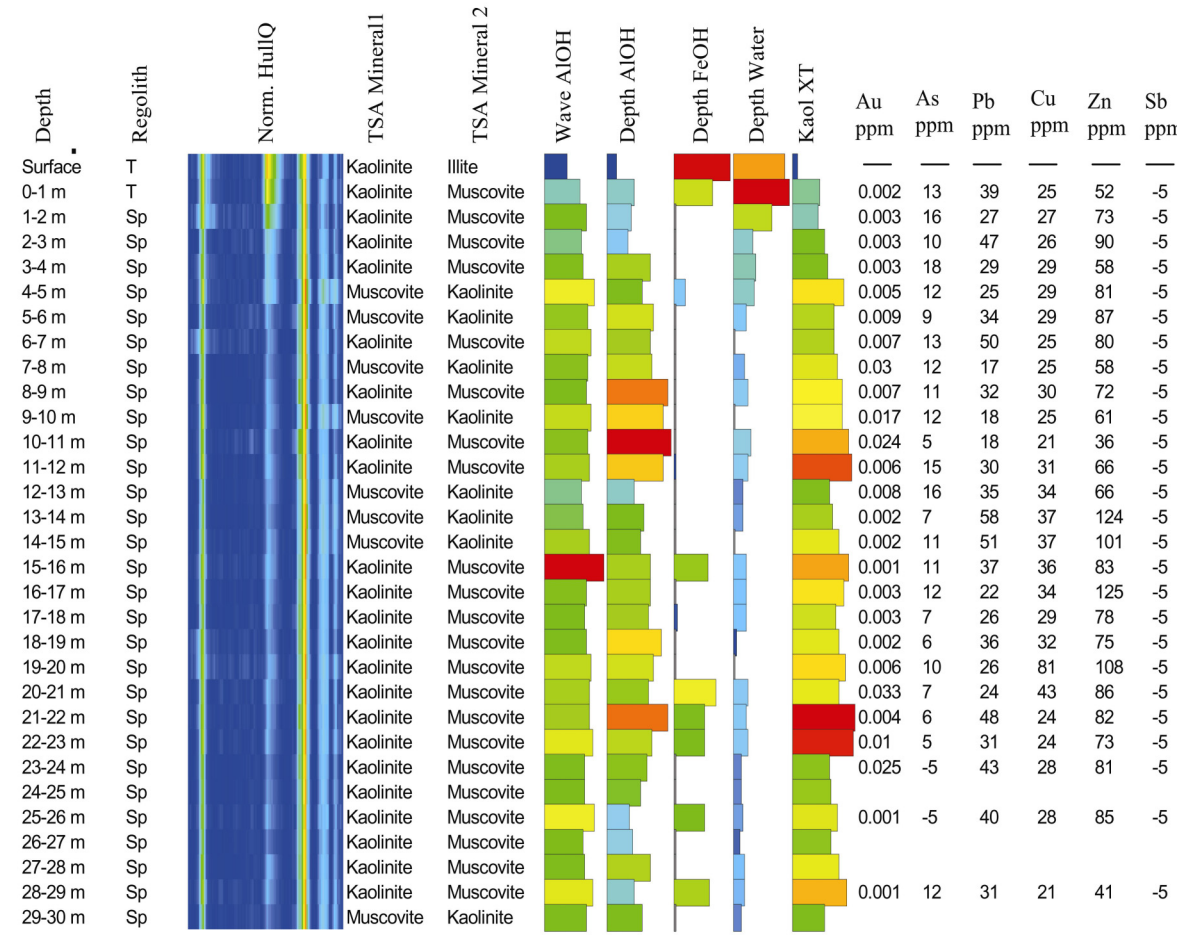

Figure 30. PIMA analysis and selected geochemical data of the regolith profile for drill hole CBAC191.

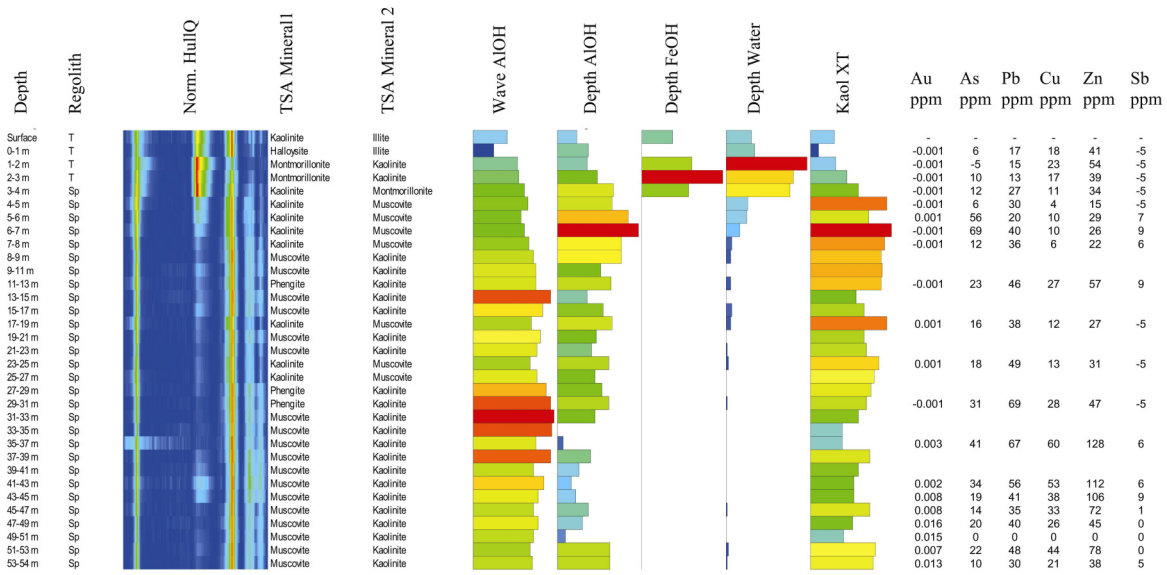

Figure 31. PIMA analysis and selected geochemical data of the regolith profile for drill hole CBAC211.

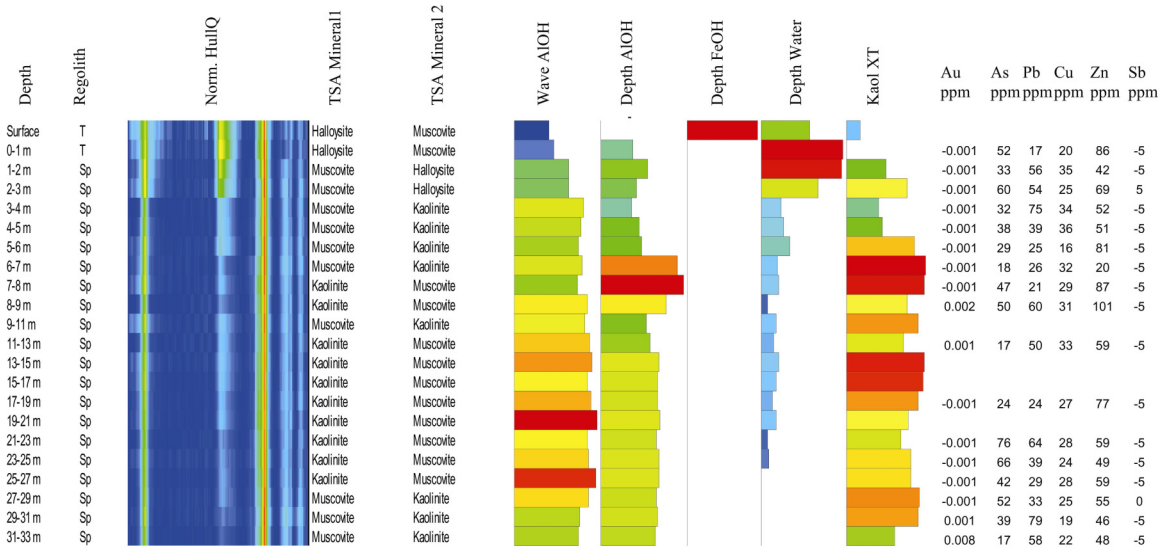

Figure 32. PIMA analysis and selected geochemical data of the regolith profile for drill hole CBAC206.

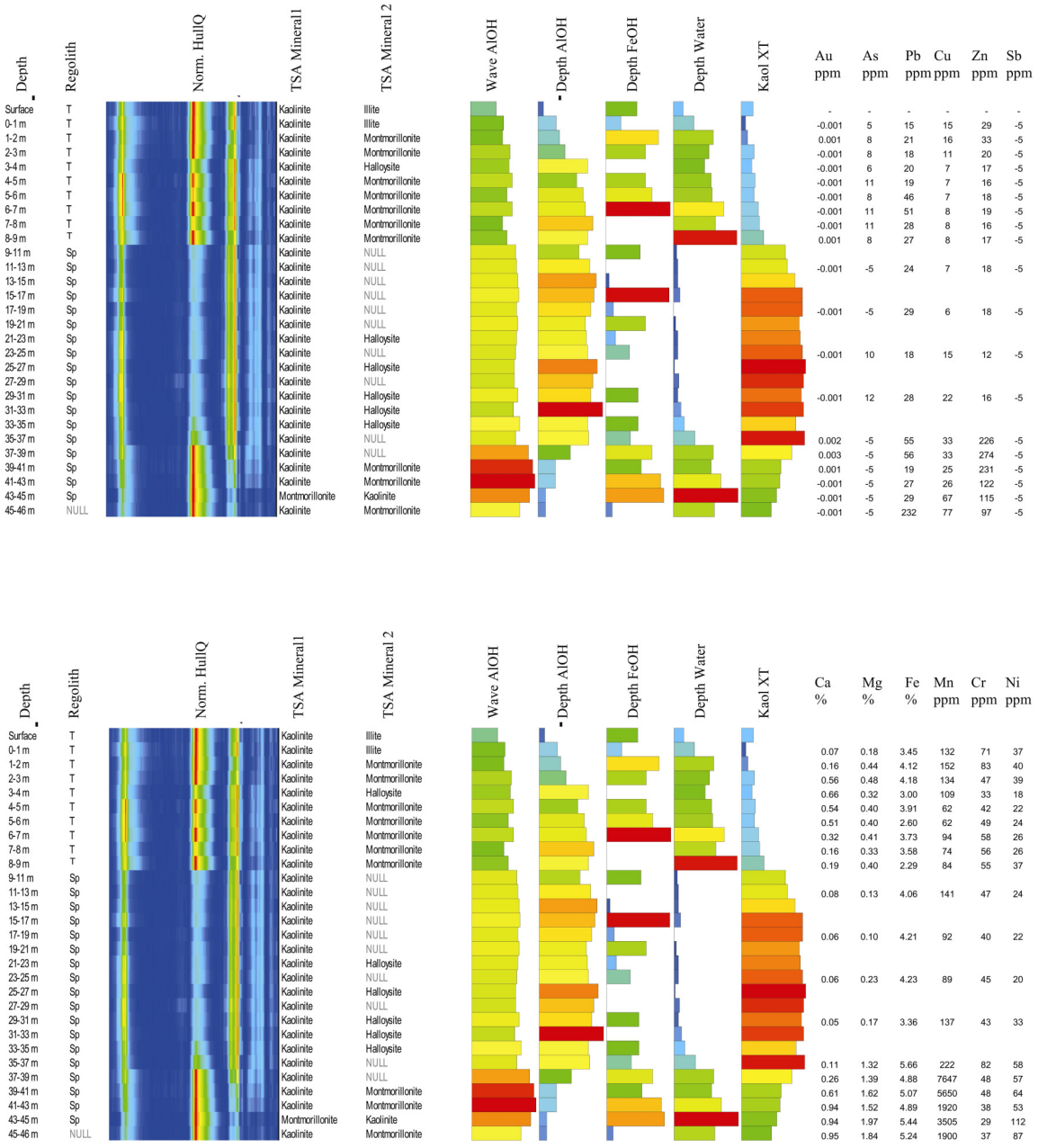

Figure 33. PIMA analysis and selected geochemical data of the regolith profile for drill hole CBAC234.

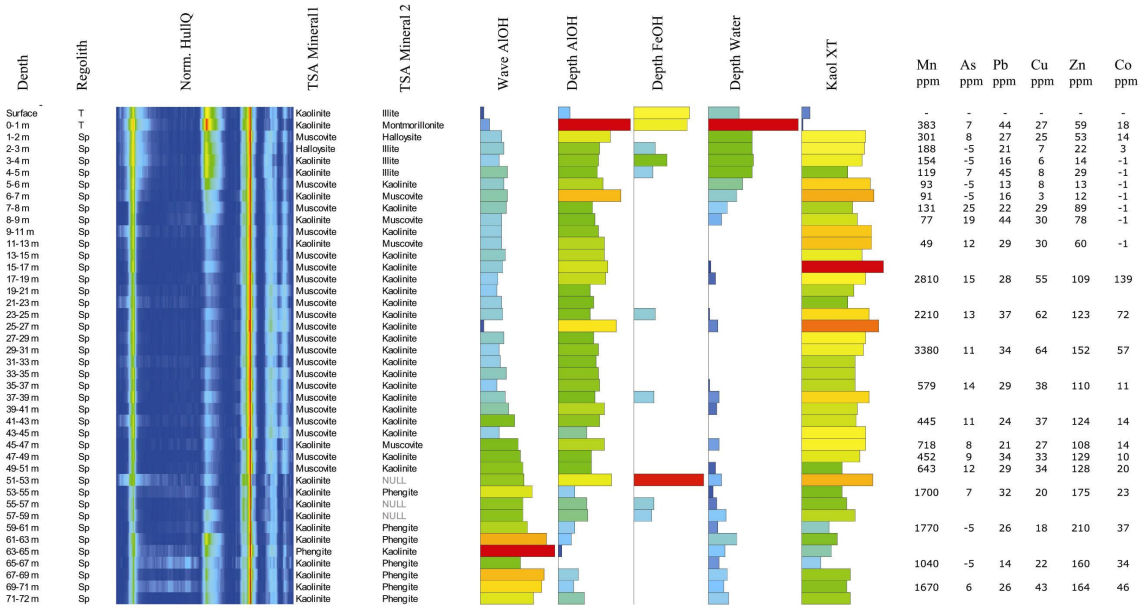

Figure 34. PIMA analysis and selected geochemical data of the regolith profile for drill hole CBAC201.

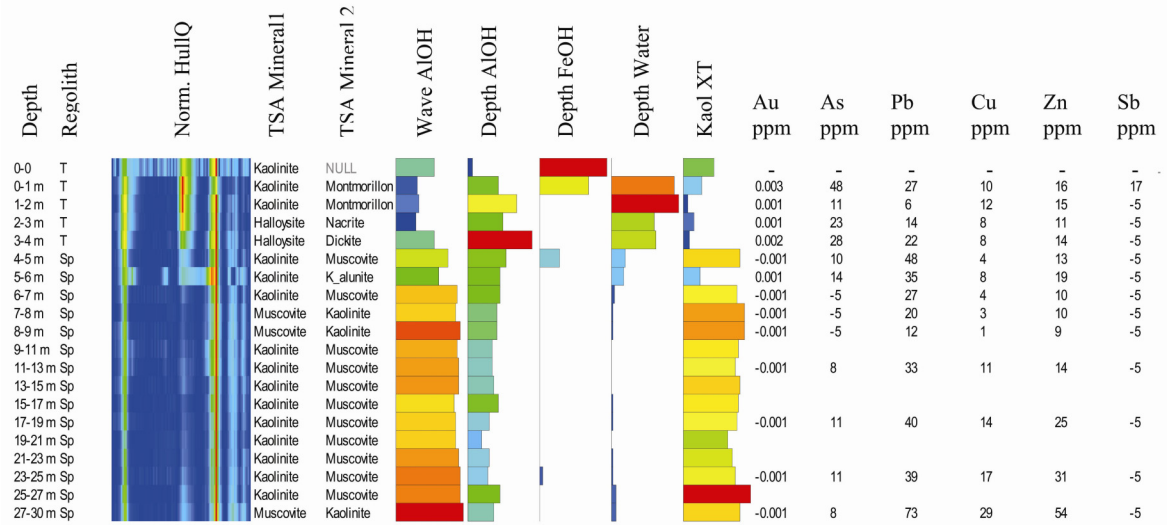

Figure 35. PIMA analysis and selected geochemical data of the regolith profile for drill hole CBAC213.

5 CONCLUSIONS

5.1 Regolith Architecture and Materials

- The regolith in the Byrock area comprises three basic units, each separated by an unconformity: Sequence 1, with inferred arid fluvial, colluvial and aeolian sediments, overlies Sequence 2, with inferred lacustrine and minor fluvial sediments, which in turn overlies *in situ* regolith (dominantly saprolite, *ie.* moderately to completely weathered bedrock). Sequence 1 sediments are up to at least 40 m thick in moderately gentle palaeovalleys up to 19 km wide. Sequence 2 sediments are up to at least 60 m thick in steep-sided palaeovalleys up to at least 8 km wide.
- Most of the Byrock area surface is covered by Sequence 1 sediments with islands and peninsulas of saprolith surrounded by rises and erosional plains covered with sheetwash deposits in the south, and depositional plains formed of sheetwash deposits and stagnant alluvial plains towards the north. The airborne radiometric imagery gives an added dimension of understanding to the regolith thickness, chemistry, provenance and degree of geomorphic activity.
- Aeolian silt-size quartz grains with clay coatings have impregnated the upper regolith layers within most regolith-landform units across the area. Aeolian sediments are highly variable in character due to different source areas and degrees of post-depositional reworking. It is therefore essential that more than one diagnostic tool be employed to ensure the correct characterisation of aeolian deposits (*i.e.* particle size, mineralogical, geochemical and morphological techniques), and that a range of different deposits are studied (ideally including sites of aeolian deposit preservation and/or where aeolian material contrasts with the underlying substrate). The aeolian component in soils of the Byrock region is predominantly in the near 70 μm size range.
- The high frequency component of airborne magnetic imagery (1VD) reveals the distribution of dendritic palaeovalleys containing magnetic sediments, which are a significant component of Sequence 1. Coincident radiometrics imagery with high thorium signature (teal colour) indicates eroded and redistributed palaeovalley sediments. Magnetic palaeosediments are mainly buried under stagnant alluvial plains and adjacent low relief depositional plains.
- The base of the palaeovalleys containing the upper sediments of Sequence 1 forms an erosional hiatus with the underlying sediments in Sequence 2. Sequence 1 sediments range from no older than mid Miocene to present, and Sequence 2 sediments are Early Miocene or older, as determined from the K/Ar date (16.8 Ma) of the leucitite flow marker.
- Some clays within Sequence 2 sediments have quartz clasts, perhaps indicating vegetation rafting in a near shore environment, or possibly a debris flow; whereas other clays have dispersed quartz grains, perhaps indicating further distance from shore, or the tail of a debris flow. Two periods of increasing and decreasing water depth, or conversely valley infilling, may be interpreted from the sequence stratigraphy of Sequence 2 sediments.
- Early Cretaceous (Aptian) Surat Basin sediments were determined from palynology on a sample from a drill hole on the western depositional plains of the Bogan River. Palynological analyses are currently continuing for Sequence 2 sediments. Sequence 1 sediments were analysed but were too oxidised for the preservation of palynomorphs incorporated into the sediment profile at the time of deposition.

- Carbonate induration occurs more commonly in Sequence 1, but does occur in Sequence 2 sediments. Ferruginous staining and induration from weathering is common in Sequence 1 sediments, whereas siliceous induration is widespread but of patchy and limited extent.
- Through detailed binocular microscopic petrography and textural analyses, with some specific validation from geochemistry, all saprolith lithologies were nominally identified, and a variety of weathering overprints (*e.g.* pink saprolite, pallid saprolite, and induration) and degree of weathering (saprolite versus saprock) were ascertained.

5.2 Mineralogy

- Two main clay mineral assemblages reflecting a toposequence association have been observed in the alluvial / colluvial / aeolian (Sequence 1) sediments:
  1. Kaolinite + illite ± muscovite ± halloysite (no smectite) assemblage mostly observed in moderate relief areas, *e.g.* CHer with thin (≤3 m) transported regolith;
  2. Kaolinite + illite + smectites ± halloysite ± muscovite assemblage is the most common mineralogical assemblage found. This material contains abundant smectites and forms thick sequences (> 3 m and up to 22 m) on stagnant alluvial plains.
- The lacustrine (Sequence 2) sediments are composed of kaolinite, and abundant illite, halloysite and smectites.
- The mineralogical assemblages observed in the *in situ* regolith reflect the nature (lithology, alteration, weathering) of the parent rocks (bedrocks), *i.e.* Girilambone Group sediments, mafic and felsic rocks, landscape and palaeolandscape position.
- Within weathered Girilambone Group rocks three main mineralogical assemblages have been distinguished:

  1. Kaolinite + muscovite ± halloysite ± smectites ± illite. Two types of profiles are observed with this mineralogical assemblage: those with muscovite and kaolinite as the only clays detected; and those with hydrated clays such as illite, halloysite and smectites in association with kaolinite or muscovite at the top of the saprolite, immediately under the transported / *in situ* unconformity;
  2. Kaolinite + muscovite + phengite ± halloysite ± illite ± smectites;
  3. Kaolinite + phengite ± halloysite ± illite ± smectites (no muscovite).
- The presence of weathered mafic rocks is indicated by:
  1. The clay mineralogy: kaolinite, halloysite and smectites/vermiculite are the only clays formed during the weathering of mafic rocks (mica and illite are not present);
  2. The clay chemical composition: kaolinite and smectites generally contain iron in their structure;
  3. PIMA TSG results show Kaolinite + NULL or NULL + NULL.
- Elevated abundances of base metals and / or gold have been detected in all the drill holes intersected by mafic intrusions.

5.3 Geochemistry

- The geochemical data confirm that the quick ICP and ICP-MS analytical methods are valuable in giving an indication of mineralisation and weathering processes.
- A number of areas with elevated gold values were detected in the Byrock region. Some of these appear to be associated with mafic rocks, including in the western part of the region near the Mt Dijou – Bald Hills area. Pathfinder elements such as

As do not appear to be strongly correlated with the anomalous gold, although Pb and Zn concentrations occur in some cases. In the Lord Carrington area, northeast of Byrock, anomalous gold occurs in weathered chlorite-phengite-magnetite bearing schists with associated intervals enriched in apatite. These schists lie in a distinctive linear to arcuate magnetic unit in the aeromagnetic imagery and may be part of a shear zone in this unit.

- Limited data on calcrete geochemistry indicate a regional enrichment of gold (*i.e.* well above a regional threshold of 4 ppb) in the area south and east of Bald Hills on the western side of the Byrock sheet. This enrichment / dispersion probably also extends into the palaeodrainage in this area.
- At one locality, anomalous Zn values were found to be associated with igneous rocks of intermediate composition (possibly monzodiorite).
- Co±Zn were found to be commonly enriched with Mn, probably reflecting redox boundaries at present or fossil water table positions.
- High levels of S (as sulfates, including gypsum and alunite) were found in some areas, related to the presence of lacustrine sediments.
- Major element geochemical data for both weathered and less weathered parts of the regolith have proved useful for interpreting the bedrock lithologies in the Byrock area. There appears to be a greater abundance of mafic rock types (probably as dykes and volcanics) in this area than in the previously studied areas to the south. The geochemical data also clearly identify the Tertiary leucitites and their weathered equivalents and the fractionated granitoids present throughout the area.
- There is potential for vein and lode-style gold mineralisation associated with mafic rocks in regolith concealed areas.

ACKNOWLEDGEMENTS

Field logging of the drill holes was done by Anthony Senior under contract to ANU. Regolith-landform mapping was done by Peter Buckley (NSW DMR). Permission to refer to regolith-landform units in Hugh Glanville's Honours Thesis (CRC LEME / ANU) of the Byrock area is acknowledged. Guy Fleming (NSW DMR) facilitated data and image procurement. Dr Peter Milligan (GA) is acknowledged for his contribution to producing the profile section lines. Christian Thun (GA) prepared samples for palynological analyses by Dr Mike MacPhail (consultant). Clive Hiliker is thanked for help with the figures for aeolian materials. Peter Lewis (NSW DMR) is thanked for his support and encouragement during this last stage, as well as the two earlier stages of this project. John Watkins (NSW DMR) is thanked for facilitating the finalisation of Plates 1, 2 and 3. Thanks also goes to the reviewers of this manuscript: Colin Pain and Dave Gibson (peer reviewers) for their timely comments; and Lisa Worrall (Program Leader) for her diligent attention to detail.

REFERENCES

Bagnold, R., 1960. *The physics of wind blown sand and desert dunes.* (Methuen: London).

Blevin, P.L. and Jones, M., 2004. Granites of the Bourke-Byrock-Brewarrina region. *In:* McQueen, K.G. and Scott, K.M (Eds). *Exploration Field Workshop Cobar Region 2004*, Proceedings, pp.10-14. CRC LEME.

Braithwaite, R.L., 1974. Exploration reports, EL 684, Bald Hills. Newmont Pty Ltd. Report. Geological Survey of New South Wales, File GS1974/399 (unpubl.).

Bureau of Meteorology, 2003. www.bom.gov.au/climate/averages/tables.

Byrnes, J.G., 1993. Bourke 1:250 000 Metallogenic Map SH/55-10. Metallogenic Study and Mineral Deposit Data Sheets. 127 pp. Geological Survey of New South Wales, Sydney.

Campbell, J., 2003. Limitations in the laser particle sizing of soils. *In*: Roach I. (Ed.). *Advances in Regolith: Regional Regolith Symposia 2003*, pp. 38-42. CRC LEME.

Capnerhurst, K.R., 2003. Geochemistry of gossan samples collected on the Bourke 1:250 000 Sheet. Geological Survey of New South Wales, Report GS 20003/437 (unpubl.).

Chan, R.A., Greene, R.S.B., de Souza Kovacs, N., Maly, B.E.R., McQueen, K.G, and Scott, K.M., 2003a. Regolith, geomorphology, geochemistry and mineralization of the Susex-Coolabah area in the Cobar-Girilambone Region, North-Western Lachlan Foldbelt, NSW. Cooperative Research Centre for Landscape Environments and Mineral Exploration, CRC LEME Report 148, second impression (first impression: CRC LEME Report 166, 2001).

Chan, R.A., Greene, R.S.B., Hicks, M., Maly, B.E.R., McQueen, K.G., and Scott, K.M., 2003b. Regolith architecture and geochemistry of the Hermidale area of the Girilambone Region, North-Western Lachlan Foldbelt, NSW. Cooperative Research Centre for Landscape Environments and Mineral Exploration, CRC LEME Open File Report 149, second impression (first impression: CRC LEME Report 179, 2002).

CRA Exploration Pty Ltd., 1982. Exploration reports EL 1869, Byrock area. Geological Survey of New South Wales, Report GS 1982/578 (unpubl.).

Fleming, G. and Hicks, M., 2003 Preparations for third programme of shallow reconnaissance aircore drilling, Byrock area, Cobar NSW. Interim Report, March 2003. GS2003/065. Geological Survey of New South Wales.

Fleming, G. and Hicks, M., 2004. Third Programme of shallow reconnaissance aircore drilling, Byrock area, Cobar NSW: GS2004/048. Geological Survey of New South Wales.

Glanville, H.D., 2004. Regolith-landform mapping, leucitite basalt and the landscape evolution of the Byrock region, northwestern NSW. Honours Thesis. CRC LEME / ANU.

Gonzalez, O.R., 2001. The geology and landscape history of the El Capitan area, Cobar, NSW., Honours Thesis, University of Canberra (unpublished).

Gray, D.R. and Foster, D.A., 2004. Tectonic framework of the Lachlan Orogen. *In*: Beirlin, F.P. & Hough, M.A. (Eds.). *Tectonics to Mineral Discovery – Deconstructing the Lachlan Orogen*, Proceedings Volume and Field Guide. MORE-SGEG Conference, Orange, NSW, July 6-8, 2004. Geological Society of Australia Abstracts No. 74, pp. 1-20.

Hicks, M.G. and Fleming, G., 2004. Girilambone-Cobar project: A collaborative venture between NSW DMR and CRC LEME. *In:* McQueen, K.G. and Scott, K.M (Eds). *Exploration Field Workshop Cobar Region 2004*, Proceedings, pp.43-45.

Mason, J.A., Jacobs, P.M., Greene, R.S.B., and Nettleton, W.D., 2003. Sedimentary aggregates in the Peoria loess of Nebraska, U.S.A. Catena, 53, 377-397.

Metals Exploration Pty Ltd., 1981. Exploration reports, ELs 1652 and 1653, Boorindal – Mt Oxley area. Geological Survey of New South Wales, File GS1984/557 (unpubl.).

McClatchie, L., 1970. Mineralisation in the Bald Hills – Mount Dijou area. Geological Survey of New South Wales, Report GS 1969/465 (unpubl.).

McQueen, K.G., 2004. The nature, origin and exploration significance of the regolith, Girilambone-Cobar region. *In:* McQueen, K.G. and Scott, K.M (Eds). *Exploration Field Workshop Cobar Region 2004*, Proceedings, pp. 51-56.

Pain, C.F., Chan, R.A., Craig, M.A., Gibson, D.L., Kilgour, P. and Wilford, J.R., 2002. RTMAP regolith database: field hand book users guide. Second Edition. CRC LEME Report 138

Scheibner, E. 1987. Paleozoic tectonic development of Eastern Australia in relation to the Pacific region. *In:* Monger, J.W.H. and Francheteau, J. (Eds.). *Circum-Pacific orogenic belts and evolution of the Pacific Ocean Basin.* Geodynamics Series Volume 18 pp 133-165. American Geophysical Union (Washington DC) and Geological Society of America (Boulder, Colorado).

Sutherland, F.L. 1985. Regional controls in eastern Australian volcanism. *In:* Sutherland F.L., Franklin B.J. & Waltho A.E. (Eds). *Volcanism in Eastern Australia*. Geological Society of Australia Publication. N.S.W. Division **1**, 13-32.

Tate, S.E., Greene, R.S.B., Scott, K.M., and McQueen, K.G., 2003. *In:* Roach, I.C. (Ed.). *Advances in Regolith: Regional Regolith Symposia 2003*, pp. 399-405. CRC LEME.

Thomson, B.R., 1949. Geological reconnaissance of M.A.D. anomalies, Cobar and adjacent land districts. The Zinc Corporation Limited, Geological Report (unpubl.) GS1949/026.

APPENDICES

APPENDIX 1: CARBONATE DETERMINATIONS (BY ACID ATTACK) FOR BYROCK DRILLING PROGRAM

HCL 1:1; M= Major effervescence and m= minor effervescence; ===: Transported / *in situ* Regolith boundary;
No carbonates in CBAC192 andCBAC243. Drill holes are grouped according to sampling intervals.

CBAC	188	189	190	191	204	219	220	221	222	223	224	225	226	227	228	229	235	237	241	247
Surface						m		m			M									
0-1 m		m		M							M	M		m						
1-2 m	m	M	M	M	M			m		M	M	M	M	m	m					
2-3 m	M	m	M	m	M		M	M			M			M						
3-4 m	M				M			m						m	M					
4-5 m	m				M		M						M		M					m
5-6 m	m				M							M	M		M					m
6-7 m					M			M	M		M		M						m	M
7-8 m								m					m		M			M		m
8-9 m								m		M		M						M		m
9-10 m	m				M				m		m	M	m		M					m
10-11 m									M		M	M	M		M					
11-12 m									m		M	m	m		M					
12-13 m					m										M					
13-14 m											m									
14-15 m											M									
15-16 m											M									
16-17 m																				
17-18 m																				
18-19 m																				
19-20 m																	m			
20-21 m																	m			
21-22 m																				
22-23 m																				
23-24 m																				
24-25 m																				
25-26 m																				
26-27 m																				
27-28 m																				
28-29 m																				
29-30 m																				

APPENDIX 1. (continued)

CBAC	199	200	201	202	205	206	207	208	209	210	211	212	213	214	230	232	234	238	239	240	244	245	246	248
Surface								m																
0-1 m			m	m	M								m	m					m	M		m		
1-2 m		M	M	M	M	M	m	m	M		m		m	m	M			m		m			m	M
2-3 m		M	M	M	M	M	M	m	M		M	M	m	m	M			M	m	m			M	M
3-4 m		m	M	M	M	M	M	m	M		M		m	M			M	M					m	m
4-5 m	m	m	M	m	M	m	M	m		M	M	m	m				M	M	M					M
5-6 m	m		M		M		m	m		M	M		m				m						m	M
6-7 m	m		M				m	m		m	M						m				M			
7-8 m	m		M				M			M														m
8-9 m	m	m	M				M			M		m				M								m
9-11 m			m				m			M						M								
11-13 m										m														
13-15 m										M														
15-17 m																								
17-19 m																								
19-21 m																								
21-23 m																								
23-25 m																								
25-27 m																								
27-29 m																								
29-31 m																								
31-33 m																								

APPENDIX 1. (continued)

CBAC	193	194	195	196	197	198	CBAC	215	217	218	231	233	236	CBAC	216	CBAC	242
Surface							Surface							Surface		Surface	
0-1 m			M				0-1 m			M				0-1 m		0-1 m	
1-2 m			M	m	M	M	1-2 m		M	M	M	M	m	1-2 m		1-2 m	
2-3 m	M	M	M	m	M	M	2-3 m	m	m	M	M	M	M	2-3 m	M	2-3 m	
3-4 m	M	M		M	m	M	3-4 m			M	M		M	3-4 m		3-4 m	M
4-5 m	M	M		M		M	4-5 m			m			M	4-5 m		4-5 m	
5-6 m		M				M	5-6 m	M		M	M		M	5-6 m	M	5-6 m	M
6-7 m		M					6-7 m		M	M	M			6-7 m	m	6-7 m	M
7-8 m	m					M	7-8 m	M	M	M	M			7-8 m	m	7-8 m	m
8-9 m	m					M	8-9 m		m		M			8-9 m	M	8-9 m	m
9-10 m							9-10 m	m	M		M			9-10 m	m	9-10 m	
10-12 m							10-11 m	m	m	m	M			10-11 m	m	10-11 m	
12-14 m							11-12 m	m	M					11-13 m	M	11-12 m	M
14-16 m							12-13 m	M	M		M			13-15 m		12-13 m	M
16-18 m							13-14 m	m		M	M			15-17 m		13-14 m	m
18-20 m							14-15 m		m				M	17-19 m		14-15 m	
20-22 m							15-16 m		m				M	19-21 m		15-16 m	
22-24 m							16-17 m		M				M	21-23 m		16-17 m	
24-26 m							17-19 m						m	23-25 m		17-18 m	
26-28 m							19-21 m						m	25-27 m		18-19 m	
28-30 m							21-23 m							27-29 m		19-20 m	
30-32 m							23-25 m							29-31 m		20-21 m	
32-34 m							25-27 m							31-33 m		21-22 m	
34-36 m							27-29 m							33-35 m		22-23 m	
36-38 m							29-31 m							35-37 m		23-25 m	m
38-40 m							31-33 m							37-39 m		25-27 m	
40-42 m							33-35 m							39-41 m		27-29 m	M
42-44 m							35-37 m							41-43 m		29-31 m	
44-46 m							37-39 m							43-45 m		31-33 m	
46-48 m							39-41 m							45-47 m		33-35 m	
48-50 m							41-43 m							47-49 m		35-37 m	
50-52 m							43-45 m							49-51 m		37-39 m	
52-54 m							45-47 m							51-53 m		39-41 m	

APPENDIX 2: PIMA PROFILES (SPECTRA AND LOGS) FOR BYROCK DRILLING PROGRAM

See Appendicies directory on this CD.

APPENDIX 3: DEPTH OF THE UNCONFORMITY (TRANSPORTED / *IN SITU* BOUNDARY), GEOSCIENCE AUSTRALIA'S SITE IDs, AND REGOLITH-LANDFORM UNITS FOR BYROCK DRILLING PROGRAM

Field ID	GA Site ID	Base of T/*IS* bdy. (m)	Regolith Landform Unit	Field ID	GA Site ID	Base of T/*IS* bdy. (m)	Regolith-Landform Unit
CBAC188	2003701026	1	Aap	**CBAC219**	2003701023	15	ACar
CBAC189	2003701027	1	Aed	**CBAC220**	2003701055	27	ACar
CBAC190	2003701028	1	CHer	**CBAC221**	2003701056	53	Aas
CBAC191	2003701029	1	CHer	**CBAC222**	2003701057	>48	Aas
CBAC192	2003701030	1	CHer	**CBAC223**	2003701058	53	Aas
CBAC193	2003701031	3	CHpd	**CBAC224**	2003701059	29	Aas
CBAC194	2003701032	1	Aed	**CBAC225**	2003701060	27	Aas
CBAC195	2003701033	1	CHer	**CBAC226**	2003701061	>51	Aas
CBAC196	2003701034	2	CHer	**CBAC227**	2003701062	24	Aas
CBAC197	2003701035	1	CHer	**CBAC228**	2003701063	>36	Aas
CBAC198	2003701036	1	CHer	**CBAC229**	2003701064	1	SSer
CBAC199	2003701037	3	CHpd	**CBAC230**	2003701065	2	SSer
CBAC200	2003701038	2	SHer	**CBAC231**	2003701066	12	Aap
CBAC201	2003701039	1	SHer	**CBAC232**	2003701067	25	CHpd
CBAC202	2003701040	1	CHer	**CBAC233**	2003701068	1	CHer
CBAC204	2003701041	7	CHpd	**CBAC234**	2003701069	9	CHpd
CBAC205	2003701042	1	CHpd	**CBAC235**	2003701070	>43	VFvp
CBAC206	2003701043	1	CHer	**CBAC236**	2003701071	>66	Aas
CBAC207	2003701044	2	CHer	**CBAC237**	2003701072	50	Aas
CBAC208	2003701045	1	CHer	**CBAC238**	2003701073	3	CHep
CBAC209	2003701046	1	CHer	**CBAC239**	2003701074	2	CHer
CBAC210	2003701047	16	Aap	**CBAC240**	2003701075	0	SSer
CBAC211	2003701048	3	CHpd	**CBAC241**	2003701076	>34	CHpd
CBAC212	2003701049	2	CHer	**CBAC242**	2003701077	>52	Aap
CBAC213	2003701050	4	CHer	**CBAC243**	2003701024	10	Aap
CBAC214	2003701051	1	CHer	**CBAC244**	2003701078	1	CHer
CBAC215	2003701052	13	CHer	**CBAC245**	2003701079	5	Aap
CBAC216	2003701053	41	CHpd	**CBAC246**	2003701080	5	CHer
CBAC217	2003701021	15	CHpd	**CBAC247**	2003701081	23	Aap
CBAC218	2003701054	14	CHpd	**CBAC248**	2003701025	2	CHer

APPENDIX 4: GEOCHEMICAL ANALYSES FOR BYROCK DRILLING PROGRAM

See Appendicies directory on this CD.

APPENDIX 5: CALCRETE ANALYSES IN BYROCK AREA

See Appendicies directory on this CD.

APPENDIX 6: END OF DRILL HOLE DEPTH FOR BYROCK DRILLING PROGRAM

Field Id	EOH (m)	Field Id	EOH (m)
CBAC188	22	CBAC219	60
CBAC189	6	CBAC220	57
CBAC190	27	CBAC221	72
CBAC191	30	CBAC222	48
CBAC192	24	CBAC223	63
CBAC193	51	CBAC224	72
CBAC194	12.5	CBAC225	69
CBAC195	33	CBAC226	51
CBAC196	27	CBAC227	72
CBAC197	33	CBAC228	36
CBAC198	51.5	CBAC229	15
CBAC199	24	CBAC230	24
CBAC200	54.5	CBAC231	53
CBAC201	72	CBAC232	49
CBAC202	13	CBAC233	28
CBAC204	57	CBAC234	46
CBAC205	18	CBAC235	43
CBAC206	33	CBAC236	66
CBAC207	51	CBAC237	57.5
CBAC208	33	CBAC238	66
CBAC209	39	CBAC239	30
CBAC210	55	CBAC240	21
CBAC211	54	CBAC241	34
CBAC212	57	CBAC242	52
CBAC213	30	CBAC243	66
CBAC214	63	CBAC244	18
CBAC215	60	CBAC245	39
CBAC216	72	CBAC246	66
CBAC217	65.5	CBAC247	64.7
CBAC218	51	CBAC248	60

APPENDIX 7: PALYNOLOGY FOR DRILL HOLE CBAC242 AT 51-52 m DEPTH, BYROCK DRILLING PROGRAM

Palynology from report by Dr. M.K. Macphail, Consultant Palynological Services.

MFP No:	1272927
Sub-basin:	western Surat
Lithology:	organic-rich dark mudstone?
Yield (Kerogen):	high, dominated by structured terrestrial
Yield (dinocysts):	none observed
Yield (spore-pollen):	high
Depositional environment:	freshwater lacustrine
'Best fit' age:	Aptian
Zone:	*Cyclosporites hughesii* Zone based on *Cyclosporites hughesii* and multiple specimens of *Pilosisporites notensis* in an assemblage which is dominated by long-ranging Early Cretaceous taxa but lacking the indicator species of the *Crybelosporites striatus* Zone
Confidence rating:	high
Maximum age:	*Cyclosporites hughesii* Zone based on rare *Cyclosporites hughesii* associated with multiple specimens of *Pilosisporites notensis* and *Trilobosporites trioreticulosus*
Minimum age:	*Cyclosporites hughesii* Zone based on absence of *C. striatus* Zone indicators
Comment:	The diversity is surprisingly low for the (very high) yield. The assemblage is unusual in that the nominate species *Cyclosporites hughesii* is very rare whilst *Foraminisporis asymmetricus* which is commonly found in samples of Aptian age, is absent. Conversely the high relative abundance of cnidoblasts is (in my experience) unique in an Early Cretaceous context.

APPENDIX 8: CLAY MINERALOGY OF THE TRANSPORTED REGOLITH FOR THE BYROCK DRILLING PROGRAM

Drill Hole	Elevation (m)	Depth (m)	Regolith Landform Unit	Kaolinite		Illite		Muscovite		Smectite		Halloysite	
				M	m	M	m	M	m	M	m	M	m
CBAC188	206	1	Aap	+			+						
CBAC189	212	1	Aed	+	+		+	+					
CBAC190	220	1	CHer	+			+		+				
CBAC191	210	1	CHer	+			+		+				
CBAC192	205	1	CHer	+			+		+				
CBAC193	196	3	CHpd	+	+		+	+					+
CBAC194	193	1	Aed	+			+						
CBAC195	192	1	CHer	+			+						
CBAC196	190	2	CHer	+			+				+		
CBAC197	190	1	CHer	+			+						
CBAC198	182	1	CHer	+			+						
CBAC199	182	3	CHpd	+			+						
CBAC200	184	2	SHer	+	+		+						
CBAC201	186	1	SHer	+			+				+		
CBAC202	186	1	CHer	+			+						
CBAC204	176	7	CHpd	+	+		+		+	+	+	+	
CBAC205	179	1	CHpd	+			+					+	
CBAC206	173	1	CHer						+			+	
CBAC207	169	2	CHer	+			+		+			+	
CBAC208	168	1	CHer	+			+					+	
CBAC209	167	1	CHer	+			+		+				
CBAC210	165	16	Aap	+			+		+		+	+	+
CBAC211	166	3	CHpd	+	+		+			+			
CBAC212	165	2	CHer	+			+						
CBAC213	161	4	CHer	+	+						+	+	
CBAC214	159	1	CHer	+			+		+				
CBAC215	158	13	CHer	+	+		+			+		+	+
CBAC216	155	41	CHpd	+	+		+		+	+	+	+	+
CBAC217	153	15	CHpd	+	+		+			+	+	+	+
CBAC218	151	14	CHpd	+	+		+			+	+	+	+

M= major clay; m: Minor clay.

APPENDIX 8. (continued)

Drill Hole	Elevation (m)	Depth (m)	Regolith Landform Unit	Kaolinite		Illite		Muscovite		Smectite		Halloysite	
				M	m	M	m	M	m	M	m	M	m
CBAC219	149	15	ACar	+	+		+			+	+	+	+
CBAC220	149	27	ACar	+	+		+			+	+	+	+
CBAC221	149	53	Aas	+	+		+		+	+	+	+	+
CBAC222	148	>48	Aas	+	+		+			+	+	+	+
CBAC223	147	53	Aas	+	+		+		+	+	+	+	
CBAC224	147	29	Aas	+	+		+			+	+		+
CBAC225	147	27	Aas	+	+		+			+	+	+	
CBAC226	146	>51	Aas	+	+		+		+	+	+		
CBAC227	145	24	Aas	+	+		+			+	+	+	
CBAC228	145	>36	Aas	+	+		+		+	+	+	+	+
CBAC229	152	1	SSer	+			+						
CBAC230	154	2	SSer	+			+			+			+
CBAC231	151	12	Aap	+	+		+	+		+	+	+	
CBAC232	149	25	CHpd	+	+		+				+	+	+
CBAC233	155	1	CHer	+			+						
CBAC234	155	9	CHpd	+			+				+		+
CBAC235	154	>43	VFvp	+	+		+		+	+	+	+	+
CBAC236	148	>66	Aas	+	+		+		+	+	+		+
CBAC237	145	50	Aas	+	+	+	+			+	+	+	
CBAC238	169	3	CHep	+	+		+				+	+	
CBAC239	188	2	CHer	+			+				+		
CBAC240	198	0	SSer	+			+						
CBAC241	155	>34	CHpd	+	+		+			+	+	+	+
CBAC242	138	>52	Aap	+	+		+			+	+	+	+
CBAC243	149	10	Aap	+	+		+			+	+		
CBAC244	176	1	CHer	+			+						
CBAC245	198	5	Aap	+	+		+				+	+	
CBAC246	185	5	CHer	+	+		+			+	+	+	
CBAC247	166	23	Aap	+	+		+			+	+	+	+
CBAC248	182	2	CHer	+			+			+			+

M= major clay; m: Minor clay.

APPENDIX 9: CLAY MINERALOGY OF THE *IN SITU* REGOLITH FOR THE BYROCK DRILLING PROGRAM

Drill Hole	K+M±H±I±Sm	K+M±Ph±H±I±Sm	K+Ph±H±I±Sm	K(Fe)±N±Null	K±H±Sm±I
CBAC188					
CBAC189					
CBAC190					
CBAC191					
CBAC192					
CBAC193					
CBAC194					
CBAC195					
CBAC196					
CBAC197					
CBAC198					
CBAC199					
CBAC200					
CBAC201					
CBAC202					
CBAC204					
CBAC205					
CBAC206					
CBAC207					
CBAC208					
CBAC209					
CBAC210					
CBAC211					
CBAC212					
CBAC213					
CBAC214					
CBAC215					
CBAC216					
CBAC217					
CBAC218					
CBAC219					
CBAC220					
CBAC221					
CBAC222	All Transported				
CBAC223	All Transported				
CBAC224					
CBAC225					
CBAC226	All Transported				
CBAC227					
CBAC228	All Transported				
CBAC229					
CBAC230					
CBAC231					
CBAC232					
CBAC233					
CBAC234					
CBAC235	All Transported				
CBAC236	All Transported				
CBAC237					
CBAC238					
CBAC239					
CBAC240					
CBAC241	All Transported				
CBAC242	All Transported				
CBAC243					
CBAC244					
CBAC245					
CBAC246					
CBAC247					
CBAC248					

K: Kaolinite; M: Muscovite; Ph: Phengite; H: Halloysite; I: Illite; Sm: Smectite.

APPENDIX 10: GEOCHEMICAL DATA QUALITY AND RELIABILITY FOR THE BYROCK DRILLING PROGRAM

A10–1. Analytical Precision

As a continuing test of analytical precision for the multi acid digest and ICP-MS and ICP-OES methods, replicates of a reference sample analysed as part of the previous (Hermidale) stage of the project were submitted for analysis with the batches of samples for this study. The results of the replicate analyses are presented in Table A10-1. They confirm previous results, which show that the multi acid digest approach was able to achieve very good precision for most major elements, except K (possibly reflecting non-total digestion of muscovite or variable formation of potassium perchlorate during the digestion process used), and to some extent Al (which is the most abundant element, with variability possibly reflecting imperfect homogenisation of the sample). Minor elements likely to be largely or partly hosted by resistate minerals, such as Ti, Cr, and Zr show significant variability. For most trace elements precision was good except for As and Bi and several elements at or very close to the limit of detection (Cd, Co, Mo and Sb). The replicate analyses for gold show values around 3-4 ppb, a little above the detection limit of 1 ppb. Comparisons between replicate analyses from the Byrock study and the mean values from the previous study are shown diagrammatically in Figure A10-1.

A10–2. Laboratory Precision and Accuracy

A series of laboratory duplicates were analysed for 136 of the samples submitted to ALS-Chemex laboratories. Results of these duplicate determinations are presented in Appendix 11. A number of internal standards were also analysed by the laboratory during analysis of the Byrock samples and results are also shown at the end of Appendix 11.

Sample No.	Au (ppm)	Ag (ppm)	Al (%)	As (ppm)	Ba (ppm)	Be (ppm)	Bi (ppm)
CB1791	0.004	-0.5	11.16	12	824	4.3	4
CB1792	0.004	-0.5	11.46	11	833	4.7	-2
CB1793	0.002	-0.5	11.61	17	849	4.7	7
CB1794	0.002	-0.5	10.13	13	760	4.7	6
CB1795	0.002	-0.5	9.78	14	716	4.8	6
CB4042	**0.004**	**-0.5**	**12.05**	**12**	**810**	**5**	**-2**
CB4043	**0.003**	**-0.5**	**13**	**14**	**880**	**5.1**	**2**
Stand dev	0.001	0.00	1.1	1.98	55	0.3	3.8

Sample No.	Ca (%)	Cd (ppm)	Co (ppm)	Cr (ppm)	Cu (ppm)	Fe (%)	K (%)
CB1791	0.01	-0.5	2	96	33	5.37	2.21
CB1792	0.01	-0.5	2	104	36	5.49	1.11
CB1793	0.01	-0.5	2	110	35	5.48	2.57
CB1794	-0.01	-0.5	2	114	35	5.23	1.98
CB1795	-0.01	-0.5	2	115	35	5.21	1.9
CB4042	**0.02**	**0.6**	**-1**	**116**	**37**	**5.66**	**3.42**
CB4043	**0.02**	**0.5**	**1**	**118**	**37**	**5.8**	**2.85**
Stand dev	0.01	0.51	1.13	8	1	0.26	0.74

Sample No.	Mg (%)	Mn (ppm)	Mo (ppm)	Na (%)	Ni (ppm)	P (ppm)	Pb (ppm)
CB1791	0.52	67	-1	0.09	24	574	32
CB1792	0.52	70	-1	0.09	26	692	33
CB1793	0.53	70	1	0.09	26	667	32
CB1794	0.47	68	-1	0.09	25	647	28
CB1795	0.45	65	-1	0.09	25	645	26
CB4042	**0.55**	**74**	**1**	**0.1**	**27**	**710**	**30**
CB4043	**0.57**	**74**	**1**	**0.1**	**26**	**730**	**30**
Stand dev	0.04	3	1.07	0.00	1.0	52	2.5

Sample No.	S (%)	Sb (ppm)	Sr (ppm)	Ti (%)	V (ppm)	W (ppm)	Zn (ppm)
CB1791	-0.01	6	41	0.13	124	-10	84
CB1792	-0.01	-5	42	0.37	131	-10	86
CB1793	-0.01	-5	44	0.34	130	-10	86
CB1794	-0.01	9	35	0.27	132	-10	85
CB1795	-0.01	-5	34	0.31	131	-10	84
CB4042	**-0.01**	**-5**	**38**	**0.34**	**132**	**-10**	**86**
CB4043	**-0.01**	**5**	**45**	**0.48**	**136**	**-10**	**89**
Stand dev	0.00	6.4	4.3	0.11	4	0.00	1.7

Sample No.	Zr (ppm)
CB1791	93
CB1792	105
CB1793	106
CB1794	102
CB1795	103
Stand dev	5

Table A10-1: Replicate analyses and standard deviations for samples from CBAC150 (31-33m). Bold samples submitted with Byrock sample batch. Other samples from previous Hermidale batch.

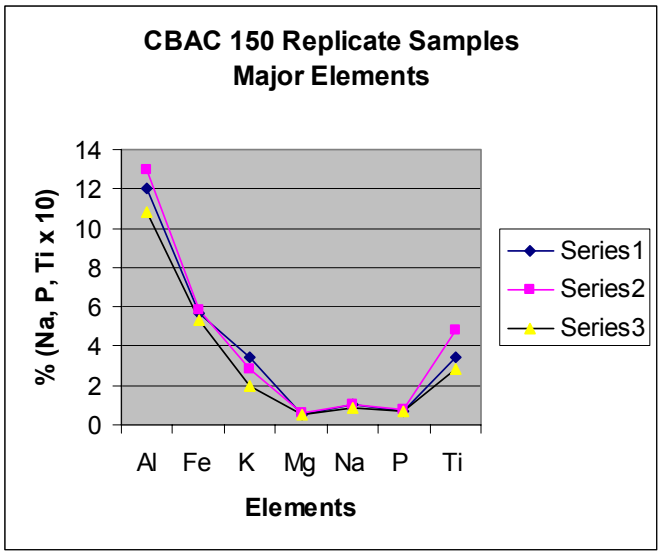

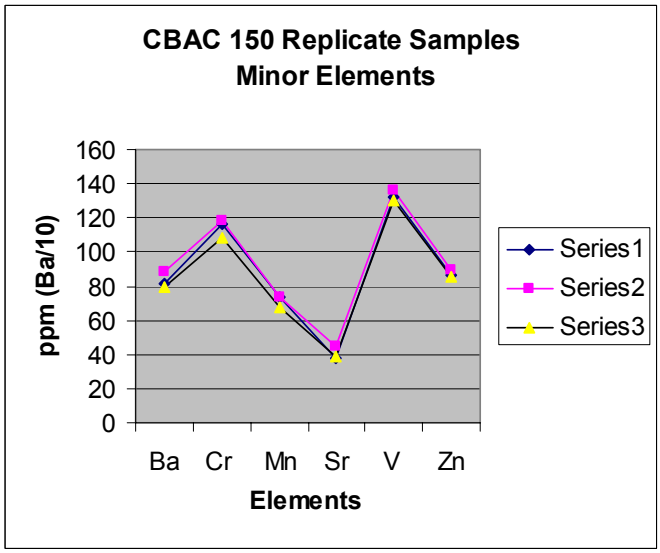

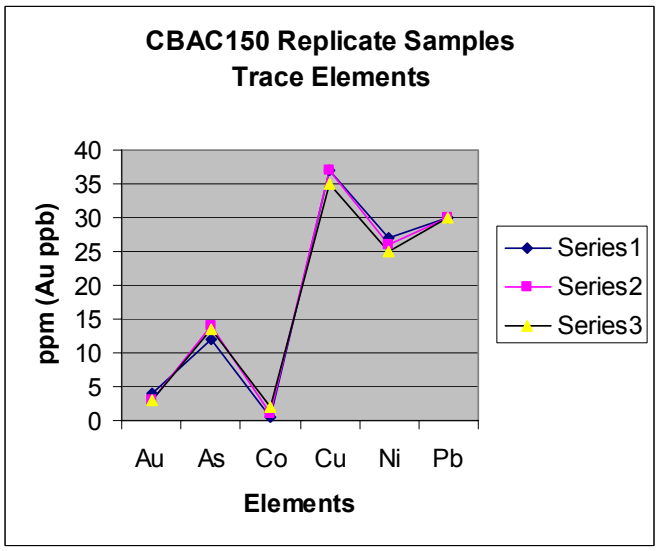

Figure A10-1. Plots showing results of replicate analyses of major, minor and trace elements for subsamples from CBAC150 32-33m. Series 1 and 2 are CB4042 and CB4043. Series 3 is mean of 5 samples analysed previously.

A10–3. Sample Representativeness

To test the degree to which samples are representative of the bulk interval sampled by air core drilling, duplicate samples were collected from the same bulk samples. Most of the duplicates were collected from the bulk sample bags during a second stage of re-sampling, one month after the original sampling. Comparisons for major, minor and trace elements for ten pairs of duplicates are presented in Figs A10-2,3,4. Most duplicates show good comparison, except for some elements including Al, K, Mn, As, Bi, Mo and Au. Some of these elements (Al and K) showed variability in the replicate samples suggesting lower analytical precision. Aluminium in particular shows poor results for this set of duplicates, especially where its abundance is greater than about 6%. This may partly reflect lower precision for Al at high concentrations. The previous Hermidale study showed better comparison of Al in duplicates but Al abundance in these previous duplicates was less than 8%. Also a large number of the duplicates for the present project were composite samples (amounts combined from a number of sample intervals) and there may have been insufficient attention paid to proper sampling, resulting in greater heterogeneity of bulked duplicates. This effect will show up most in major elements that are hosted by particular components of the sample e.g. clay versus quartz. Gold in the duplicates does not compare as well as in the previous study, again possibly reflecting poor sampling procedure. Iron and elements associated with iron oxides/oxyhydroxides (such as Cu, Zn, Pb, Cr and V) compare well and have been less effected by heterogeneity between duplicates (possibly because these oxide phases are more evenly distributed between samples). The duplicates compare poorly for As and Bi, probably reflecting poor analytical precision for these elements. These results combined with those from the previous Hermidale study suggest that the bulk samples from the air core drilling technique are reasonably well homogenised and that 0.5 kg samples from a single bulk sample give a good representation of the total sample. However, care needs to be taken when making up composite samples from several sample intervals to ensure that the same volume of sample is taken from each bulk. We suggest that equal amounts be carefully taken from each sample with a sampling spear, rather than the grab sample approach that appears to have been taken by the field technician in this case.

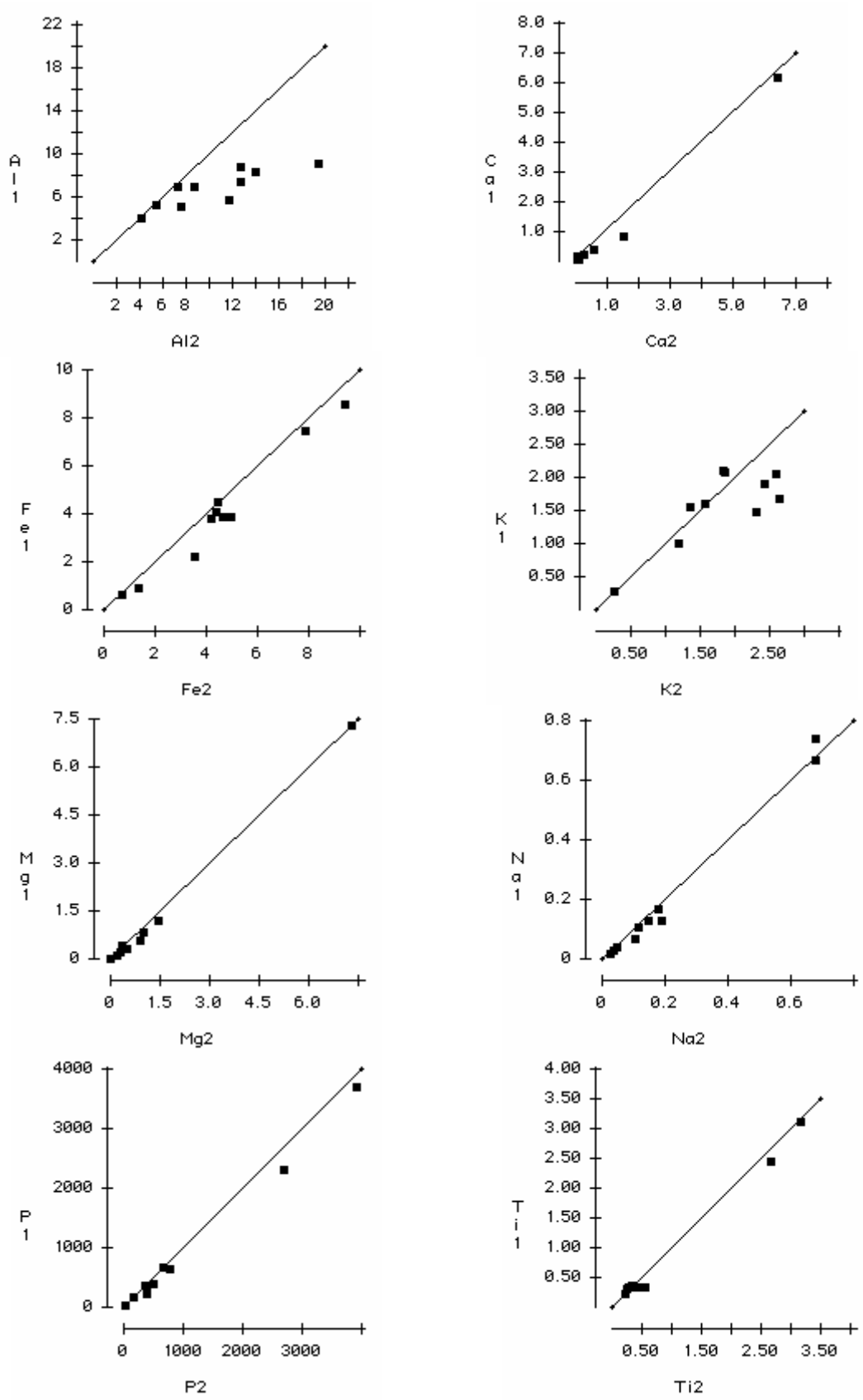

Figure A10-2. Determinations of duplicate samples for Al, Ca, Fe, K, Mg, Na and Ti (%) and P (ppm).

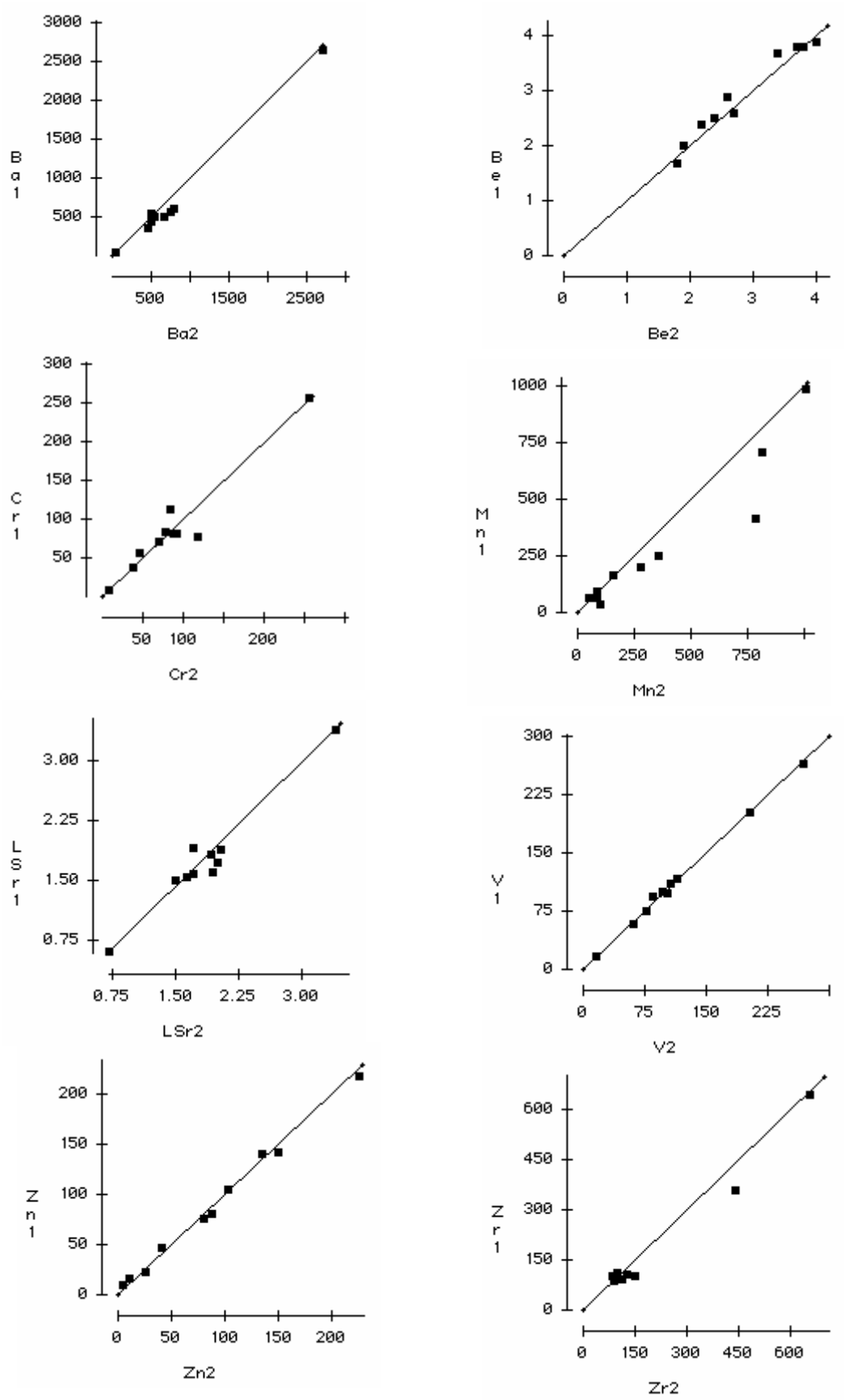

Figure A10-3. Determinations of duplicate samples for Ba, Be, Cr, Mn, log Sr, Zn and Zr (ppm).

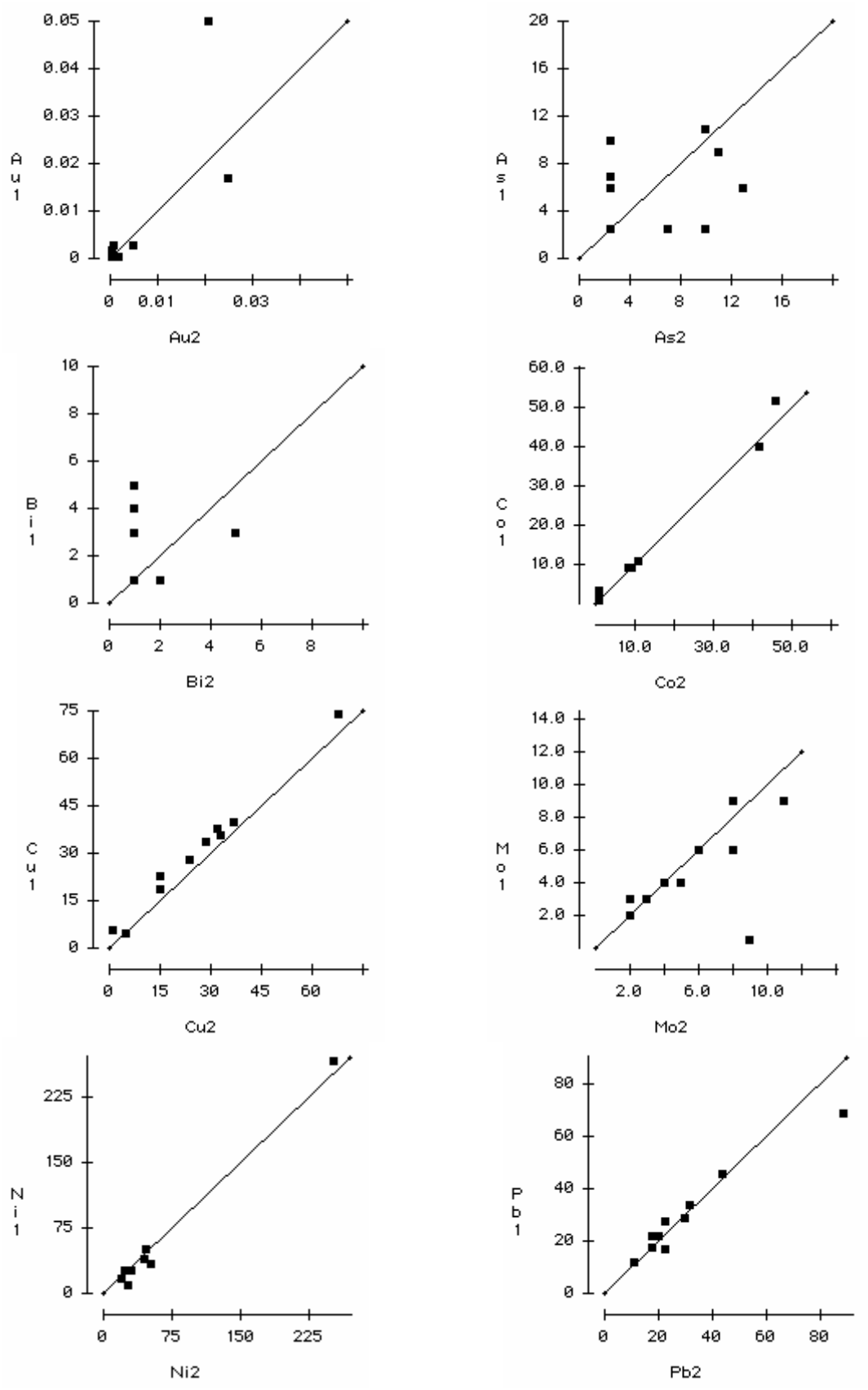

Figure A10-4. Determinations of duplicate samples for Au, As, Bi, Co, Cu, Mo, Ni and Pb (ppm).

APPENDIX 11: ALS CHEMEX GEOCHEMICAL DATA REPORT:

See Appendicies directory on this CD.